Coordination Chemistry

DOI: 10.1002/anie.200702075

Supramolecular Coordination Chemistry: The Synergistic Effect of Serendipity and Rational Design**

Rolf W. Saalfrank, Harald Maid, and Andreas Scheurer*

Keywords:
coordination chemistry · coordination polymers · magnetic properties · molecule dynamics · supramolecular chemistry

Dedicated to Professor Jean-Marie Lehn

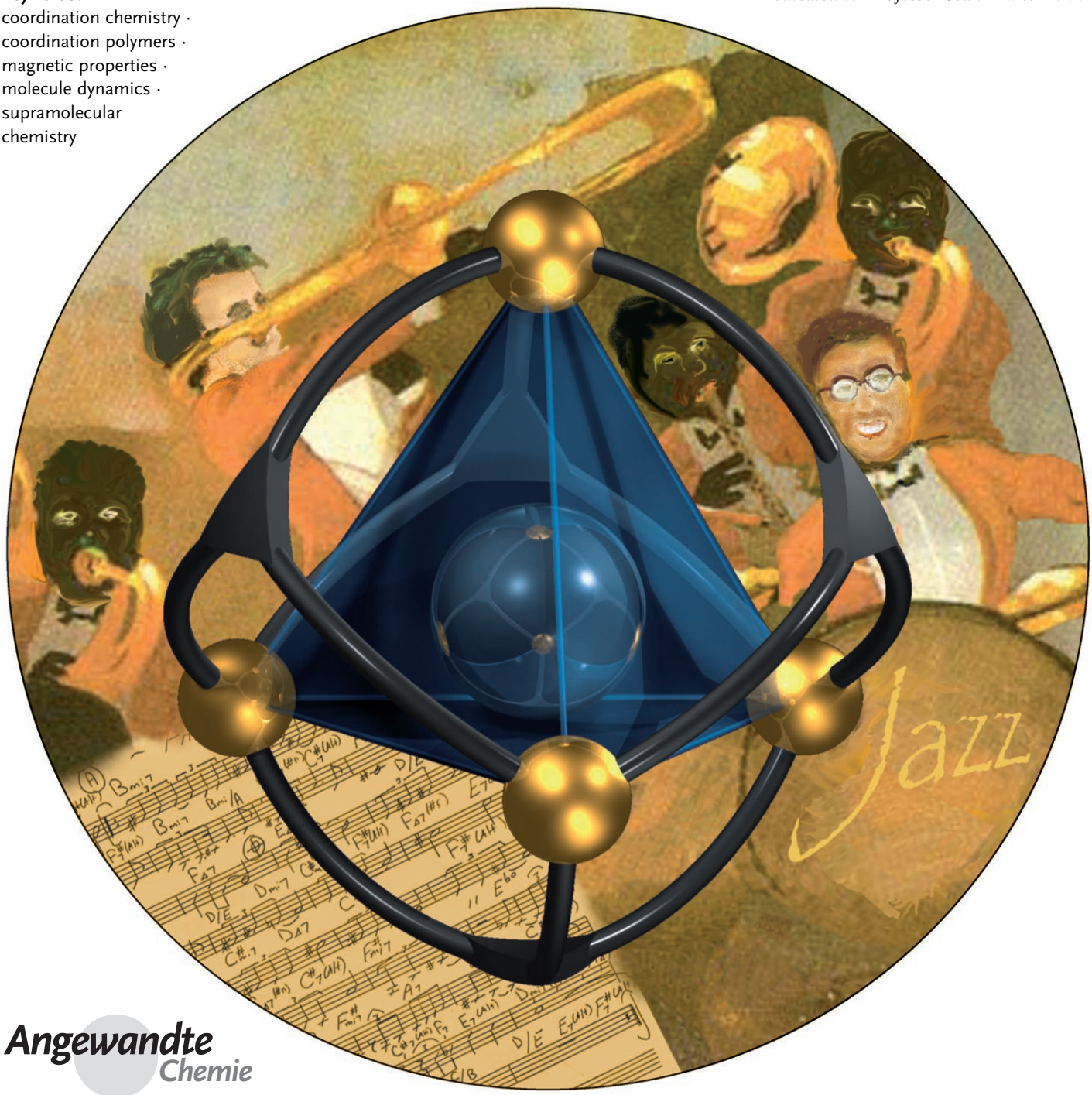

Supramolecular coordination compounds bear exceptional advantages over their organic counterparts. They are available in one-pot reactions and in high yields and display physical properties that are generally inaccessible with organic species. Moreover, their weak, reversible, noncovalent bonding interactions facilitate error checking and self-correction. This Review emphasizes the achievements in supramolecular coordination chemistry initiated by serendipity and their materialization based on rational design. The recognition of similarities in the synthesis of different supramolecular assemblies allows prediction of potential results in related cases. Supramolecular synthesis obeys guidelines comparable to the "lead sheet" used by small jazz ensembles for improvisation and therefore more often leads to unpredicted results. The combination of detailed symmetry considerations with the basic rules of coordination chemistry has only recently allowed for the design of rational strategies for the construction of a variety of nanosized systems with specified size and shape.

"*Ever present never twice the same*"
Robert Irwin. Paul Getty Museum, Central Garden, Los Angeles.

From the Contents

1. Introduction

Lehn has described supramolecular chemistry as an information science in which molecular subunits that contain the necessary information self-assemble into large specific structures.[1] Complementary and explicit interaction of individual components with the appropriate symmetry and geometry generates the product assembly. Consequently, self-assembly has been recognized as a powerful tool for the construction of supramolecular scaffolds, as demonstrated by numerous excellent contributions.[2]

In 1988,[3] we demonstrated that the synergistic effects of serendipity and rational design,[4] based on the well-known rules of coordination chemistry, enable assembly of metallotopomers of the classical purely organic coronates and of bi- and tricyclic cryptates. Compared with the conventional organic-based nitrogen-bridged structures **2** and **3**, the new complexes **5** and **6** feature metal ions that act as bridgeheads linked by bis(bidentate) chelating ligands. The oxygen donors of the ligands are shared between the metal bridgeheads and the encapsulated cations. The transition-metal complexes **4**–**6**, essentially analogous to **1**–**3**, are accessible on a gram scale and in excellent yields by simply mixing the bis(bidentate) chelating ligands and metal ions in solution (Figure 1). Only recently has significant progress been made towards the generation of numerous complexes with predesigned molecular architectures by choosing rigid ligands that have strong preference for specific coordination modes. For instance,

[*] Prof. Dr. R. W. Saalfrank, Dr. H. Maid, Dr. A. Scheurer
Department Chemie und Pharmazie
Lehrstuhl für Allgemeine und Anorganische Chemie
Friedrich-Alexander-Universität Erlangen-Nürnberg
Egerlandstrasse 1, 91058 Erlangen (Germany)
Fax: (+49) 9131-85-27396
E-mail: saalfrank@chemie.uni-erlangen.de
Homepage: http://www.chemie.uni-erlangen.de/oc/saalfrank/

[**] Roots: Part II. Roots: Part I: Reference [42a].

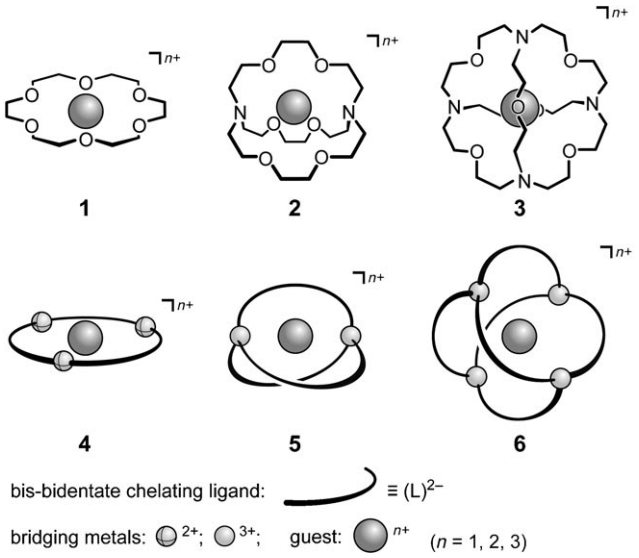

Figure 1. The pictograms reveal the close relationship between the supramolecular structures **1**–**3** and their corresponding metallotopomers **4**–**6**.

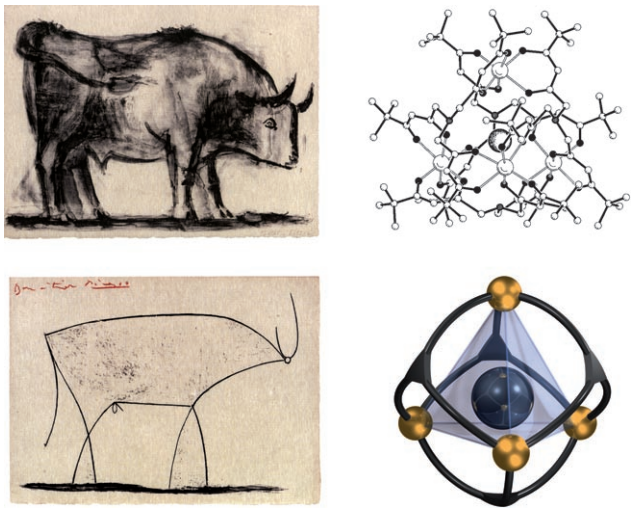

Figure 2. Comparison of Pablo Picasso's series "Le taureau" (left) and the X-ray structure of cation $[Cs\subset\{Fe^{II}Fe^{III}_3(L)_4\}]^+$ of **57** (top right; Cs void, In segment) and its cartoon (bottom right; Cs blue, In yellow, L black).

there have been many endeavors to control structure by use of the symmetry-interaction model or the molecular-library model.[2c,5]

As the systems discussed in this Review gradually become more and more complex, their presentation became more and more difficult. Therefore, to enhance understanding without loss of information, we have put much effort into the design of self-explanatory cartoons. The importance of abstraction and minimization for rapid recognition of complex pictures is impressively exemplified by Pablo Picasso's series "Le taureau".

In Figure 2, a part of this series is contrasted with the original X-ray structure and the iconified version of cationic indium complex $[Cs\subset\{In_4(L)_4\}]^+$ of **57** (Section 8.2). All structural motives presented in this Review are based on single crystal X-ray structure analyses and displayed as POVRAY stereoviews (side-by-side). Unless stated otherwise, protons, disorder, and solvent molecules are omitted for clarity. We recommend the reader viewing the figures take the time sometimes necessary for the brain to adapt in order to experience the 3D world. The additional information the 3D pictures reveal is well worth this effort.

The breadth of supramolecular chemistry has become progressively more apparent. Recent years have seen an explosive growth, as documented by the increasing number of laboratories joining the field whose work has been reported in an immense number of publications. It is therefore impossible to provide an exhaustive account of this field. We do not claim to give a comlete overview, and examples are selected and highlighted according to their originality and are taken mainly from our own work. This Review provides a personal account of how new synthetic tools were developed and put to use in our current work.

2. Cation-Mediated Formation of Metallocoronates

2.1. Coronates, Double-Decker, Triple-Decker, and Sandwich Complexes

In the Introduction, we pointed out the structural analogy between coronates and {2}- and {3}-cryptates and their topologically equivalent metallocoronates and metallocryptates. If the principles of organic crown ether chemistry are

Rolf W. Saalfrank studied and received his Ph.D.at the University of Erlangen-Nürnberg. After a one-year postdoctoral stay with Prof. Donald G. Farnum (Michigan State University, East Lansing, USA), he moved to the German Cancer Research Center at Heidelberg. In 1973 he returned to Erlangen and completed his habilitation in 1976 on push–pull substituted allenes. In 1980 he was appointed professor for organic chemistry. He is Overseas Visiting Scholar at St. John's College, University of Cambridge, UK. Since 1987 his research has concentrated on supramolecular coordination chemistry.

Harald Maid studied chemistry at the Friedrich-Alexander-Universität Erlangen-Nürnberg (FAU). He received his Ph.D. in 2000 for research on the synthesis of coordination polymers under Prof. R. W. Saalfrank. He stayed in the group of Prof. Saalfrank, where he investigates polynuclear transition-metal complexes. He is particularly interested in the computer-aided visualization of chemistry.

applied to the chemistry of metallocrown ethers (MCs), the complexation of differently sized cations by MCs should lead to metallocoronates of varying structures. As the ionic radii of alkali- and alkaline-earth-metal cations differ significantly, while the diameter of the metallocrowns does not change substantially, the inclusion of small cations, such as Na^+ or Ca^{2+}, should lead to a complex with a $Ca^{2+}/MC = 1:1$ stoichiometry. In contrast, encapsulation of the larger K^+ ion should lead to a metallocrown ether sandwich complex with a $K^+/MC = 1:2$ stoichiometry. Consequently, reaction of ketipinate H_2L^1 with copper(II) acetate in the presence of calcium nitrate led to green crystals of the neutral trinuclear metallocoronate $[(Ca\subset\{Cu_3(L^1)_3\})(NO_3)_2]$ (**7**; Scheme 1, Figure 3).[6a] The copper ions are linked along the circumference of the metallocoronate through bis(bidentate) diethyl ketipinate dianions $(L^1)^{2-}$, and each copper(II) ion is coordinated in a square-planar fashion to four oxygen donors. Additional coordination of water, tetrahydrofuran, and nitrate ions leads to a square-pyramidal coordination sphere at each copper ion. The guest Ca^{2+} ion, whose charge is compensated by the two axially coordinated nitrate ions, is located in the center of the metallocoronand host.

However, double deprotonation of diethyl ketipinate H_2L^1 with sodium hydroxide in the presence of sodium tetrafluoroborate and treatment of the dianion $(L^1)^{2-}$ with copper(II) chloride yielded the metallocoronate dimer $[\{(Na\subset\{Cu_3(L^1)_3\})BF_4\}_2]$ (**8**) (Scheme 1, Figure 4).[6b] The monomer of **8** is composed of a $\{Cu_3(L^1)_3\}$ metallocoronand core with a sodium ion located in the center and a BF_4^- counterion. The two monomers are linked through two Na^+ ions, which are each bound to one ring oxygen atom of the neighboring coronate, to give double-decker **8**.

In **8**, both planes are blocked by solvent molecules and counterions. However, in the absence of coordinating water, the most suitable ligation around copper(II) and the sodium ions is achieved by the formation of the triple-decker metallocoronate $[\{(Na\subset\{Cu_3(L^1)_3\})BF_4\}_3]$ (**9**; Scheme 1, Figure 5).[6b]

Whereas encapsulation of the small cations Na^+ and Ca^{2+} led to host-guest systems **8** and **9** with a $M/MC = 1:1$ stoichiometry, double deprotonation of di-*tert*-butyl ketipinate H_2L^2 with 2 N potassium hydroxide and reaction of the dianion $(L^2)^{2-}$ with copper(II) chloride in methanol afforded the metallocrown ether sandwich complex $[(K\subset\{Cu_3(L^2)_3\}_2)OMe]$ (**10**) with a $K/MC = 1:2$ stoichiometry (Scheme 1, Figure 6).[6a,c] It is constructed of two neutral trimetallocrown building blocks that are rotated relative to each other by 60° and are connected by a potassium ion. The coordination spheres of the six copper(II) centers are saturated by methanol molecules, and, thus, each copper(II) ion is surrounded by oxygen donors in a square-pyramidal fashion. The counterion MeO^- is coordinated to potassium.

Andreas Scheurer studied chemistry at the Friedrich-Alexander-Universität Erlangen-Nürnberg (FAU) and at the Université de Rennes 1. For his doctoral thesis he developed novel catalytic systems for asymmetric synthesis at the Ecole Nationale Supérieure de Chimie de Rennes (ENSCR) und FAU. After a postdoctoral stay at the ENSCR with Dr. P. Mosset, he returned to Prof. Saalfrank's group at the FAU, where he works on the synthesis and study of polynuclear transition-metal complexes as model systems for intramolecular electron transfer and single-molecule magnetism.

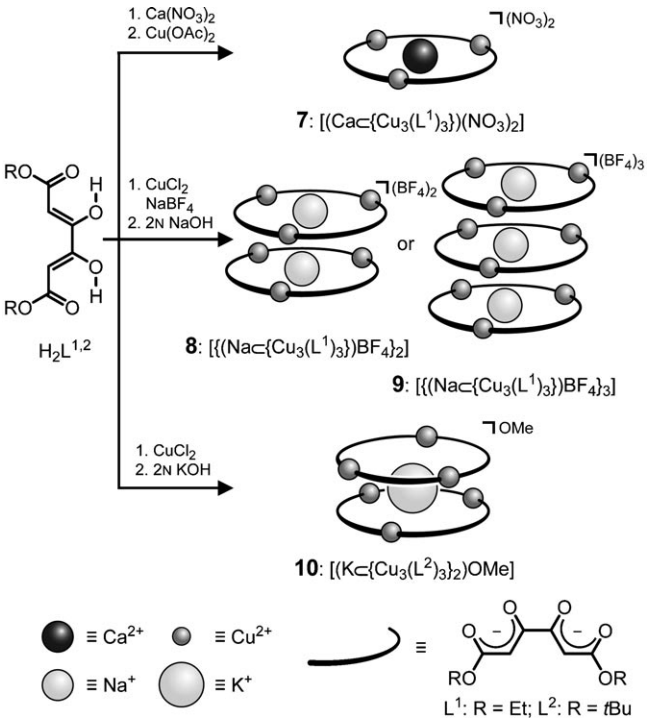

Scheme 1. Synthesis and schematic presentation of **7**–**10**. Please note: the ligand numbering applies only the section in which it appears.

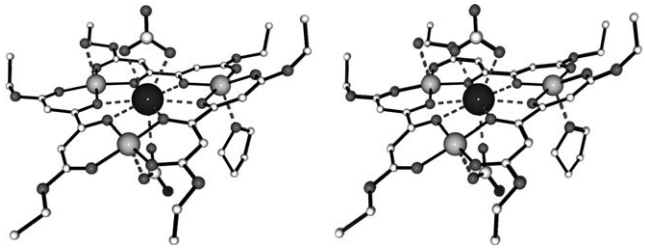

Figure 3. Stereo presentation of metallocoronate **7** in the crystal. Please note: for all figures, the presentation of the atoms is the same as in the corresponding scheme.

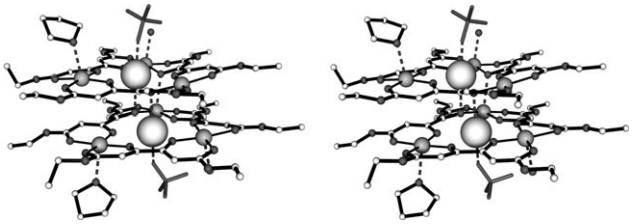

Figure 4. Stereo presentation of double-decker metallocoronate **8** in the crystal.

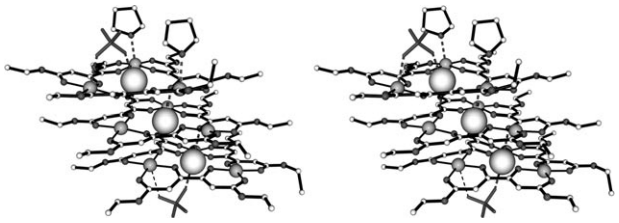

Figure 5. Stereo presentation of the cation of triple-decker metallocoronate **9** in the crystal.

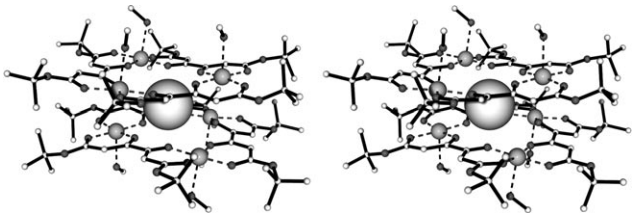

Figure 6. Stereo presentation of the cationic sandwich $\mathbf{10}^{+}$. The disordered counterion MeO^{-} is omitted for clarity.

The cyclic structures **7**–**10**, analogous to classical organic crown ethers **1** (Figure 1), are accessible by simply substituting every-other ethylene bridge with a transition-metal ion. This metallocrown analogy has proven to be highly successful for the controlled preparation of homonuclear, heteronuclear, and mixed-valent assemblies of moderate nuclearity with predesigned molecular architectures.[7]

2.2. Octanuclear [2×2]⊂[2×2] Grids of Magnesium, Calcium, Manganese, and Cadmium

In extension of the aforementioned experiments, Claisen condensation of alkyl acetates or methyl ketones with dialkyl oxalates yielded the ketipinates and tetraketones H_2L^{1-5},[6b] which reacted with cadmium, manganese, or calcium dichloride in the presence of aqueous ammonia to afford the octanuclear [2×2]⊂[2×2] grids $[Cd_8(L^{1-5})_8]$ (**11**), $[Mn_8(L^{1-5})_8]$ (**12**), or $[Ca_8(L^1)_8]$ (**13**; Scheme 2).[6b,8,9] The ^1H and ^{13}C NMR spectra of the diamagnetic cadmium grids **11** indicate two sets of identical ligands and that two halves of each ligand are in different magnetic environments. In **12a**, eight manganese(II) ions form the corners of one of two squares of different sizes but with the same center (Figure 7). The smaller square is

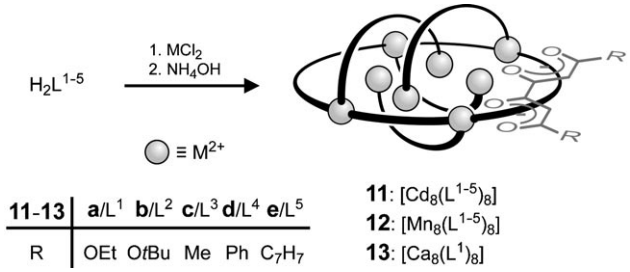

Scheme 2. Synthesis and schematic presentation of the grids **11**–**13**.

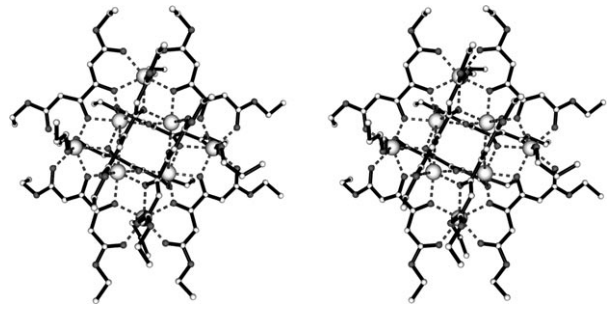

Figure 7. Stereo presentation of the structure of **12a** in the crystal.

rotated by 45° relative to the larger one. All eight Mn^{II} ions are coordinated sevenfold. The calcium grid $[Ca_8(L^1)_8]$ (**13**) is isostructural with $[Mn_8(L^1)_8]$ (**12a**).

2.3. From Metallocoronates to One-Dimensional Coordination Polymers: Threading Cesium Ions

Further studies on the supramolecular coordination chemistry of copper(II) focused on the synthesis of oligonuclear complexes by self-assembly with the pentadentate ligand $(L)^{2-}$ with 2,6-pyridinyl-spacers.[10] To this end, H_2L was treated with calcium hydride and copper(II) acetate to give the metallocoronate $[(Ca\subset\{Cu_2(L)_2\})(OAc)_2]$ (**14**; Scheme 3). In the crystal, **14** is present as a dinuclear copper(II) coronate in which a calcium ion is encapsulated in the center; two acetates act as counterions.

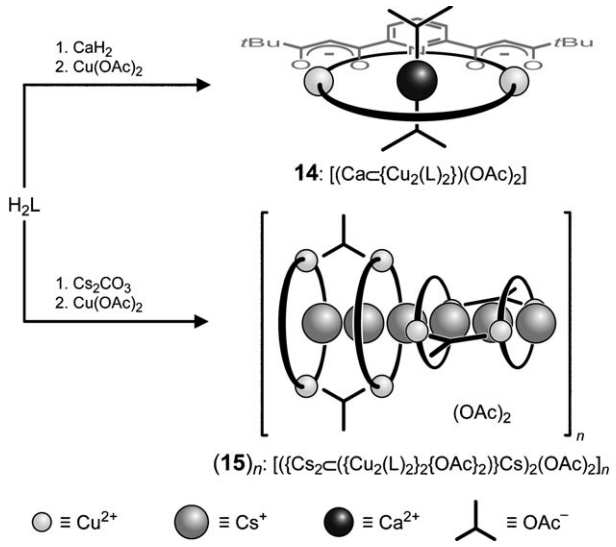

Scheme 3. Synthesis and schematic presentation of **14** and $(\mathbf{15})_n$.

In contrast, treatment of a solution of H_2L with copper(II) acetate and cesium carbonate does not yield a metallocoronate similar to **14**. Instead, the larger cesium ion, which prefers a higher coordination number, functions as a template for the formation of the one-dimensional coordination polymer $[\{(\{Cs_2\subset(\{Cu_2(L)_2\}_2\{OAc\}_2)\}Cs)_2(OAc)_2\}_n]$ $(\mathbf{15})_n$ (Scheme 3). The individual modules of $(\mathbf{15})_n$ are composed

of two concave $\{Cu_2(L)_2\}$ metallocoronands linked by two bidentate acetate ions. Endohedral encapsulation of two cesium ions and two molecules of ethanol in the container $(\{Cu_2(L)_2\}_2\{OAc\}_2)$ gives the cryptate $\{(Cs{\cdot}EtOH)_2\subset(\{Cu_2(L)_2\}_2\{OAc\}_2)\}$. Exohedral coordination of a further cesium ion to the cryptate generates the self-complementary unit $(\{(Cs{\cdot}EtOH)_2\subset(\{Cu_2(L)_2\}_2\{OAc\}_2)\}Cs)^+$. Linkage of these building blocks, alternately rotated by 90°, finally affords the dicationic monomer $[(\{(Cs{\cdot}EtOH)_2\subset(\{Cu_2(L)_2\}_2\{OAc\}_2)\}Cs)_2]^{2+}$ of the one-dimensional coordination polymer $(\mathbf{15})_n$. Charge compensation is achieved by acetate ions. The interatomic distances of the threaded cesium cations in $(\mathbf{15})_n$ are the shortest measured to date (Figure 8).

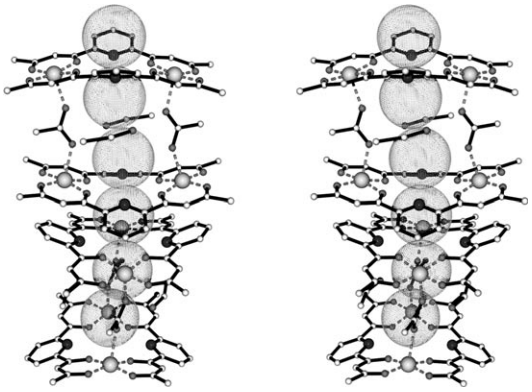

Figure 8. Stereo presentation of the of the dicationic repeating unit of one-dimensional coordination polymer $(\mathbf{15})_n$ in the crystal, indicating the close contact of the cesium ions. *t*Bu groups are replaced by Me.

3. Ligand- and Metal-Directed Syntheses of {2}-Metallocryptands, {2}-Metallocryptates, One-Dimensional Coordination Polymers, and Octanuclear Bis(Triple Helicates)

3.1. {2}-Metallocryptands and {2}-Metallocryptates of Iron

A number of review articles have described the syntheses and properties of {2}-metallocryptands and {2}-metallocryptates together with structures of variable nuclearity.[2k,11] The use of suitable tailored ligands made further {2}-metallocryptands and {2}-metallocryptates available, which we designed as metallotopomers of the corresponding organic {2}-cryptands and {2}-cryptates (Figure 1). To this purpose, H_2L^1 was treated with triethylamine and iron(III) chloride to yield dark red microcrystals. Spectroscopic data indicated that the isolated product is the {2}-ironcryptand $[Fe_2(L^1)_3]$ (**16**; Scheme 4).[11d,e,j,12,13]

In **16**, each of the two iron centers is octahedrally surrounded by six oxygen donors. In the racemic mixture of the triple helicate **16**, the two iron centers have either a (Δ,Δ)-*fac* or a (Λ,Λ)-*fac* configuration. The donating power in the interior of the metallocryptand is insufficient for the complexation of alkali metal cations, and, above all, three hydrogen atoms of the phenylene spacers of **16** are directed towards the empty interior cavity.

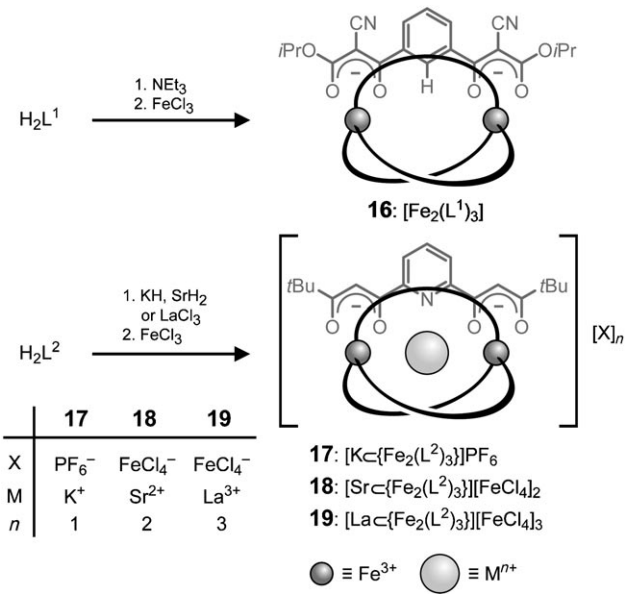

Scheme 4. Synthesis and schematic presentation of iron cryptand **16** and iron cryptates **17**–**19**.

To synthesize the {2}-ironcryptates $[M\subset\{Fe_2(L^2)_3\}][X]_n$ (**17**–**19**, $n=1$–3), the *m*-phenylene spacer of H_2L^1 was substituted for an *m*-pyridylene spacer to give H_2L^2, which then was treated with potassium hydride, strontium hydride, or lanthanum(III) chloride and subsequently with iron(III) chloride (Scheme 4).[13] The cavity of {2}-metallocryptate $[K\subset\{Fe_2(L^2)_3\}]PF_6$ (**17**) is occupied by a potassium ion, with ninefold coordination to six ligand oxygen atoms and to three pyridine nitrogen donors (Figure 9). There is a hexafluoro-

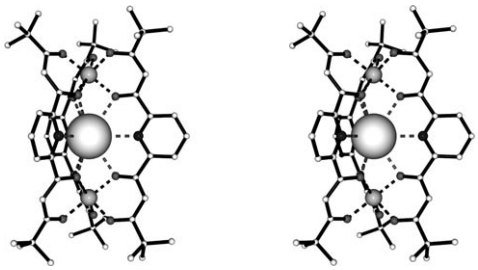

Figure 9. Stereo presentation of the structure of the cation of *meso*-**17** in the crystal.

phosphate counterion, and the two iron bridgeheads are octahedrally surrounded by six oxygen donors. However, in contrast to *rac*-(Δ,Δ)/(Λ,Λ)-*fac*-**16**, the two iron centers in *meso*-(Δ/Λ)-*fac*-**17** have opposite configurations.

The cyclic voltammogram (CV) of the {2}-metallocryptand $[Fe_2(L^1)_3]$ (**16**) displays a single quasi-reversible, one-potential, two-electron transfer process. However, {2}-metallocryptate $[K\subset\{Fe_2(L^2)_3\}]PF_6$ (**17**) undergoes two well-separated, quasi-reversible one-electron transfer processes. This behavior clearly demonstrates a sensitive depend-

ence of the electrochemical properties on electrostatic interactions, which are enhanced by the inclusion of the potassium ion in **17**.

3.2. Octanuclear Bis(Triple-Helical) Complexes of Manganese, Zinc, and Cadmium

Furthermore, the formation of metallosupramolecular structures is highly sensitive to the oxidation state of the metal ions involved, as demonstrated for the reaction of the topologically equivalent ligands $(L^1)^{2-}$ and $(L^2)^{2-}$ with manganese, zinc, and cadmium salts[14] instead of iron(III) chloride. While the iron(III) salt gives rise to $[K\subset\{Fe_2(L^2)_3\}]PF_6$ (**17**) (Section 3.1), when H_2L^1 or H_2L^2 were treated with cadmium or manganese dichloride with aqueous ammonia or with zinc(II) acetate, the coordination complexes **20**–**22** were isolated (Scheme 5). ^1H and ^{13}C NMR spectros-

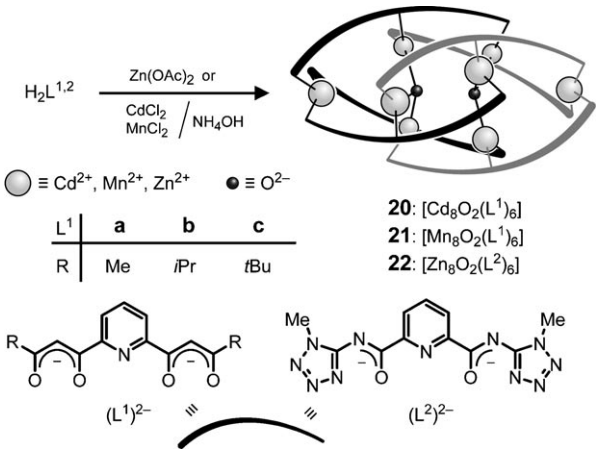

Scheme 5. Synthesis and schematic presentation of the octanuclear bis(triple-helical) complexes **20**–**22**.

copy studies of the diamagnetic cadmium complex $[Cd_8O_2(L^{1c})_6]$ (**20c**), for instance, revealed that all six ligands are identical but that the two halves of each ligand are in different magnetic environments.

To establish the structure of the octanuclear systems **20**–**22**, the manganese complex $[Mn_8O_2(L^{1b})_6]$ (**21b**) was selected as a representative example for X-ray crystallographic analysis (Figure 10). The core of **21b** consists of eight manganese(II) ions forming a twofold capped, slightly twisted trigonal prism with a μ_3-O^{2-} ion centered in each of the two inner triangular faces. Each of the six doubly negatively charged pentadentate ligands $(L^{1b})^{2-}$ is linked to three manganese(II) ions. In the neutral, octanuclear, bis(triple-helical) complex **21b**, all manganese(II) ions are octahedrally coordinated. The zinc(II) complex $[Zn_8O_2(L^2)_6]$ (**22**) is isostructural with **21b**. The similarity between the core of the octanuclear complex **22** and the metal framework of the iron–molybdenum cofactor of the nitrogenase MoFe protein is noteworthy. [15]

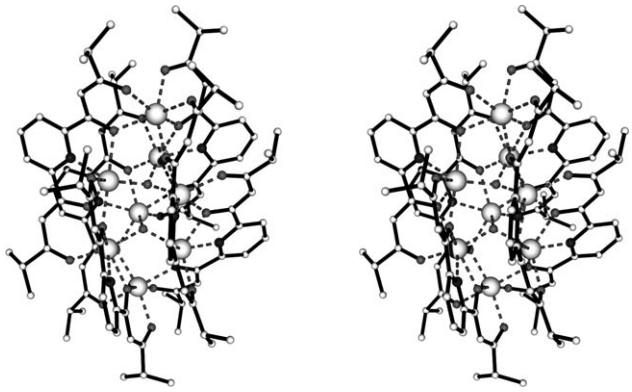

Figure 10. Stereo presentation of the structure of the octanuclear complex **21b** in the crystal.

3.3. A Bis(Double Helicate) and its Cryptatoclathrate

On the other hand, racemic, homochiral complex $[\{Zn_2(L)_2\}_2]$ (**23**) was generated in a self-assembly process starting from achiral CH-acidic bis(tetrazolylmethylketone) H_2L and zinc(II) acetate. The formation of the chiral building blocks $(\Delta,\Delta)/(\Lambda,\Lambda)$-$\{Zn_2(L)_2\}$ and their linkage is governed by chiral self-recognition (Scheme 6).[16]

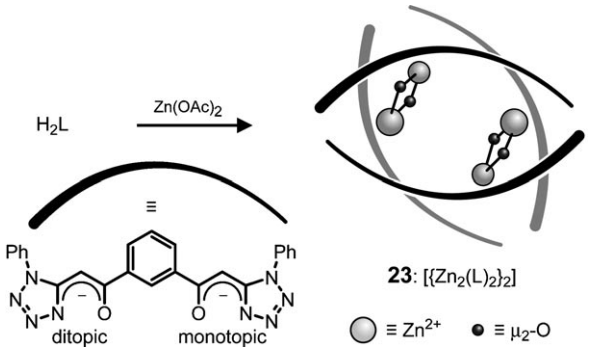

Scheme 6. Synthesis and schematic presentation of bis(double helicate) **23**.

According to NMR spectroscopy studies, intact tetranuclear **23** is present in solution, and an X-ray diffraction analysis reveals that $[\{Zn_2(L)_2\}_2]$ (**23**) exists in the crystal as a neutral tetranuclear bis(double helicate). The core of **23** is formed by the overall tritopic tetradentate ligands $(L)^{2-}$, leading to a distorted cuboid whose eight corners are occupied by alternating zinc ions and μ_2-keto oxygen donors. The enantiomeric, tetranuclear (*P*)- and (*M*)-bis(double helicates) **23** are composed of two self-complementary, homochiral, double-helical substructures $\{Zn_2(L)_2\}$. Pairwise aggregation of the bis(double helicates) **23** in the crystal leads to the inclusion of two molecules of tetrahydrofuran, resulting in the homochiral cryptatoclathrate $[(thf)_2\subset(\{Zn_2(L)_2\}_2)_2] \equiv [(thf)_2\subset(\mathbf{23})_2]$ (Figure 11).

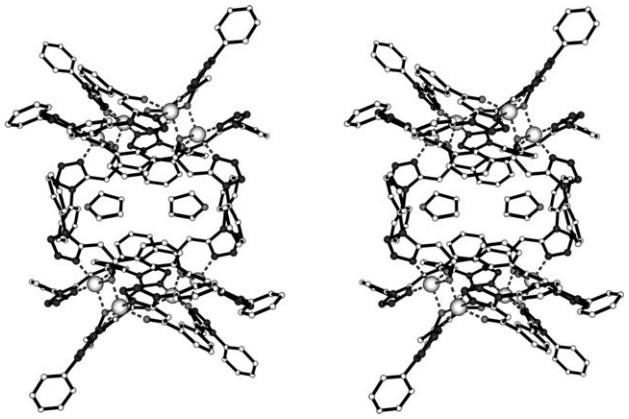

Figure 11. Stereo presentation of the structure of cryptatoclathrate $[(thf)_2\subset(\mathbf{23})_2]$ in the crystal.

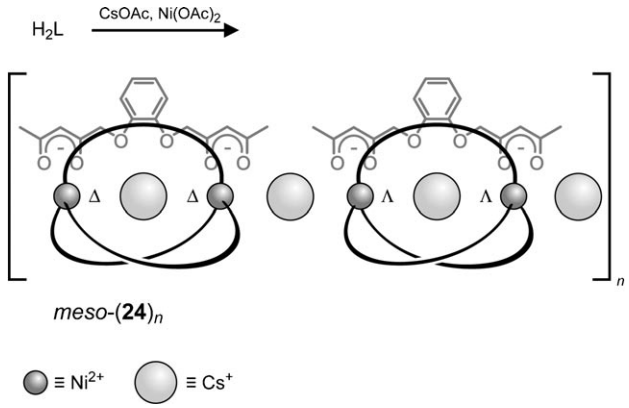

Scheme 7. Synthesis and schematic presentation of one-dimensional polymer *meso*-$(\mathbf{24})_n$.

3.4. One-Dimensional Coordination Polymers via Self-Complementary {2}-Metallocryptates

3.4.1. Meso and Racemic Polymer Strings

As noted in Section 2, the template-mediated self-assembly of tetradentate ketipinate dianions and copper(II) ions yielded trinuclear copper coronates or copper crown ether sandwich complexes. On the other hand, reaction of tetradentate 1,3-diketo dianions with *m*-phenylene spacers or pentadentate 1,3-diketo dianions with *m*-pyridylene spacers with iron(III) gave rise to {2}-metallocryptands or {2}-metallocryptates (Section 3). The prediction of these structures is based on the careful selection of matching metal/ligand combinations. However, for further developments in the field of supramolecular coordination chemistry, it is of great interest to investigate how nature copes with electronically mismatched metal/ligand combinations. In other words, this type of approach transfers the intellectual responsibility for design to the molecules themselves.[17] To expand the void in complexes derived from ligands mentioned so far, a catecholate spacer was adapted to the bis-1,3-diketo ligand system. For instance, reaction of six-coordinate nickel(II) in the presence of cesium ions with hexadentate bis-1,3-diketo dianion $(L)^{2-}$ yielded the neutral {2}-metallocryptate *meso*-$(\mathbf{24})_n$ (Scheme 7).[18]

This {2}-metallocryptand $\{Ni_2(L)_3\}^{2-}$ core is composed of two nickel centers linked through three bis-1,3-diketo dianions $(L)^{2-}$ with catecholate spacers (Figure 12). The resulting {2}-metallocryptands are homochiral with either (Δ,Δ)-*fac* or (Λ,Λ)-*fac* stereochemistry at the nickel centers and can host a cesium ion in the cavity, which is coordinated by six carbonyl and six catecholate oxygen donors. Charge compensation of the thus formed enantiomers $(Cs\subset\{(\Delta,\Delta)/(\Lambda,\Lambda)\text{-}Ni_2(L)_3\})^-$ is achieved through extra external cesium ions to give the neutral self-complementary building blocks $\{(Cs\subset\{(\Delta,\Delta)/(\Lambda,\Lambda)\text{-}Ni_2(L)_3\})Cs\}$. These self-complementary building blocks aggregate alternately end-on through the external cesium ions to yield the one-dimensional coordination polymer *meso*-$(\mathbf{24})_n$.

When H_2L was treated with magnesium(II) acetate in the presence of cesium acetate, the cesium ions again function as templates. However, in contrast to the nickel case, which afforded *meso*-$(\mathbf{24})_n$, with magnesium(II) ions *rac*-$(\mathbf{25})_n$ was formed. Homochiral building blocks $\{(Cs\subset\{(\Delta,\Delta)/(\Lambda,\Lambda)\text{-}Mg_2(L)_3\})Cs\}$ aggregate end-on across the external cesium ions to give the one-dimensional homochiral strings $[\{(Cs\subset\{(\Delta,\Delta)\text{-}Mg_2(L)_3\})Cs\}_n]$ (Δ-$(\mathbf{25})_n$) and $[\{(Cs\subset\{(\Lambda,\Lambda)\text{-}Mg_2(L)_3\})Cs\}_n]$ (Λ-$(\mathbf{25})_n$), which are packed in the crystal in alternating homochiral layers (Scheme 8, Figure 13).[19]

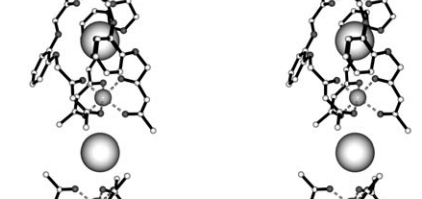

Figure 12. Stereo presentation of the repeating unit of the structure of *meso*-$(\mathbf{24})_n$ in the crystal.

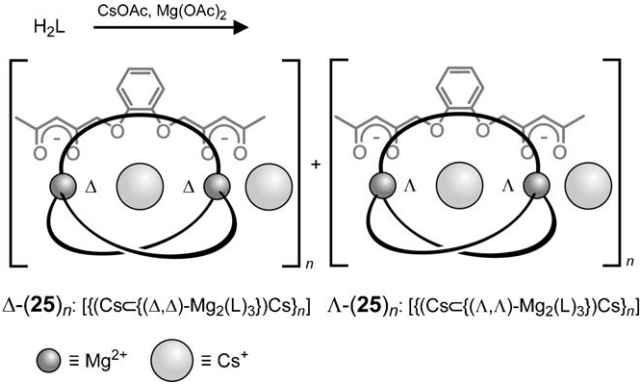

Scheme 8. Synthesis and schematic presentation of the homochiral linear one-dimensional polymers Δ-$(\mathbf{25})_n$ and Λ-$(\mathbf{25})_n$.

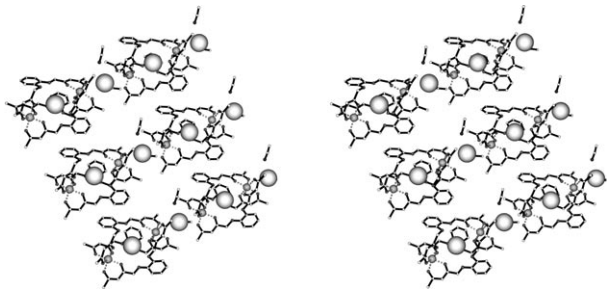

Figure 13. Stereo presentation of a layer of Λ-(**25**)$_n$ in the crystal.

3.4.2. *Meandering meso-Polymer Strings*

To suppress the formation of self-complementary monomers and their polymerization by making the external pockets of the cryptates too small to host the external cesium ions, H_2L with bulkier phenyl groups was used. To that end, stoichiometric amounts of H_2L, alkali acetates, and divalent hexacoordinate metal acetates were reacted (Scheme 9). Since the polymers *meso*-(**26**)$_n$ are isostructural, only the structure of *meso*-(**26e**)$_n$ is discussed in detail. In *meso*-(**26e**)$_n$, two enantiomers are linked end-on by only one cesium ion to give a *meso* fragment, and a second fragment is coordinated side-on to these units, giving meandering polymer *meso*-(**26e**)$_n$. Therefore, Cs_{end} links the enantiomers (Cs⊂-{(Δ,Δ)/(Λ,Λ)-$Co_2(L)_3$})$^-$ to give *meso*-{(Cs⊂{(Δ,Δ)-$Co_2(L)_3$})Cs_{end}(Cs⊂{(Λ,Λ)-$Co_2(L)_3$})}$^-$, while Cs_{side} links the *meso* fragments across their homochiral {2}-metallocryptate halves. The meandering strands of the isostructural *meso*-(**26e**)$_n$ polymers are packed in parallel in the crystal (Figure 14).[19]

3.5. *Diastereoselective Self-Assembly: Enantiomerically Pure Copper(II) Cubanes from Chiral Bis(1,3-Diketones)*

Whereas bis(1,3-diketones) with catecholate spacers and hexacoordinate metal(II) ions yielded polymers (Section 3.4), reaction of bis(1,3-diketone) H_2L with a glycolate spacer, an excess of alkali metal acetates (M = K^+, Rb^+, Cs^+), and pentacoordinate copper(II) ion yielded the racemic double-stranded metallocoronates (*P*/*M*)-[(M⊂{$Cu_2(L)_2$})OAc] ((*P*/*M*)-(M-**27**), Scheme 10, Figure 15).[18]

In the course of these studies on supramolecular coordination chemistry, the development of stereoselective syntheses attracted our attention. For that purpose, $H_2L^{(S,S)}$ and $H_2L^{(R,R)}$ were generated starting from L- or D-tartaric acid. Reaction of two equivalents of copper(II) acetate, one equivalent of $H_2L^{(S,S)}$, and one equivalent of cesium acetate yielded not the expected chiral metallocoronate but the copper(II) cubane (*C*,*C*,*C*,*C*)-[$Cu_4(L^{(S,S)})_2(OMe)_4$] (**28**) as a single enantiomer (Scheme 11).

Cubane **28** possesses a [$Cu_4(\mu_3\text{-}O)_4$] core consisting of two interpenetrating tetrahedra, one made up of four copper(II) ions and one of four μ_3-OMe co-ligands (Figure 16).[20] Similarly, (*A*,*A*,*A*,*A*)-[$Cu_4(L^{(R,R)})_2(OMe)_4$] (*ent*-**28**) was prepared from $H_2L^{(R,R)}$.

Circular dichroism (CD) measurements of the copper(II) cubanes **28** and *ent*-**28** confirm the enantiomeric nature of

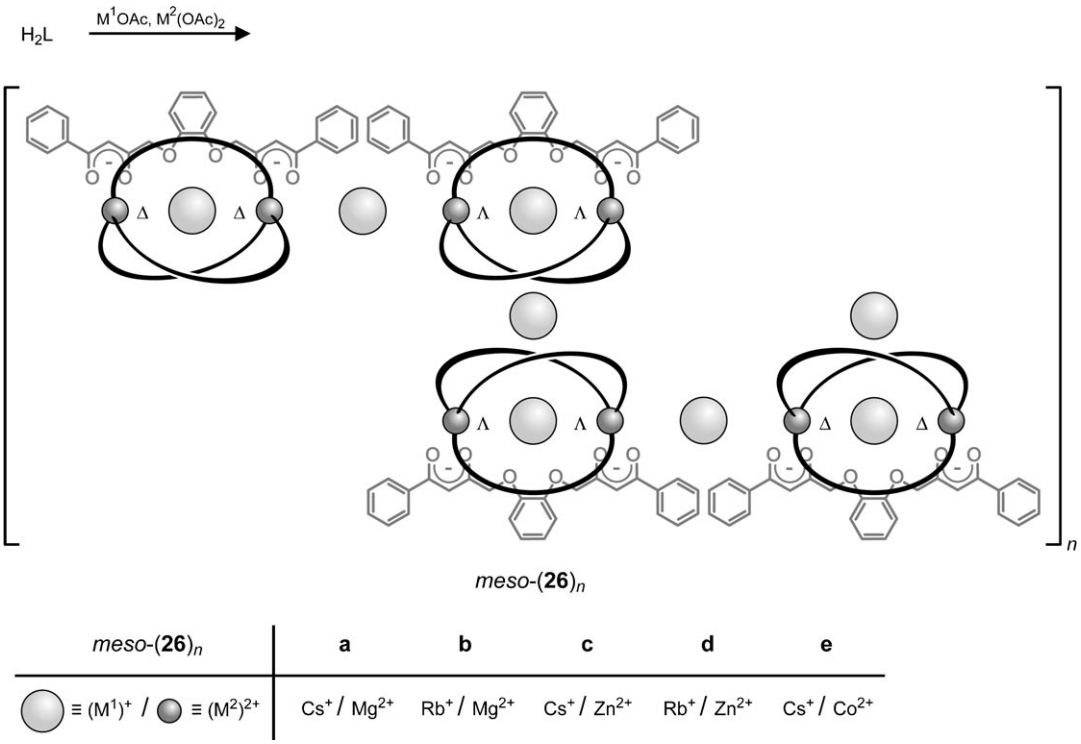

Scheme 9. Synthesis and schematic presentation of one-dimensional *meso*-(**26**)$_n$.

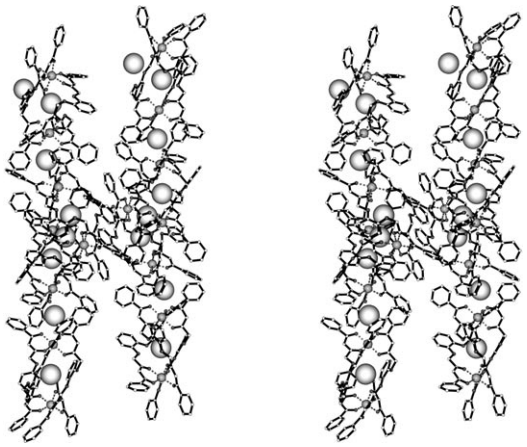

Figure 14. Stereo presentation of the repeating unit of *meso*-(**26e**)$_n$ in the crystal.

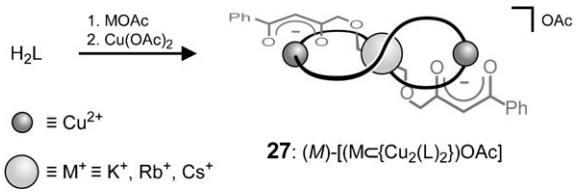

Scheme 10. Synthesis and schematic presentation of **27**.

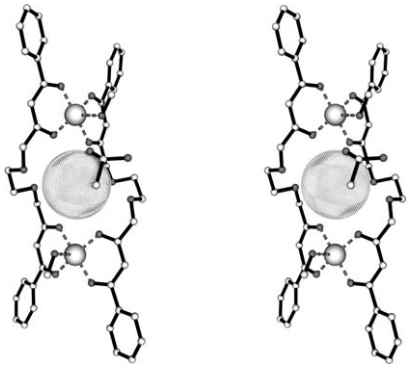

Figure 15. Stereo presentation of the double-stranded metallocoronate (*P*)-(Cs-**27**) in the crystal.

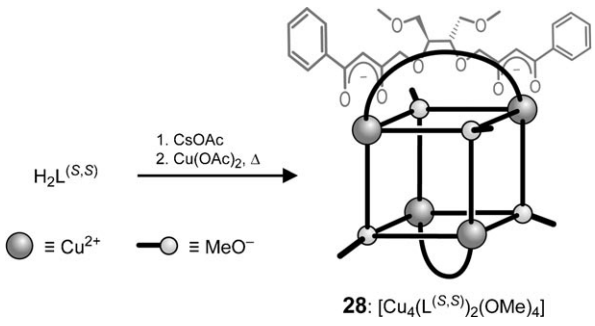

Scheme 11. Synthesis and schematic presentation of **28**.

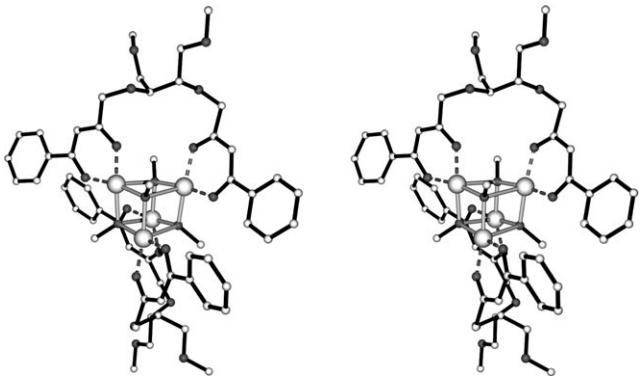

Figure 16. Stereo presentation of the structure of **28** in the crystal.

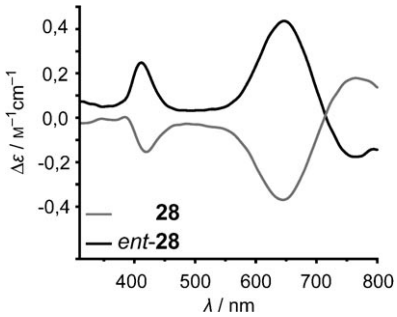

Figure 17. CD spectra of **28** and *ent*-**28**.

these complexes. The CD spectrum of **28** exhibits two negative and one positive Cotton effect, while *ent*-**28** shows Cotton effects of the opposite sign at the same wavelengths (Figure 17).[21]

3.6. Threading of Copper(II) and Palladium(II) Ions

In Section 3.5 we demonstrated the enormous sensitivity of supramolecular coordination compounds to the stoichiometry of the starting materials. Consequently, when the stoichiometry of the alkali-metal ions to ligand was changed again and $H_2L^{(S,S)}$ was treated with five equivalents of potassium acetate and one equivalent copper(II) acetate, neither a coronate nor a cubane was formed. Instead the homochiral helical complex (*P*)-[$Cu_2(L^{(S,S)})_2$] (**29**) with a square-planar coordination environment at the copper(II) centers was isolated. Analogously, (*P*)-[$Pd_2(L^{(S,S)})_2$] (**30**) could be obtained from palladium(II) acetate in the presence of one equivalent of pyridine (Scheme 12).[21] Interestingly, the molecules **29** and **30** are packed in the crystal in parallel, leading to copper and palladium metal strings with short intra- and intermolecular metal–metal separations (Figure 18).[21]

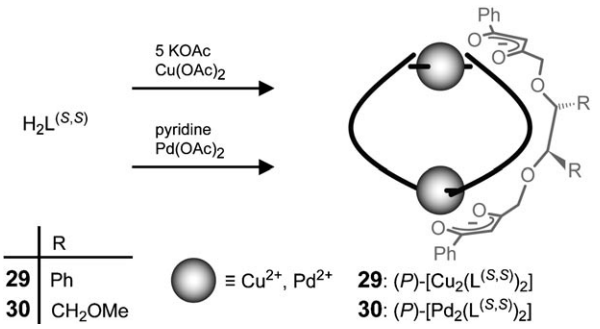

Scheme 12. Synthesis and schematic presentation of **29** and **30**.

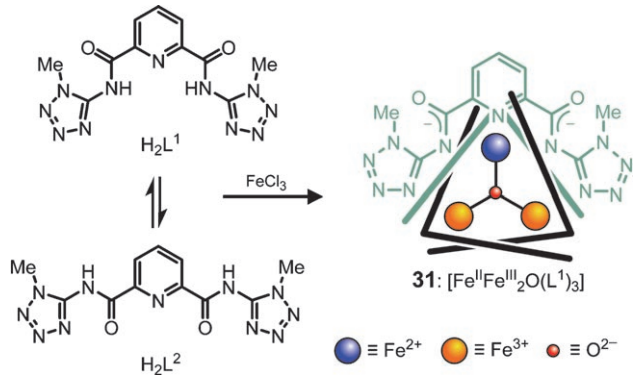

Scheme 13. Synthesis and schematic presentation of **31**.

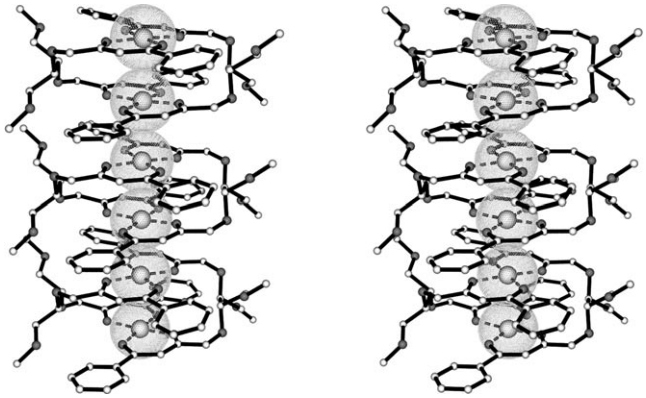

Figure 18. Stereo presentation of the packing of homochiral, helical complex (*P*)-**30** in the crystal, highlighting the short metal–metal distances by dotted (light gray) van der Waals radii of palladium(II).

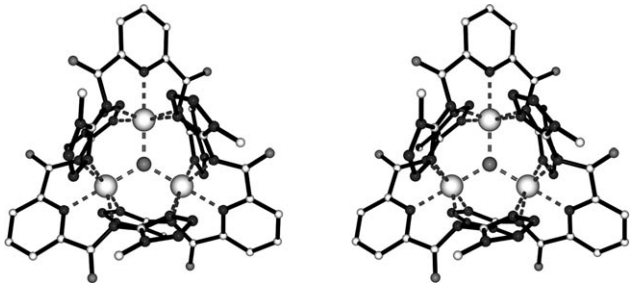

Figure 19. Stereo presentation of the structure of μ_3-oxo-centered mixed-valent **31** in the crystal. Fe light gray (large), μ_3-O^{2-} dark gray.

4. The Synthetic Potential of Ligand Rotamers and Ligand Tailoring

4.1. A Neutral, Triple-Helical, Mixed-Valent, Oxo-Centered Triiron Complex

As noted in Section 3.2, octanuclear bis(triple-helical) complexes $[Zn_8O_2(L^2)_6]$ (**22**) are accessible with linear H_2L^2. In linear $(L^2)^{2-}$ the coordinating atoms are two oxygen and three nitrogen donors. However, in solution pentadentate $(L^2)^{2-}$ is in equilibrium with its angular rotamer $(L^1)^{2-}$. Interestingly, when $H_2L^{1/2}$ was deprotonated with triethylamine and treated with iron(III) chloride, racemic μ_3-oxo-centered mixed-valent complex $[Fe^{II}Fe^{III}_2O(L^1)_3]$ (**31**) was formed (Scheme 13).[22]

In triangular **31** all iron ions are coordinated in a distorted octahedral fasion to five nitrogen donors and a common μ_3-O^{2-} ion (Figure 19). The tetrazolyl nitrogen donors of the pentadentate, tritopic ligands $(L^1)^{2-}$ attack neighboring iron centers at opposite sides of the (Fe,Fe,Fe) triangular plain, resulting in a triple-helical, D_3-symmetric arrangement of **31**. In principle, oxo-centered complexes related to $[Fe_3^{III}O(O_2CR)_6(H_2O)_3]^+$ are interesting as model compounds for ironoxo proteins, oxidation catalysts, and corrosion inhibitors.[23]

4.2. Rectangular [2×2] Grids of Nickel and Zinc

β-Alaninehydroxamic acid and salicylhydroxamic acid react with appropriate metal ions to give tetranuclear metallocoronates.[24] A common feature of the cyclic linkage of the four metal ions in these complexes is the fact that in **32** and **33** the ligands may generate five- or six-membered chelates. Likewise, oligodentate *N*-(2-alkyl-2*H*-tetrazol-5-yl)picolinamide of type **34** proved to be suitable for the formation of metallocycles, as **34** matches the geometric conditions of the structurally analogous modules **32** and **33** (Figure 20).

Moreover, fragment **34** is simply derived from *N*,*N*′-bis(tetrazolyl)pyridyldicarboxamide (Section 4.1, H_2L^2) by removing the substituent at one side of the central pyridine ring. Reaction of HL^1 with nickel(II) acetate readily yielded $[Ni_4(L^1)_8]$ (**35**; Scheme 14). The zinc complex $[Zn_4(L^2)_8]$ (**36**) was obtained in a similar manner from HL^2 and is isostructural with **35**.[25]

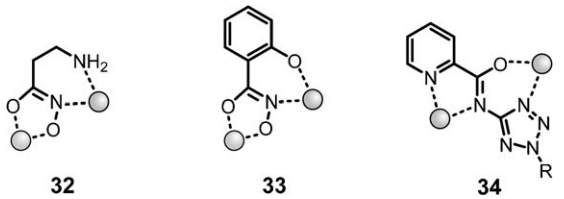

Figure 20. Geometric relationship between the fragments **32**–**34**. Gray balls: metal ions.

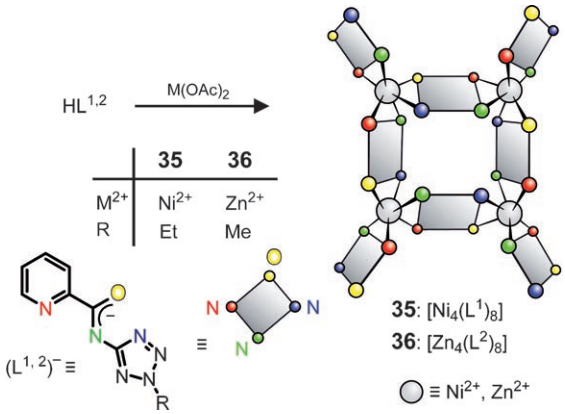

Scheme 14. Synthesis and schematic presentation of **35** and **36**.

$[Ni_4(L^1)_8]$ (**35**) is present in the crystal as a square $[2\times2]$ grid. One of the main structural characteristics of **35** is the presence of two different sets of bonding modes (bidentate and tetradentate) observed for potentially tetradentate $(L^1)^-$ (Figure 21). The temperature dependence of the magnetic susceptibility indicates intramolecular ferromagnetic coupling of the nickel(II) ions in **35**.[25a,c]

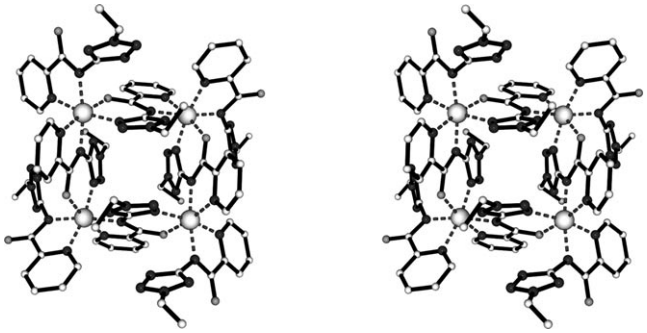

Figure 21. Stereo presentation of the structure of **35** in the crystal.

4.3. Oxo-Centered Tetranuclear Heteroleptic Zinc Complexes

Pentadentate *N*-(2-methyl-2*H*-tetrazol-5-yl)picolinamide fragment **37** forms five- and six-membered chelates suitable for the linkage of metal ions to give oligonuclear complexes (Section 4.2). Even though tetradentate *N*-(5-methylthiazol-2-yl)thiazole-2-carboxamide fragment **38** matches the geometric conditions of **37**, it does not react as a tetradentate ligand but rather as its tridentate rotamer, with only the three nitrogen donors coordinating (Figure 22).[26a] Reaction of HL with zinc(II) acetate produced $[Zn_4O(L)_4(OAc)_2]$ (**39**; Scheme 15). NMR spectroscopy studies of diamagnetic **39** revealed that all four ligands are chemically identical. An X-ray crystallographic structure analysis revealed the tetranuclear structure of **39**. In **39**, the module $[Zn_2(L)_2]^{2+}$ is generated from two ditopic tridentate ligands $(L)^-$ and two zinc(II) ions (Figure 23). Two of these building blocks are arranged such that the four Zn^{II} ions form the vertices of a

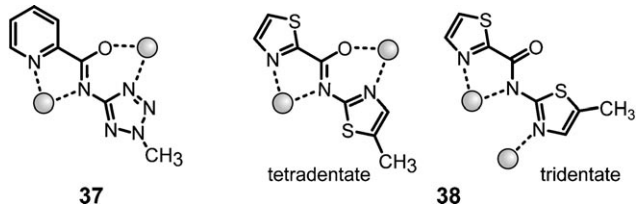

Figure 22. Comparison of the fragments **37** and **38**. Gray balls: metal ions.

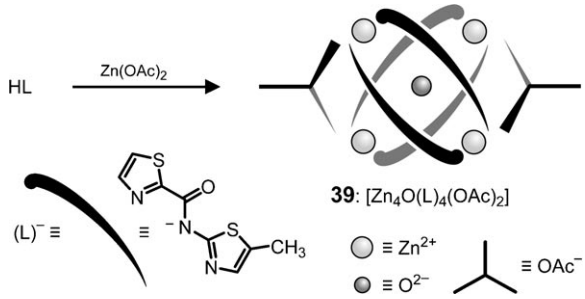

Scheme 15. Synthesis and schematic presentation of **39**.

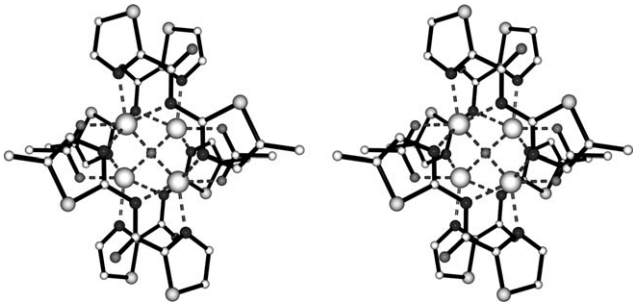

Figure 23. Stereo presentation of the structure of μ_4-oxo-centered **39** in the crystal.

tetrahedron in which two edges are bridged by two acetate clamps. Charge compensation is provided by a μ_4-O^{2-} ion in the center of the tetrahedron.

4.4. Homovalency and Mixed Valency: Tri- and Hexanuclear Oxo-Centered Iron and Nickel/Iron Complexes

In extension of the studies in Section 4.3, HL from Scheme 15 was treated with iron(II) acetate in fluorobenzene under aerobic conditions to give the racemic μ_3-O^{2-}-centered mixed-valent complex $[Fe^{II}Fe^{III}_2O(L)_3(OAc)_3]$ (**40**),[26b,c] whereas iron(II) acetate in chloroform under aerobic conditions led to the racemic homovalent oxo-bridged dimer $[\{Fe^{III}_3O(L)_2(OAc)_4\}_2O]$ (**41**; Scheme 16).[26a,b] Notably, the metal/ligand/co-ligand ratio $(Fe/(L)^-/(OAc)^-)$ in mixed-valent **40** is 1:1:1, whereas the ratio in homovalent **41** is 3:2:4.

As there were no single crystals of **40** suitable for an X-ray structure analysis, **40** was transformed by exchange of the $(OAc)^-$ co-ligands with $(OBz)^-$ ions into $[Fe^{II}Fe^{III}_2O(L)_3(OBz)_3]$ (**42**). According to its crystal structure, benzoate **42** is

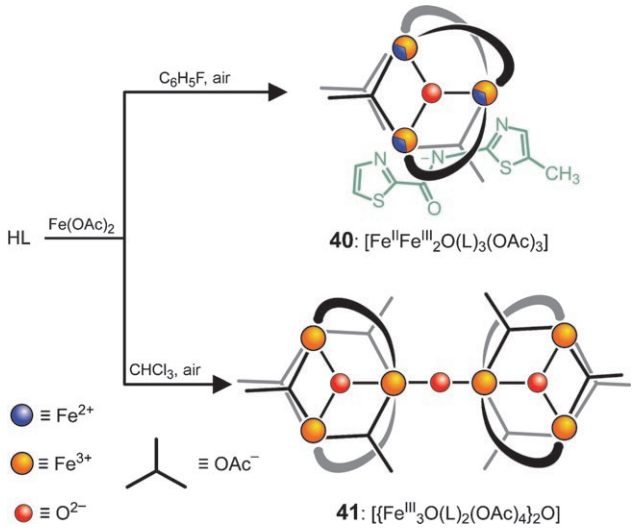

Scheme 16. Synthesis and schematic presentation of **40** and **41**.

made up of three ditopic, tridentate ligands $(L)^-$ and three bridging benzoate co-ligands, which fix the three ions ($Fe^{II}Fe^{III}_2$) in the corners of a triangle with a μ_3-O^{2-} ion in the center. All three iron ions in mixed-valent complex $[Fe^{II}Fe^{III}_2O(L)_3(OBz)_3]$ are differently octahedrally coordinated and statistically distributed over the different sites, as demonstrated by Mössbauer spectroscopy (Figure 24).

Dimer $[\{Fe^{III}_3O(L)_2(OAc)_4\}_2O]$ (**41**) is composed of two $\{Fe^{III}_3O(L)_2(OAc)_4\}^+$ fragments linked by a μ_2-O^{2-} oxo bridge. Each of these two building blocks represents an isosceles triangle with three Fe^{III} ions located in the corners and a μ_3-O^{2-} ion in the center. All iron(III) ions are octahedrally coordinated (Figure 25).[26a]

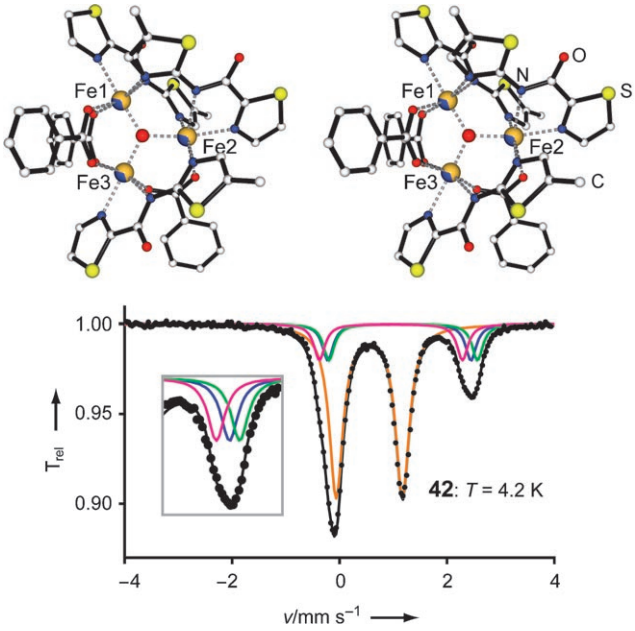

Figure 24. Top: Stereo presentation of the structure of μ_3-oxo-centered **42** in the crystal. Bottom: Mössbauer spectrum of **42** (experiment black dots; simulation black line; Fe^{II} magenta, blue, green; Fe^{III} orange); inset: enlargement of the band near 2.4 mm s^{-1}.

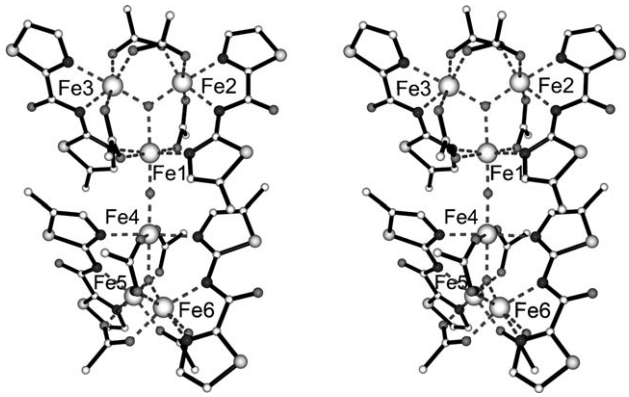

Figure 25. Stereo presentation of the structure of oxo-bridged dimer **41** in the crystal.

To generate heteronuclear species, mixed-valent iron complex $[Fe^{II}Fe^{III}_2O(L)_3(OAc)_3]$ (**40**) was reacted with nickel(II) acetate in chloroform to give the mixed-valent, heterotrinuclear complex $[Ni^{II}Fe^{III}_2O(L)_3(OAc)_3]$ (**43**; Scheme 17).[26b,c] Complex **43** was further subjected to co-ligand exchange with sodium benzoate and transformed into

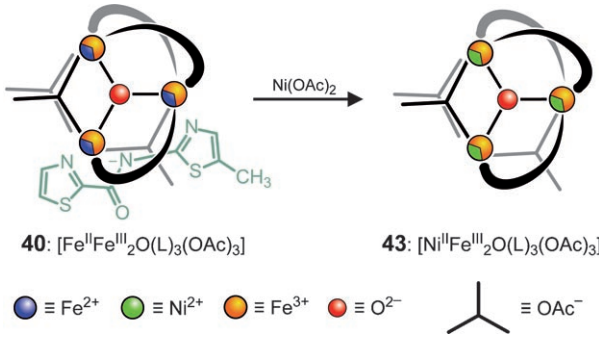

Scheme 17. Synthesis and schematic presentation of **43**.

$[Ni^{II}Fe^{III}_2O(L)_3(OBz)_3]$ (**44**), which is isostructural with $[Fe^{II}Fe^{III}_2O(L)_3(OBz)_3]$ (**42**). The reversible CV of redox-active $[Fe^{II}Fe^{III}_2O(L)_3(OAc)_3]$ **40** displayed two processes attributed to the reduction of **40** from $Fe^{II}Fe^{III}_2$ to $Fe^{II}_2Fe^{III}$ and oxidation to the all-Fe^{III} species. Consequently, the CVs of redox-active **43** and **44** represent the reduction of $Ni^{II}Fe^{III}_2$ to $Ni^{II}Fe^{II}Fe^{III}$ and reoxidation to $Ni^{II}Fe^{III}_2$. The mixed-valent character of the asymmetrically substituted complexes **40**, **42**–**44** was further established by Mössbauer spectroscopy. The Mössbauer spectra of **40** and **42** at room temperature are almost identical, and both exhibit two quadrupole doublets with an area ratio of 1:2 for the high-spin Fe^{II} and two Fe^{III} ions. On the other hand, for **42** at 4.2 K slow electron exchange leads to almost equal population within the three differently substituted iron sites in **42**, resulting in three separated quadrupole doublets for the Fe^{II} species (Figure 24). The heteronuclear complexes **43** and **44** displayed only one quadrupole doublet with a quadrupole splitting and isomeric shift corresponding to high-spin Fe^{III} ions.[26b,c]

5. Tetrahemispheraplexes of Octahedrally Coordinating Metal(II) Ions with Exohedral Guests

With completely different goals in mind,[4] we tried to doubly deprotonate dialkyl malonates with methyl Grignard or methyllithium. After addition of magnesium chloride and oxalyl chloride and subsequent workup with aqueous ammonium chloride or alkylammonium chloride solutions, tetraammonium tetramagnesium chelate complexes $[(R^2NH_3)_4\cap\{Mg_4(L^{1,2})_6\}]$ (**45**) were isolated.[3,27] The ditopic, bis(bidentate) ligands $(L^{1,2})^{2-}$ are obtained by C–C coupling of two dialkyl malonate monoanions with oxalyl chloride and spontaneous deprotonation of the bis(enol) intermediates (Scheme 18). Simple replacement of magnesium chloride by the chlorides of divalent transition metals allows the syntheses of the corresponding tetranuclear complexes $[(NH_4)_4\cap\{M_4(L^{1,2})_6\}]$ ($M = Mn^{2+}$, Co^{2+}, Ni^{2+}, Zn^{2+}).[9,27a,c]

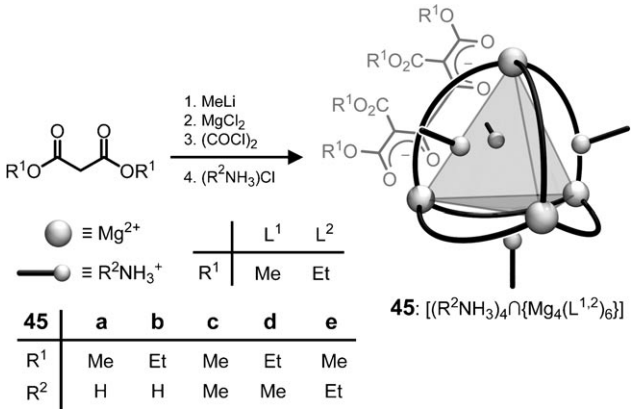

R¹	L¹	L²
Me	Me	Et

45	a	b	c	d	e
R¹	Me	Et	Me	Et	Me
R²	H	H	Me	Me	Et

Scheme 18. Synthesis (direct method) and schematic presentation of **45**.

To tune the physical and chemical properties of $[(NH_4)_4\cap\{Mg_4(L^{1,2})_6\}]$ (**45a**), the direct method described in the preceding paragraph was extended by the exchange method (Scheme 19).[27b] Addition of an excess of *n*-alkylamines leads to replacement of the ammonium ions in **45a** with *n*-alkylammonium ions to form the tetrakis(alkylammonium) tetrahemispheraplexes $[(R^3NH_3)_4\cap\{Mg_4(L^1)_6\}]$ (**46**) or $[(NH_4)_2(p\text{-}MeOC_6H_4CH_2NH_3)_2\cap\{Mg_4(L^1)_6\}]$ (**47**).

Exchange of the four ammonium ions in $[(NH_4)_4\cap\{Mg_4(L^2)_6\}]$ (**45b**) by alkali-metal cations is achieved by stirring a solution of **45b** with potassium or cesium hydroxide to give the tetra-alkali-metal tetramagnesium chelate complexes $[M_4\cap(H_2O\subset\{Mg_4(L^2)_6\})]$ ($M = K^+$, Cs^+) with an extra endohedrally encapsulated water molecule.[27b] When **45b** is stirred in solution with an excess of cobalt(II) chloride for several hours, the magnesium(II) ions are exchanged for cobalt(II) ions. Furthermore, the study presented above reveals that the space available at the surface of the tetrahedral, tetraanionic cores $\{Mg_4(L^{1,2})_6\}^{4-}$ depends on the steric demand of the ligands $(L^{1,2})^{2-}$, forcing the formation of **47** or $[Na(EtNH_3)_3\cap\{Mg_4(L^2)_6\}]$.[27b]

All the tetrahedral complexes are formed as racemic mixtures with either (Δ,Δ,Δ,Δ)-*fac* or (Λ,Λ,Λ,Λ)-*fac* configurations at the stereogenic metal centers. Since the complexes **45**–**47** are basically isostructural, only the solid-state structure of **47** will be discussed as an example. The $\{Mg_4(L^1)_6\}^{4-}$ core of **47** is a distorted tetrahedron composed of four magnesium(II) ions, which are linked along each of the six edges by the bis(bidentate) ligands $(L^1)^{2-}$, so that each of the four magnesium(II) ions is octahedrally coordinated. Charge compensation of the tetraanionic core $(\mathbf{47})^{4-}$ to give $[(NH_4)_2(p\text{-}MeOC_6H_4CH_2NH_3)_2\cap\{Mg_4(L^1)_6\}]$ (**47**) is achieved by two ammonium and two *p*-methoxybenzylammonium counterions, which are each hydrogen-bonded to three oxygen donors of the ligands at the triangular faces (Figure 26).

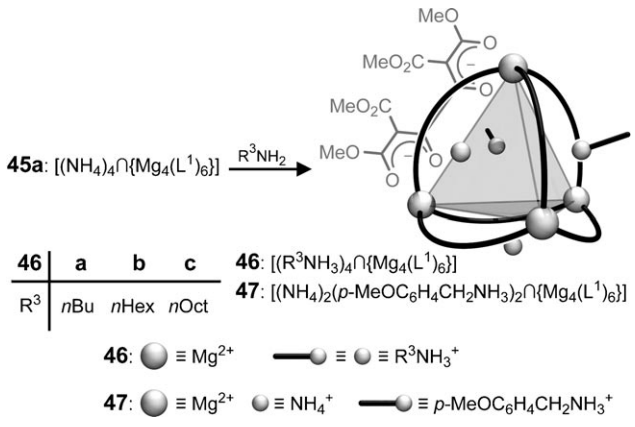

46	a	b	c
R³	*n*Bu	*n*Hex	*n*Oct

Scheme 19. Synthesis (exchange method) and schematic presentation of **46** and **47**.

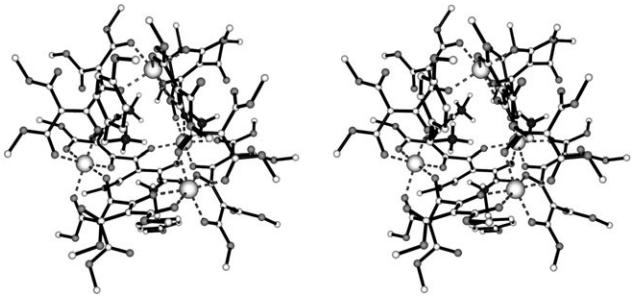

Figure 26. Stereo presentation of the structure of (Λ,Λ,Λ,Λ)-*fac*-**47** in the crystal.

6. Enantiomerization of Tetrahedral Homochiral $[(RNH_3)_4\cap\{Mg_4(L)_6\}]$ Complexes

The tetranuclear chelate complex $[(NH_4)_4\cap\{Mg_4(L^1)_6\}]$ (**45b**) is formed by the direct method from diethyl malonate (Section 5), while $[(NH_4)_4\cap\{Mg_4(L^2)_6\}]$ (**48**)[6b] and $[(EtNH_3)_4\cap\{Mg_4(L^2)_6\}]$ (**49**) are generated from diethyl ketipinate.[28] The most striking difference between $(L^1)^{2-}$ and $(L^2)^{2-}$ is the fact that $(L^2)^{2-}$ lacks two bulky ester groups (Scheme 20).

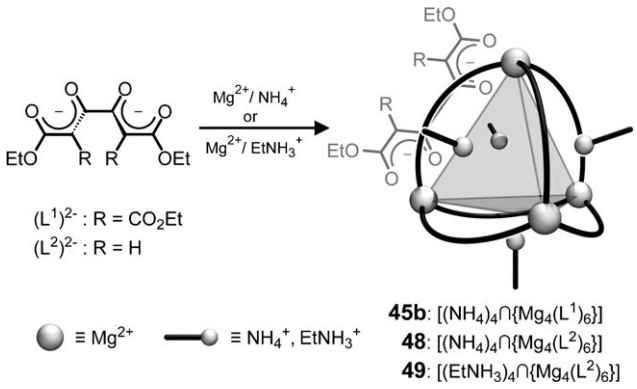

Scheme 20. Synthesis and schematic presentation of **45b**, **48**, and **49**.

Temperature-dependent ^{1}H NMR spectroscopy studies showed homochiral, racemic $(\Delta,\Delta,\Delta,\Delta)/(\Lambda,\Lambda,\Lambda,\Lambda)$-$[(NH_4)_4\cap\{Mg_4(L^1)_6\}]$ (**45b**) to be kinetically stable on the NMR timescale. Owing to steric hindrance, rotation around the central C–C bond in $(L^1)^{2-}$ is blocked, which prevents **45b** from enantiomerization. Surprisingly, the ^{1}H NMR spectrum of racemic **48** reveals dynamic temperature dependence. This phenomenon can be explained by simultaneous Bailar twists at the four octahedrally coordinated magnesium centers synchronized with sterically unhindered atropenantiomerization processes around the C–C single bonds of the six ligands $(L^2)^{2-}$, leading to the unprecedented enantiomerization $(\Delta,\Delta,\Delta,\Delta)$-(**48**)⇄$(\Lambda,\Lambda,\Lambda,\Lambda)$-(**48**). This profound, non-dissociative transformation can be monitored by NMR spectroscopy, which reflects the enantiotopization of the diastereotopic methylene protons.[11j,29] Supplementary support for the interpretation of the temperature-dependent dynamic ^{1}H NMR spectra of **48** is presented by additional studies of $(\Delta,\Delta,\Delta,\Delta)/(\Lambda,\Lambda,\Lambda,\Lambda)$-$[(EtNH_3)_4\cap\{Mg_4(L^2)_6\}]$ (**49**). In **48** and **49**, the methylene protons of the ligands exhibit identical variable-temperature (VT) NMR spectra. Moreover, the diastereotopic methylene protons of the ethyl ammonium counterions of **49** display similar temperature-dependent coalescence as the ligand vinylether methylene protons (Figure 27).

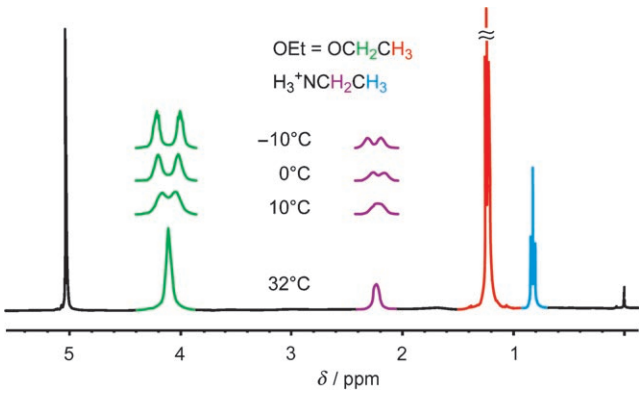

Figure 27. Variable-temperature ^{1}H NMR spectrum of **49**.

7. Homovalent and Mixed-Valent Tetranuclear Iron Chelate Complexes $[M\subset\{Fe^{II}{}_nFe^{III}{}_{4-n}(L)_6\}]^{0\pm}$ as Endoreceptors

The neutral mixed-valent complexes $[M\subset\{Fe^{II}Fe^{III}{}_3(L)_6\}]$ (**50**) are available according to the direct method in a one-pot reaction from dialkyl malonates with methyllithium, iron(II) chloride, and oxalyl chloride ($FeCl_2/(COCl)_2 = 20{:}1$) with subsequent aerobic aqueous ammonium chloride or alkali-metal chloride workup (Scheme 21).[30]

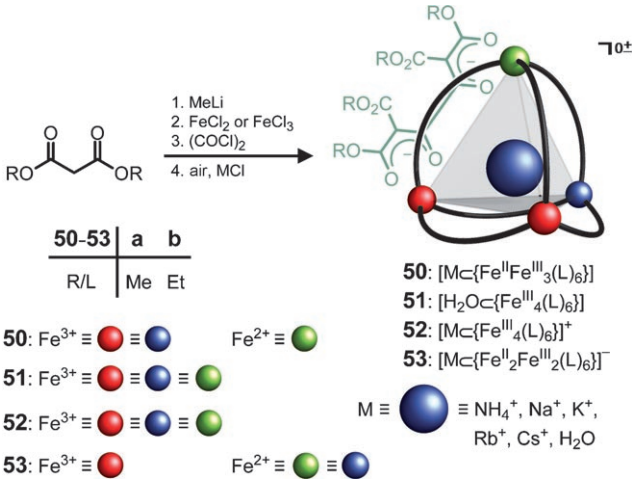

Scheme 21. Synthesis and schematic presentation of **50**–**53**.

However, when aqueous solutions of tetramethylammonium chloride, lithium chloride, or alkaline-earth-metal chlorides were used, aerobic workup afforded the all-iron(III) complexes $[H_2O\subset\{Fe^{III}{}_4(L)_6\}]$ (**51**). Accordingly, $[NH_4\subset\{Fe^{III}{}_4(L)_6\}]^+$ (NH_4-**52**) was synthesized directly, starting with iron(III) chloride and followed by workup with an aqueous solution of ammonium acetate instead of ammonium chloride. Furthermore, the all-iron(III) complexe cations $[K\subset\{Fe^{III}{}_4(L)_6\}]^+$ (K-**52**) and $[Cs\subset\{Fe^{III}{}_4(L)_6\}]^+$ (Cs-**52**) are accessible from **51** by simple exchange of the encapsulated water molecule for the corresponding alkali metal ions. Finally, the mixed-valent complex anion $[NH_4\subset\{Fe^{II}{}_2Fe^{III}{}_2(L)_6\}]^-$ (NH_4-**53**) is available from dialkyl malonates with methyllithium, iron(II) chloride, and oxalyl chloride ($FeCl_2/(COCl)_2 = 1.5{:}1$) after rapid aerobic workup with an aqueous ammonium chloride solution (Scheme 21).[30] The mixed-valent or all-iron(III) nature of Cs-**50b**, Cs-**52b**, K-**52b**, and NH_4-**53b** was determined by Mössbauer spectroscopy.[31] The complexes **50**–**53** are formed as racemic mixtures and are basically isostructural, with $(\Delta,\Delta,\Delta,\Delta)/(\Lambda,\Lambda,\Lambda,\Lambda)$-configuration at the octahedrally coordinated iron centers; the complexes have approximately *T* molecular symmetry. The four iron centers are located in the apices of a tetrahedron with water or cations encapsulated in the center, and the six edges are bridged by the doubly negatively charged, ditopic, tetradentate chelate ligands. Figure 28 displays the X-ray structure of $[NH_4\subset\{Fe^{II}Fe^{III}{}_3(L)_6\}]$ (NH_4-**50a**).

To enlarge the size of the cavity of the tetrahedral complexes mentioned so far, 4,4′-phenylene and 4,4′-biphen-

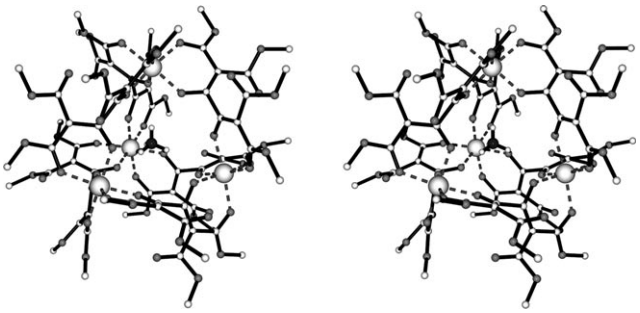

Figure 28. Stereo presentation of the structure of (Δ,Δ,Δ,Δ)-(NH_4-**50a**) in the crystal. Fe light gray (large).

ylene spacers were introduced. For instance, when tetramethyl terephthaloyldimalonate was deprotonated with sodium hydride and the doubly negatively charged ditopic, tetradentate ligand $(L^{phen})^{2-}$ treated with iron(III) chloride, complex $[Fe_4(L^{phen})_6]$ with an empty cavity was isolated. In contrast to racemic (Δ,Δ,Δ,Δ)/(Λ,Λ,Λ,Λ)-**50**–**53**, complex (Δ,Δ,Λ,Λ)-$[Fe_4(L^{phen})_6]$ is achiral (*meso*-form) and has S_4 molecular symmetry in the crystal.[32]

8. Tripodal Tris(Bidentate) Chelators: Synthesis of Tetrahedral and Trigonal Antiprismatic Complexes

8.1. Benzene as Center of Tripodal Ligands

Compared with the *T*-symmetric edge-bridged complexes described in Sections 5–7, there are far fewer examples of *T*-symmetric complexes in which the octahedrally coordinated metal centers in the vertices of a tetrahedron are linked by tripodal tris(bidentate) ligands that occupy the tetrahedral faces. In a one-pot reaction, the tetranuclear iron(III) chelate complex $[Fe_4(L^1)_4]$ (**54**) was generated from benzene-1,3,5-tricarboxylic acid trichloride, bis-*tert*-butyl malonate, methyllithium, and iron(II) chloride under aerobic conditions (direct method).

Alternatively, hexanuclear trigonal antiprismatic iron chelate complex $[Fe_6(L^2)_6]$ (**55**) was formed starting from bis-*para*-tolyl malonate by employing the same reaction conditions as for the synthesis of **54**. Further tetranuclear tetrahedral and hexanuclear trigonal antiprismatic complexes were generated from the tripodal benzene-1,3,5-chelators $(L^3)^{6-}$ and $(L^4)^{3-}$ (Scheme 22).[33]

The all-iron(III) nature of **54** and **55** was determined by Mössbauer spectroscopy. In $[Fe_4(L^1)_4]$ (**54**), four octahedrally coordinated iron centers constitute the apices of a tetrahedron, and the four tripodal, tris(bidentate) ligands $(L^1)^{3-}$ are centered above the triangular faces of the tetrahedron.[33a] Hence, **54** has nearly *T* molecular symmetry, and the crystals are composed as racemic mixtures of homoconfigurational (Δ,Δ,Δ,Δ)/(Λ,Λ,Λ,Λ)-*fac* stereoisomers. There is no evidence that the cavity of the tetrahedron hosts a guest (Figure 29), as observed in other cases (Sections 7 and 8.2).[34]

Complex $[Fe_6(L^2)_6]$ (**55**) can be described as having idealized D_3 molecular symmetry. The iron centers define

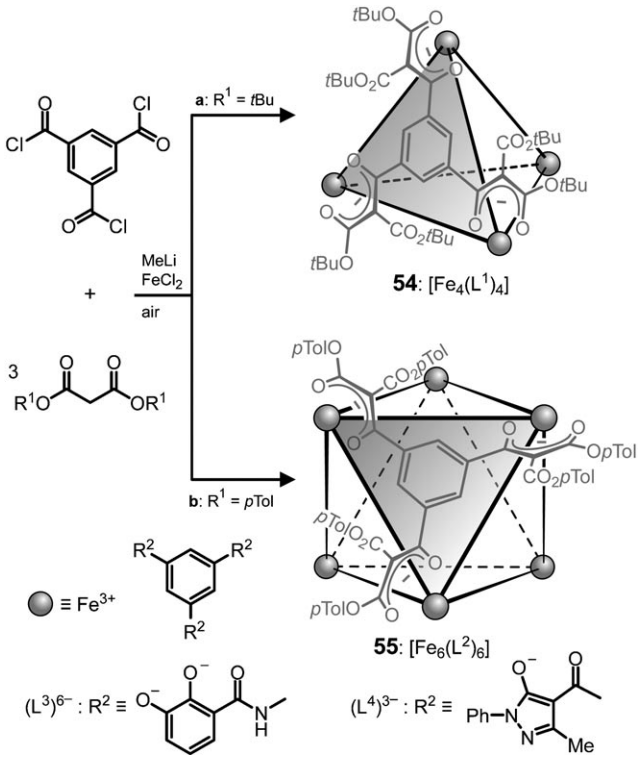

Scheme 22. Synthesis and schematic presentation of **54** and **55**. *p*Tol = *para*-tolyl

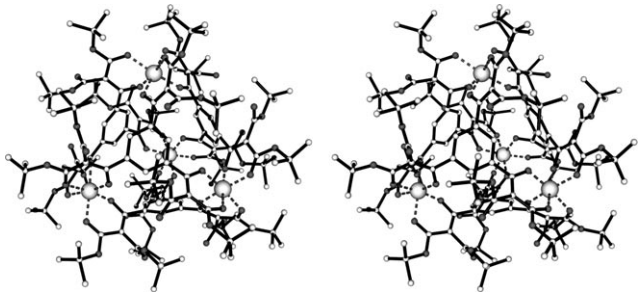

Figure 29. Stereo presentation of the structure of (Δ,Δ,Δ,Δ)-**54** in the crystal.

the apices of a distorted trigonal antiprism in which six tripodal, tris(bidentate) ligands $(L^2)^{3-}$ make up the equatorial faces, leaving the top and bottom triangles unoccupied. All six iron(III) ions are identically octahedrally coordinated, and **55**

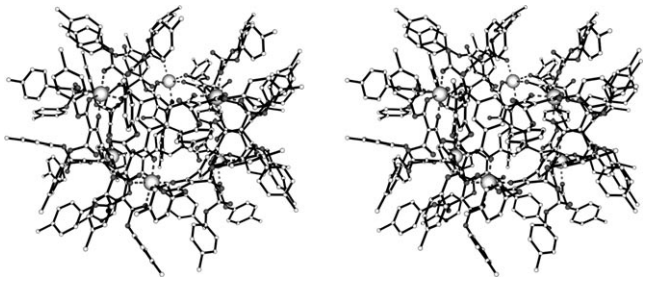

Figure 30. Stereo presentation of the structure of (Δ,Δ,Δ,Δ,Δ,Δ)-**55** in the crystal.

exists as a racemic mixture of homoconfigurational (Δ,Δ,Δ,Δ,Δ,Δ)/(Λ,Λ,Λ,Λ,Λ,Λ)-*fac* stereoisomers (Figure 30).

8.2. Nitrogen as the Center of a Tripodal Ligand

In earlier work, threefold symmetric tris(5,5-dimethyl-2,4-dioxohexyl)amine H_3L was shown to readily isomerize in a domino cascade (aldol addition/hemiketal formation/hemiketal formation/epimerization) to dioxaazaadamantane **56** when treated with a catalytic amount of methanolic potassium hydroxide.[35] Furthermore, N-centered tripodal heptadentate ligand $(L)^{3-}$ should be suitable for complexation and bridging of appropriate metal ions, leading to oligonuclear aggregates. Therefore, when H_3L was treated with cesium carbonate and indium(III) perchlorate, pentanuclear host–guest complex $[Cs\subset\{In_4(L)_4\}]ClO_4$ (**57**) was isolated. When the experiment was repeated in absence of an alkali base, the N-protonated tetranuclear In^{III} complex $[In_4(H^NL)_4](ClO_4)_4$ (**58**) was obtained. However, reaction of indium(III) perchlorate and H_3L with subsequent addition of triethylamine afforded the neutral tetranuclear complex $[In_4(L)_4]$ (**59**). Complex **59** was also prepared simply by deprotonation of **58** with triethylamine (Scheme 23).[34,36]

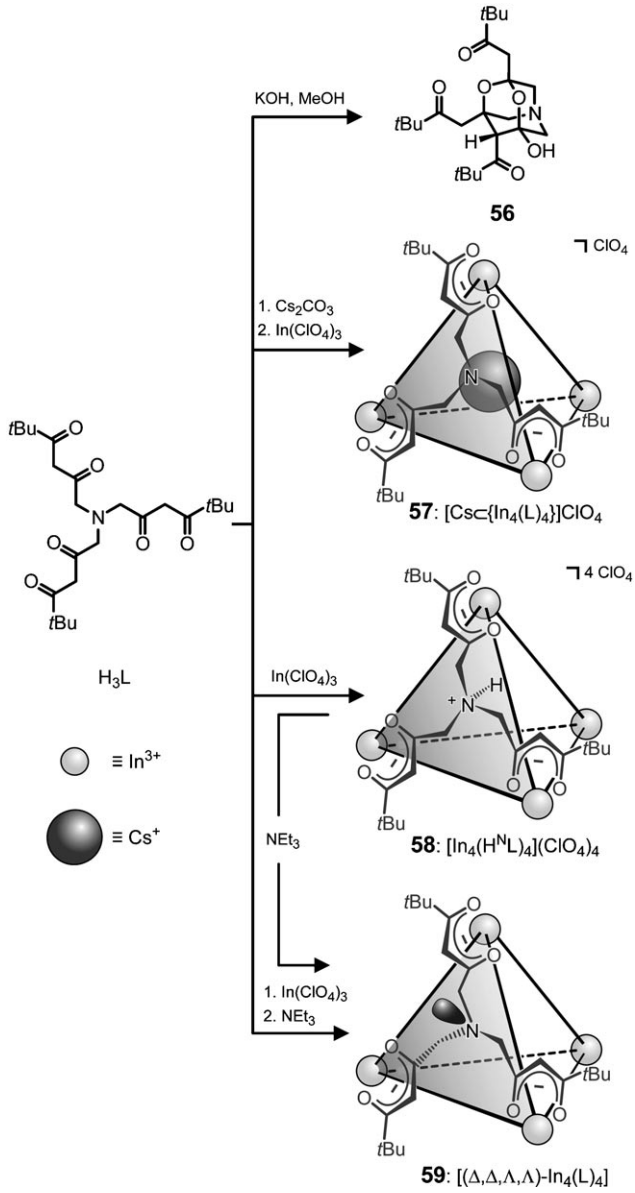

Scheme 23. Isomerization of tripodal H_3L to give heteroadamantane **56** and synthesis and schematic presentation of **57**–**59**.

The composition of the compounds **57**–**59** results from charge-balance calculations, mass spectrometry, and elemental analyses. The structure determination of **57**–**59** was accomplished by ^1H and ^{13}C NMR spectroscopy. In racemic, homochiral (Δ,Δ,Δ,Δ)/(Λ,Λ,Λ,Λ)-*fac* **57** and **58**, four indium ions constitute the apices of a tetrahedron, and the four tripodal ligands $(L^1)^{3-}$ are centered above the triangular faces of the tetrahedron. Hence, **57** and **58** have nearly *T* symmetry, with the indium ions octahedrally coordinated by six oxygen donors; there is a cesium ion or four protons at the nitrogen atoms in the cavity of the tetrahedron. Single crystal X-ray diffraction was used to confirm unequivocally the tetrahedral geometry of **57**–**59** (Figure 31).[36] At first glance, **59** had a

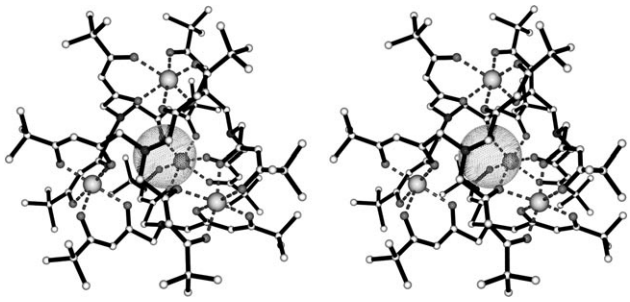

Figure 31. Stereo presentation of the structure of cation of (Δ,Δ,Δ,Δ)-**57** in the crystal.

confusing ^1H NMR spectrum for a high-symmetry molecule. Whereas in the complexes **57** and **58** with *T* molecular symmetry, all four ligands are equivalent, a tripling of the signals was observed in both the ^1H and ^{13}C NMR spectra of **59**. This result implies that the C_3 symmetry of the ligands is broken during deprotonation of **58**. According to the X-ray structure, (Δ,Δ,Λ,Λ)-$[In_4(L)_4]$ (**59**) has idealized S_4 molecular symmetry, and the indium ions have a distorted octahedral coordination sphere with alternative Δ or Λ configuration. Most interestingly, the driving force to break the symmetry of the C_3-symmetrical N-centered ligands $(L)^{3-}$ during deprotonation of $[In_4(H^NL)_4](ClO_4)_4$ (**58**) to give **59** is the repulsive power of the lone pairs at nitrogen of the N-centered ligands, which are displaced from the interior in **57** and **58** to the surface in **59**.

9. Template-Mediated Self-Assembly of Ferric Wheels with Ethanolamines

9.1. Six- and Eight-Membered Iron Coronates with Triethanolamine

Aside from the use of bis(bidentate) ditopic ligands, by which tetranuclear iron chelate complexes of type

$[M\subset\{Fe^{II}Fe^{III}_3(L)_6\}]$ (**50**) are available (Section 7), the precapping[37] of iron ions by a tripodal, tridentate, monotopic co-ligand and subsequent linkage of these building blocks by bidentate ditopic ligands should also lead to similar tetrahedral complexes. Along these lines, Huttner and co-workers[38] achieved tetrahedral host–guest complex $[\{H_3CC(CH_2PPh_2)_3Fe\}_4(NC(CH_2)_2CN)_6\subset(BF_4)]^{7+}$ by reacting triphos caps, iron(II) ions, fumaronitrile ligands, and tetrafluoroborate ions.

When we chose triethanolamine H_3L (Scheme 24) as the tridentate capping co-ligand, we did not consider that it acts, in fact, as a tetradentate ligand. Therefore, when triethanolamine was reacted with sodium hydride, iron(III) chloride, and fumaronitrile, contrary to the expected tetranuclear iron chelate complex $[\{(L)Fe\}_4(NC(CH_2)_2CN)_6\subset(Cl)]^-$, a yellow solid material was isolated that did not contain any dinitrile. Therefore, when the experiment was repeated without the addition of fumaronitrile, an identical material was isolated, which proved to be $[Na\subset\{Fe_6(L)_6\}]Cl$ (**60**) (Scheme 24).[39]

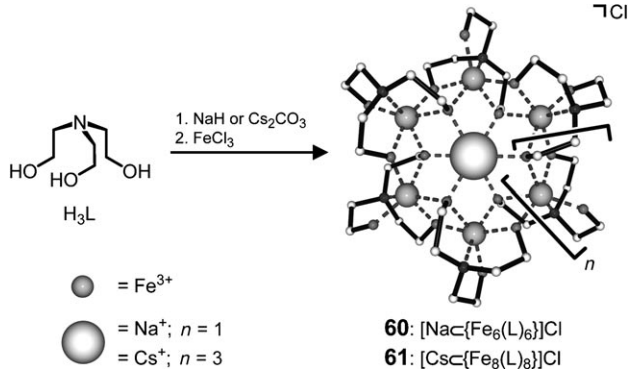

Scheme 24. Synthesis and schematic presentation of **60** and **61**.

According to Lehn et al.,[22d] amidst a set of possibilities in the template-mediated self-assembly of a supramolecular system, the one combination of building blocks is realized that leads to the best receptor for the substrate. Therefore, the six-membered cyclic structure **60** is exclusively selected from all the possible iron triethoxyamine oligomers when sodium ions are present. In the presence of cations with different ionic radii, different structures are expected. Consequently, when triethanolamine H_3L was reacted with cesium carbonate and iron(III) chloride, the octanuclear centrosymmetric ferric wheel $[Cs\subset\{Fe_8(L)_8\}]Cl$ (**61**) was isolated (Scheme 24).[39]

In the crystal, $[Na\subset\{Fe_6(L)_6\}]Cl$ (**60**) is present as an S_6-symmetric cyclic iron(III) complex with an encapsulated sodium ion in the center and a chloride counterion. The six crystallographically equivalent iron centers of the centrosymmetric cation $[Na\{Fe_6(L)_6\}]^+$ are located in the corners of a regular hexagon and are octahedrally coordinated. Consequently, the triethoxyamine trianions act as tetradentate, tetratopic chelating ligand, which each link three iron(III) ions and one sodium ion (Figure 32).

At low temperatures, the magnetization of $[Na\subset\{F_6(L)_6\}]Cl$ (**60**) exhibits a step at a critical field B_c, arising from a field-induced level crossing. By means of high-field torque magnetometry, a hysteretic behavior was observed at the level crossing with a characteristic butterfly shape, which is analyzed in terms of a dissipative two-level model. It has been demonstrated that **60** allows cooling by adiabatic demagnetization as well as by adiabatic magnetization.[40]

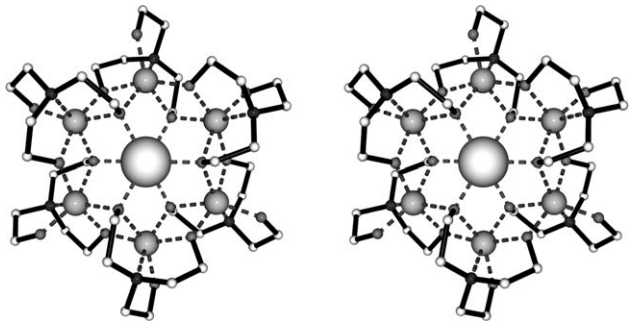

Figure 32. Stereo presentation of cation of **60** in the crystal.

9.2. Six-Membered Iron Coronands with N-Substituted Diethanolamines

A common feature of the complexes $[Na\subset\{Fe_6(L)_6\}]Cl$ (**60**) and $[Cs\subset\{Fe_8(L)_8\}]Cl$ (**61**; Section 9.1) is that the μ_1-O^- ethoxide donors do not participate in the formation of these ferric wheels. They function solely as ligands for the coordinative saturation of the iron centers. Therefore, any monoanionic donor, such as a chloride ion, could also be a candidate for this function. As expected, reaction of *N*-alkyldiethanolamines H_2L with calcium hydride and iron(III) chloride yielded the neutral iron coronands $[Fe_6Cl_6(L)_6]$ (**62**) with unoccupied centers (Scheme 25).[41]

To prepare single crystals suitable for X-ray analysis, some of the chloro complexes $[Fe_6Cl_6(L)_6]$ (**62**) were transformed with thiocyanate ions to give the corresponding thiocyanate complexes $[Fe_6(SCN)_6(L)_6]$ (**63**). In principle, all the six-membered ferric wheels **62** and **63** are isostructural and have idealized S_6 molecular symmetry. However, there are fundamental differences concerning their crystal packing. The ferric wheels **62a–d**,**f**,**g** and **63a**,**b** crystallize in the space group $R\bar{3}$ and **62e** in the space group $P\bar{3}$. The crystal packing of the ferric wheels **62a–f** and **63a**,**b** is essentially the same. For example, all the disk-like molecules of **62a** are arranged in parallel and are piled in cylindrical columns, with all the iron centers superimposed. Each column is surrounded by six parallel columns, which are alternately dislocated by $^1/_3\,c$ and $^2/_3\,c$ against the central one (Figure 33).

An additional interesting feature of some ferric wheels is their readiness to create various superstructures, depending on the nature of their side arms. For instance, van der Waals interactions cause the side arms of **62d** and **62e** to interlock and give rise to the formation of compartments occupied by disordered chloroform. In contrast, the side arms of **63a** give rise to a ball-shaped capsule lacking further intermolecular interactions (Figure 34). An especially interesting example of crystal packing, leading to porous three-dimensional frame-

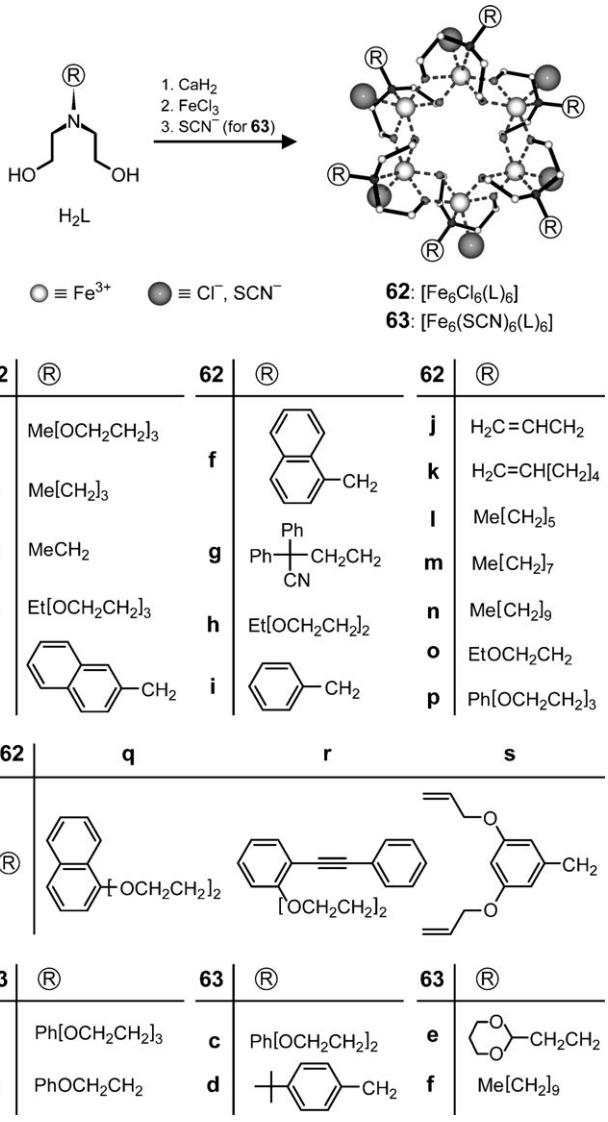

Scheme 25. Synthesis and schematic presentation of the coronands **62** and **63**.

works, is caused by π–π stacking of the naphthyl groups at the side arms of the ferric wheels **62f** (Figure 35). Unlike **62a–f** and **63a,b** the ferric wheels of **62g** are not arranged in parallel but rather are three-dimensionally perpendicular, a well-known arrangement for 3D coordination polymers (Figure 36).[42] Moreover, the crystal packings of the ferric wheels **62h,i** and **63c** are almost identical, with five wheels in the unit cell, and generally differ only by the angle between the two groups of parallel wheels (Figure 37).

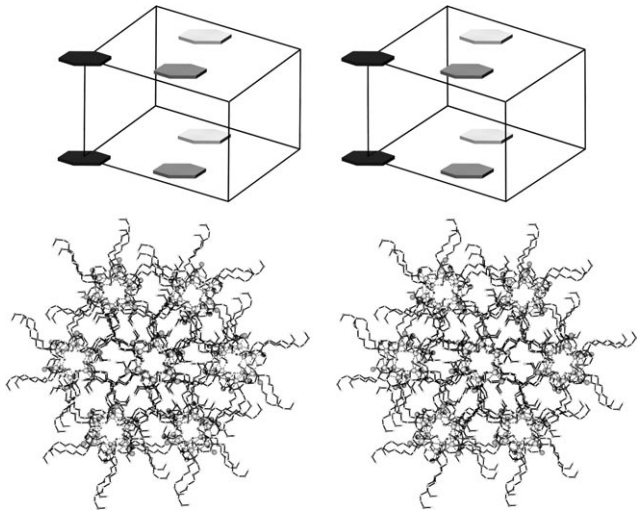

Figure 33. Top: Schematic stereo presentation of the crystal packing of **62a–f**, **63a,b**. Bottom: Stereo presentation of the crystal packing of the ferric wheel **62a**. View along the *c* axis.

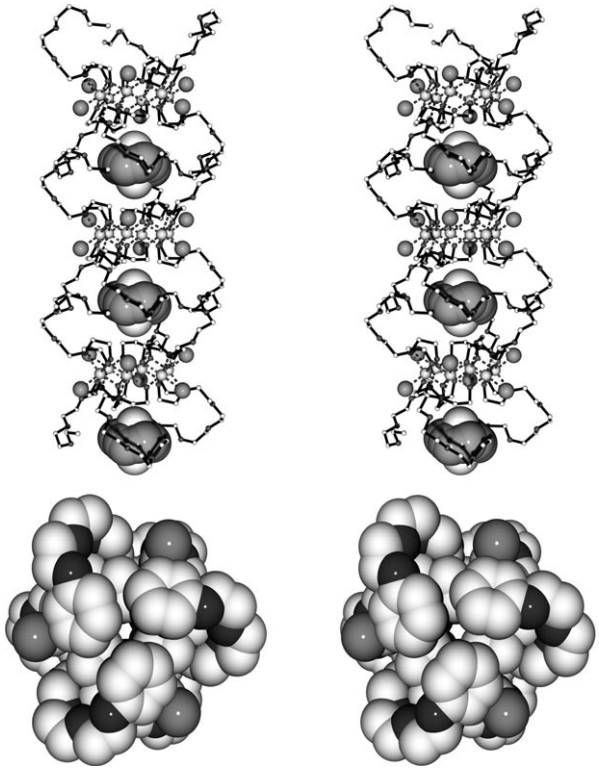

Figure 34. Top: Stereo presentation of the columnar crystal packing of **62d**, highlighting the compartments with encapsulated disordered chloroform. Bottom: Stereo presentation of a space-filling depiction of ball-shaped **63a**.

9.3. The Ferric Star: $[Fe\{Fe(L)_2\}_3]$ A Single-Molecule Magnet

To date, little is known about the mechanistic aspects of self-assembly processes.[43] To shed light on this subject, *N*-methyldiethanolamine H_2L (Scheme 26) was deprotonated with sodium hydride. Careful titration of the dianion $(L)^{2-}$ with a solution of iron(III) chloride in THF afforded a colorless suspension of intermediate $\{Fe(L)_2\}^-$, with a iron/ligand ratio of 1:2. Further addition of iron(III) chloride to this suspension up to a iron/ligand ratio of 1:1.5 resulted in the isolation of amber microcrystals of the ferric star $[Fe\{Fe(L)_2\}_3]$ (**65**). However, at an iron/ligand ratio of 1:1, the known ferric wheel $[Fe_6Cl_6(L)_6]$ (**64**) was generated as the final product. This process was shown to be reversible. As a consequence of

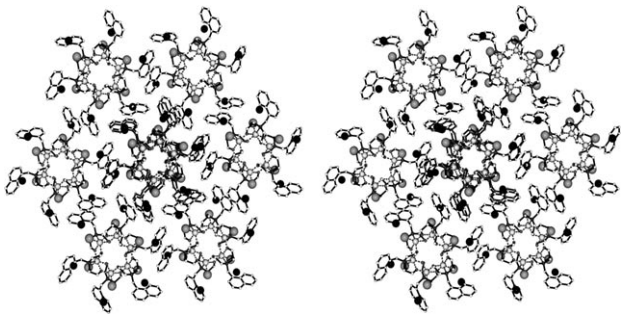

Figure 35. Stereo presentation of the crystal packing of **62 f**, highlighting the π–π interactions, together with cocrystallized water (black spheres).

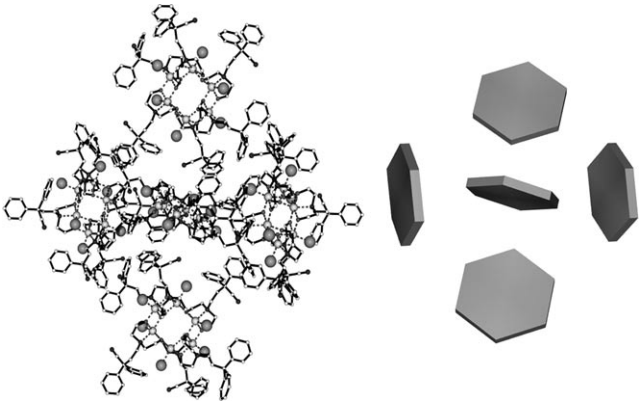

Figure 36. Left: Crystal packing of **62 g**. Right: Graphical presentation highlighting the three-dimensional perpendicular arrangement of the ferric wheels.

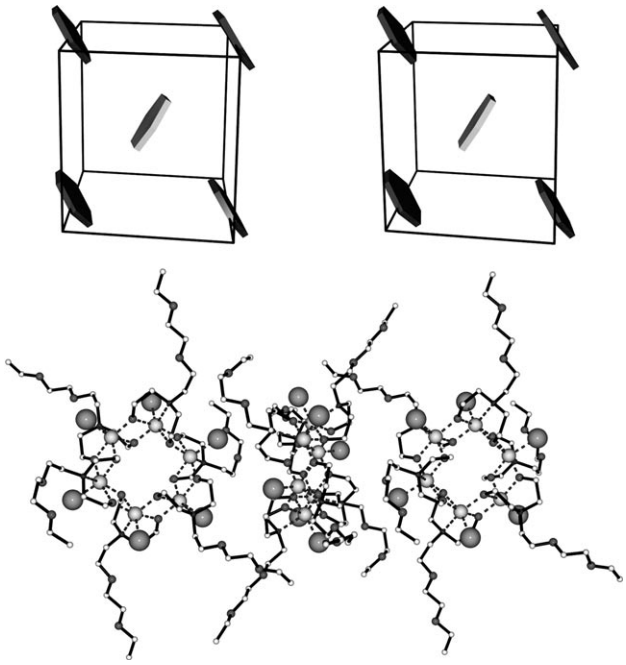

Figure 37. Top: Schematic stereo presentation of the crystal packing of **62 h**,**i** and **63 c**. Bottom: Presentation of the two orientations of **62 h** in the crystal.

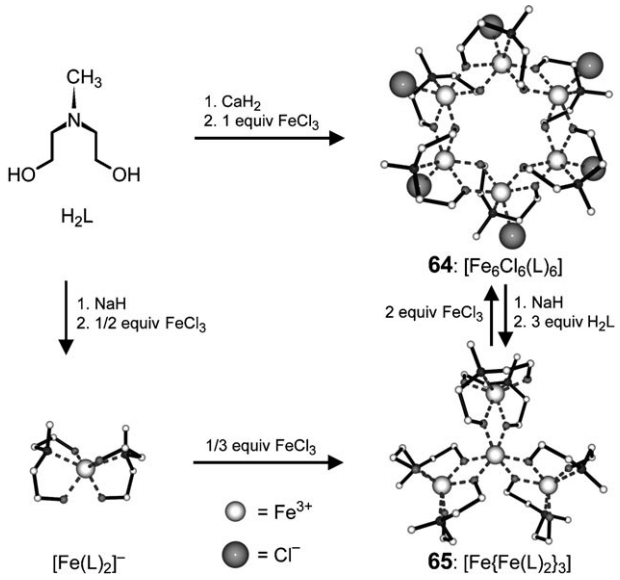

Scheme 26. Synthesis and schematic presentation of the ferric wheel **64** and the ferric star **65**, depending on the stoichiometry of Fe^{III}/H_2L.

these mechanistic studies, $[Cr\{Fe(L)_2\}_3]$ or $[Al\{Fe(L)_2\}_3]$ were isolated when intermediate $\{Fe(L)_2\}^-$ was reacted with a solution of $CrCl_3$ or $AlCl_3$.[41b]

In the racemic, star-shaped complex $[Fe\{Fe(L)_2\}_3]$ (**65**), the central iron ion is octahedrally coordinated by two μ_2-alkoxo bridges from each of the three peripheral building blocks $\{Fe(L)_2\}^-$. During the coordination of $(L)^{2-}$ to iron, the nitrogen atom becomes a stereogenic center (Figure 38).

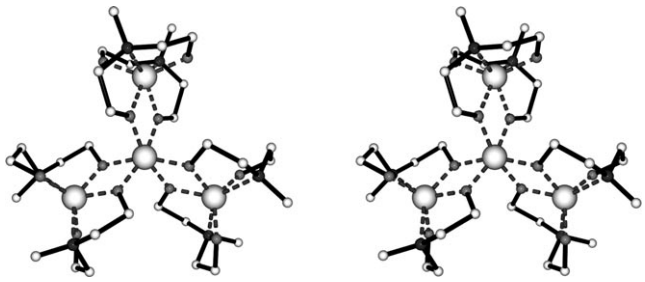

Figure 38. Stereo presentation of [Δ-(*R*,*R*)(*S*,*S*)(*S*,*S*)]-**65** in the crystal.

SQUID measurements of **65**·4 $CHCl_3$ revealed a strong antiferromagnetic intramolecular coupling $J = -30$ K, resulting in a $S = 10/2$ ground-state multiplet. Since the ground-state multiplet is energetically well-separated from the excited multiplets, the magnetic properties were described using a giant-spin Hamiltonian. The magnetization curves along the crystallographic axes show a magnetic anisotropy of the easy-axis type. Both the high-spin ground state and the easy-axis anisotropy suggest that ferric star **65** is a single-molecule magnet (SMM). Magnetization measurements using a 2DEG-Hall sensor showed hysteresis below a blocking temperature of about 1.2 K (Figure 39) that revealed the

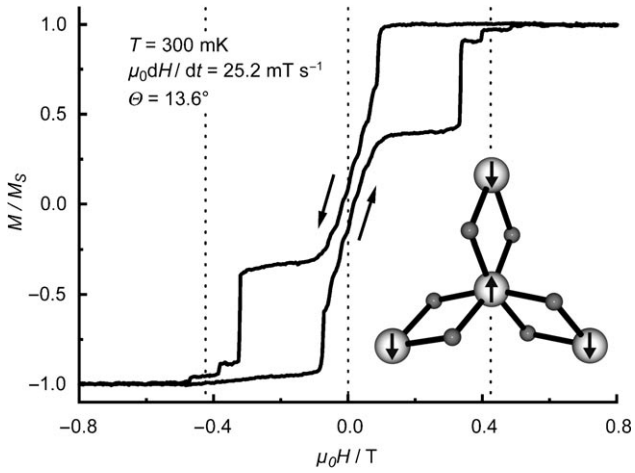

Figure 39. Hysteresis loop of a 2DEG-Hall probe magnetization measurement of **65**·4 $CHCl_3$. Level crossings are indicated by dotted lines. Inset: Magnetic coupling scheme.

typical sweep rate and temperature dependency of SMMs.[44,45]

9.4. Dynamics of Six-Membered Indium Metallodendrimers

In the reaction of the N-substituted diethanolamines H_2L^{1-3} [46] with calcium hydride and subsequent addition of iron(III) chloride or indium(III) chloride, the iron wheels $[Fe_6Cl_6(L^1)_6]$ (**66**) and $[Fe_6Cl_6(L^2)_6]$ (**67**) or indium wheels $[In_6Cl_6(L^1)_6]$ (**68**), $[In_6Cl_6(L^2)_6]$ (**69**), and $[In_6Cl_6(L^3)_6]$ (**70**) were formed in excellent yields (Scheme 27).[47]

Single crystal X-ray structure analysis found iron wheel **66** to be isostructural with the indium wheel **68**.[47] In the solid state, the N-substituted diethoxyamine ligands of S_6-**68** are desymmetrized through metal coordination. ESI mass spectroscopy demonstrated that **68** is the only species present in solution. In contrast to the paramagnetic ferric wheels **66** and **67**, the diamagnetic indium wheels **68**–**70** could be studied by NMR spectroscopy.[47] A major feature of the desymmetrized $(L^1)^{2-}$ ligands of these compounds is the diastereotopicity of the 12 ethoxide arms, established by ^{1}H NMR spectroscopy. As a result, there is a set of four distinguishable methylene groups, which, like the six N-benzylic methylene groups, exhibit characteristic AB splitting patterns for their diastereotopic methylene protons. Variable-temperature ^{1}H NMR spectroscopy studies on the enantiomerization of tetrahedral homochiral **48** and **49** (Section 6) prompted us to also study the dynamic behavior of $[In_6Cl_6(L^1)_6]$ (**68**). The high-temperature ^{1}H NMR spectra (Figure 40) indicate time-averaged pseudo D_{3d} molecular symmetry for **68**, arising from rapid, non-dissociative enantiomerization S_6-**68**$\rightleftarrows S_6$-**68′**.[48]

As shown exemplarily for the N-benzylic diastereotopic methylene protons of **68**, coalescence is observed at 130 °C. The activation parameters for the molecular enantiotopization have been derived from a line-shape analysis and verified by density functional calculations.[47] For unambiguous characterization of dendritic $[In_6Cl_6(L^2)_6]$ (**69**) and $[In_6Cl_6(L^3)_6]$ (**70**; Figure 41), ^{1}H and ^{13}C NMR spectra were recorded.

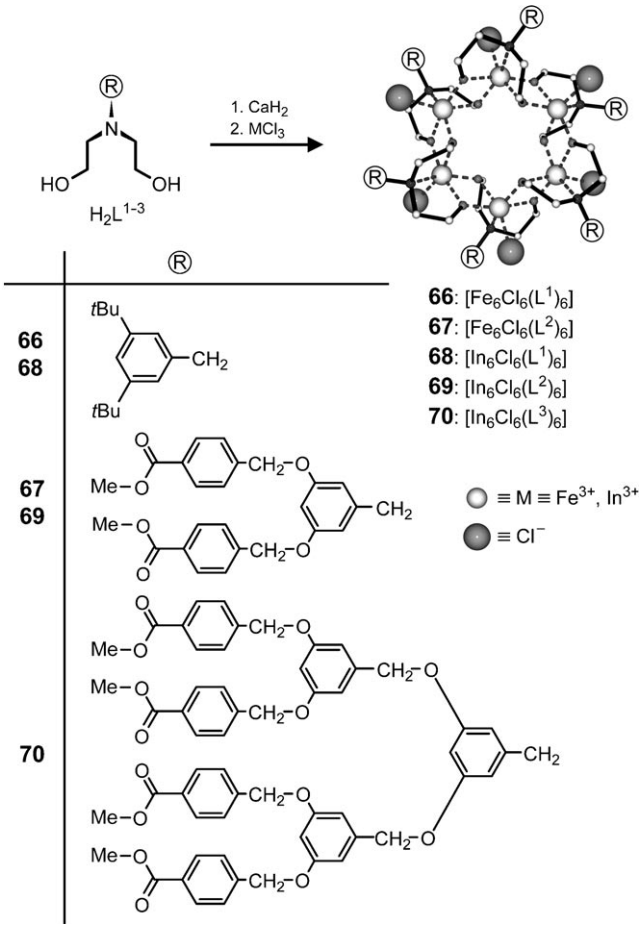

Scheme 27. Synthesis and schematic presentation of the iron wheels **66**, **67** and the indium wheels **68**–**70**.

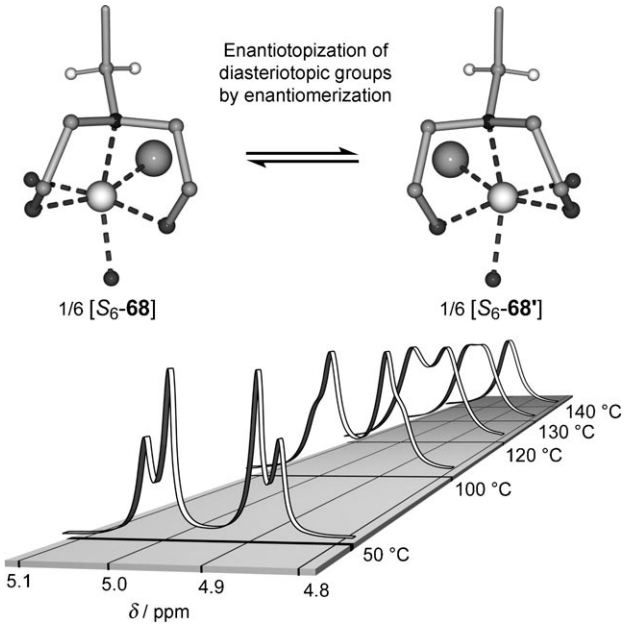

Figure 40. Top: Enantiomerization of one indium(III) center of **68** $\{^1/_6[S_6\text{-}\mathbf{68}]\rightleftarrows{}^1/_6[S_6\text{-}\mathbf{68'}]\}$. Bottom: Variable-temperature ^{1}H NMR spectroscopy signals of the enantiotopization of the diastereotopic *N*-benzylic methylene protons of **68**.

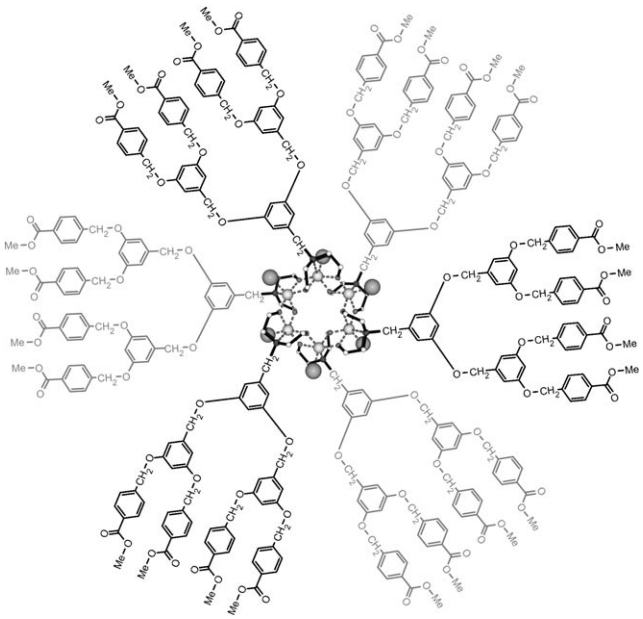

Figure 41. Presentation of the molecular formula of metallodendrimer **70**. In light gray (large), Cl gray (large).

10. Gyroscope-Shaped Copper Complexes and Heteronuclear Boxes of Copper and Cobalt: Template- and Ligand-Directed Product Formation

10.1. Gyroscope-Shaped Copper Complexes

In the six-membered iron coronands $[Fe_6X_6(L)_6]$ (**62**, **63**; Section 9.2), the μ_2-O^- ethoxide donors of the *N*-alkyldiethoxyamine ligands are structure-determining. Completion of the octahedral coordination sphere at the iron center and charge compensation is achieved by the halide or pseudohalide co-ligands. By changing from hexacoordinate iron(III) to pentacoordinate copper(II), it should be possible to synthesize neutral, unoccupied metallocrowns without the need of extra co-ligands. Consequently, reaction of the *N*-alkyldiethanolamines $H_2L^{1,2}$ (Scheme 28) with sodium hydride or lithium hydride and copper(II) bromide or copper(II) chloride yielded the complexes $[(NaBr)_2\cap\{Cu_6(L^1)_6\}]$ (**71**) and $[(LiCl)_2\cap\{Cu_6(L^2)_6\}]$ (**72**).[49]

Complexes **71** and **72** are isostructural and, therefore, only the structure of **71** is discussed here (Figure 42). The six copper centers of centrosymmetric **71** are located in the corners of a regular hexagon. Each ligand $(L^1)^{2-}$ acts as a tridentate tritopic clamp and links three copper(II) ions. The square-pyramidal coordination sphere of the Cu^{II} ions is composed of one nitrogen donor, two μ_2-oxygen donors, and two μ_3-oxygen donors. In contrast to the ferric wheel $[Na\subset\{Fe_6(L)_6\}]Cl$ (**60**) ($L = N(CH_2CH_2O^-)_3$, Section 9.1), no endohedral cation inclusion is observed for **71**. Instead, for $[(NaBr)_2\cap\{Cu_6(L^1)_6\}]$ (**71**) two sodium ions are found exohedrally bound to the outer faces of the copper wheel by three of the six μ_3-oxygens each. The tetrahedral coordination sphere of the sodium ions is completed by bromide ions, giving complex **71** the shape of a molecular gyroscope. The sodium and bromide ions are located on the molecular C_3 axis. The distance between Na^+ and Br^- is remarkably short.

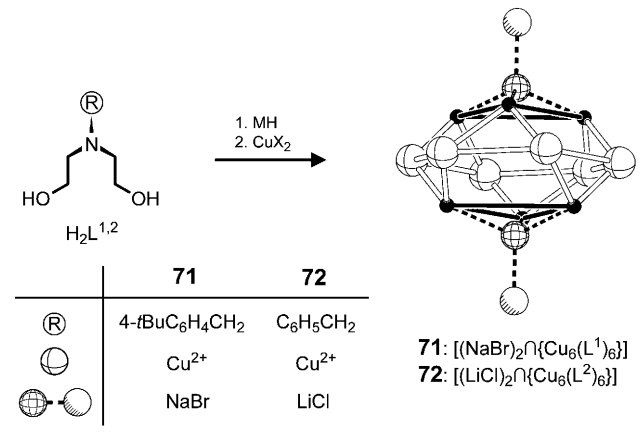

Scheme 28. Synthesis and schematic presentation of **71** and **72**. **71**: M = Na, X = Br; **72**: M = Li, X = Cl.

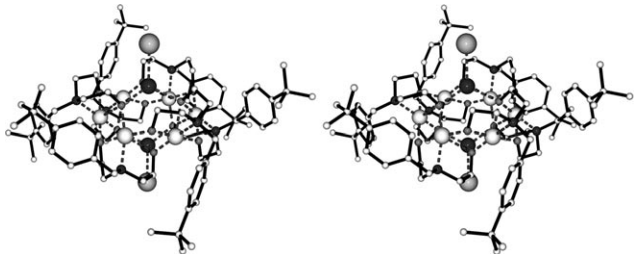

Figure 42. Stereo presentation of the copper wheel **71** in the crystal. Cu light gray (large), Br gray (large), Na black (large).

It is not necessarily the templating effect of the cations alone that determines the product, as was found when copper(II) acetate was treated with diethanolamine H_2L^3 and lithium hydride. The reaction product was identified in the solid state as the one-dimensional coordination polymer $1D\text{-}[\{Cu_4(HL^3)_4(OAc)_4\}_n]$ (**74**), built up from the self-complementary tetranuclear building blocks $[Cu_4(HL^3)_4(OAc)_4]$ (**73**) by their linkage through hydrogen bonds (Scheme 29).[49]

In module **73**, four copper centers are linked by four $(HL^3)^-$ ligands. The square-pyramidal coordination geometry at the inner and outer copper centers is completed by four acetate ligands. Generation of the ideal conformation necessary for the polymerization of the self-complementary building block **73** is assisted by additional intramolecular H-bonds. The modules **73** polymerize to $1D\text{-}[\{Cu_4(HL^3)_4(OAc)_4\}_n]$ (**74**) across NH···O···HO hydrogen bonds (Figure 43).

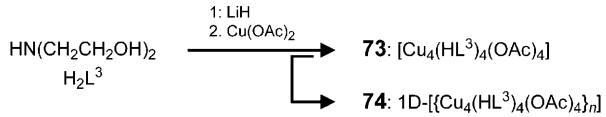

Scheme 29. Synthesis of polymeric strand **74**.

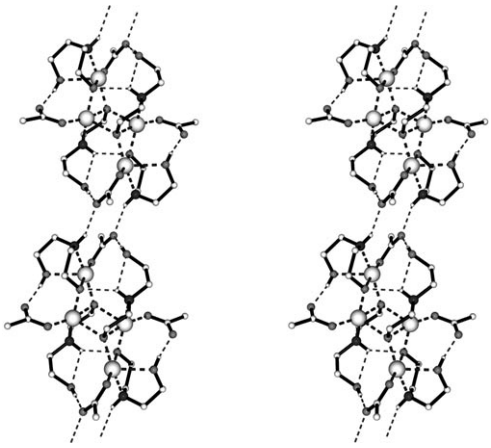

Figure 43. Stereo presentation of single-stranded 1D polymer **74** in the crystal, showing the linkage of the self-complementary building blocks **73** through hydrogen bonds. Cu gray (large), H white (small).

10.2. A Hetero-Octanuclear Molecular Box of Copper and Lithium Linked by Bis(Diethoxyamine) Ligands

When bis(diethanolamine) H_4L was allowed to react with lithium hydride and copper(II) acetate, complex $[Cu_4(L)_2(HOAc)_4]$ (**75**) was formed. In contrast, reaction of H_4L with copper(II) chloride yielded the hetero-octanuclear molecular box $[Li_4(Cu_4O)(L)_2]Cl_2$ (**76**; Scheme 30).[50]

Complex **75** is present in the crystal as the bis(bimetallic) cyclophane. Furthermore, four HOAc molecules are coordinated to the copper ions across their carbonyl oxygen donors and are associated to the μ_1-O^- donors of the ligands $(L)^{4-}$ through hydrogen bonds, as are the two dichloromethane solvent molecules (Figure 44). Although $[Li_4(Cu_4O)(L)_2]Cl_2$

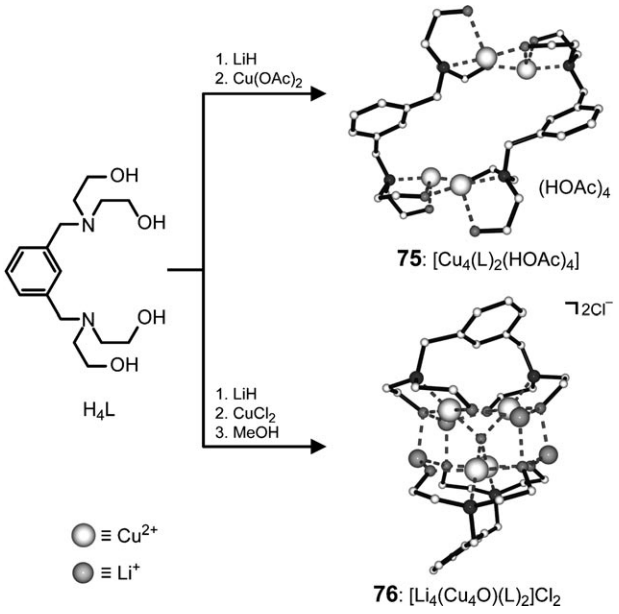

Scheme 30. Synthesis and schematic presentation of **75** and **76**.

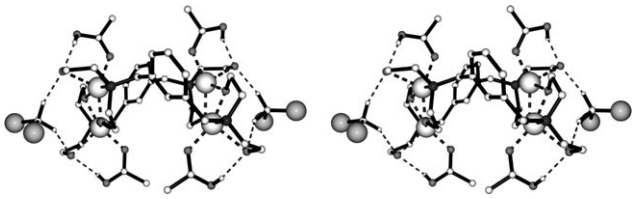

Figure 44. Stereo presentation of the structure of **75** in the crystal with coordinated dichloromethane. Cu light gray (large), Cl gray (large).

(**76**) seems to be a quite complex system, its building plan is rather straightforward. In principle, **76** is composed of two metallocrown ether subunits $[Li_2Cu_2(L^2)]^{2+}$ bridged by an extra μ_4-O^{2-} anion in the center (Figure 45). The overall two

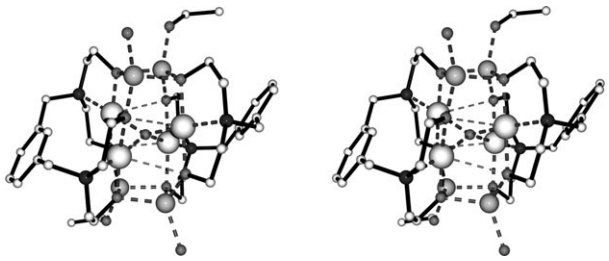

Figure 45. Stereo presentation of the structure of dication of **76** in the crystal with the coordinated water and ethanol molecules. Cu light gray (large), Li gray (large).

positive charges of the square box are compensated by two extra chloride anions, which are not in close contact with the supramolecular core.

10.3. An Octadecanuclear Square Box of Cobalt and Sodium Composed of a Total of 52 Single Components

A challenging problem arises from the reaction of N-substituted diethanolamines with hexacoordinate divalent metal ions. Assuming a hexanuclear coronand is formed, the twelve positive charges from the metal ions would be compensated by the six tridentate dianionic ligands; however, they would leave each metal center only pentacoordinated. To guarantee both coordinative saturation and charge compensation at the metal centers, a more complex assembly, rather than a hexanuclear wheel, may be expected. Therefore, when tridentate ligand H_2L was allowed to react with cobalt(II) acetate, the novel octadecametallic square box $[(Na\{Co_4(HL)_3(OAc)_5\}_2)_2(HCO_2)_2]$ (**77**) was isolated (Scheme 31).[51]

Racemic supramolecule **77** has idealized D_2 symmetry with both enantiomers present in the crystal. Although **77** represents a rather complex assembly of 52 single components, its building plan is quite straightforward. Supramolecule **77** comprises four tetrahedral $[Co_4(HL)_3(OAc)_5]$ modules, which are linked across the cobalt(II) ions in the apex in pairs by a sodium cation to give cationic building block $(Na\{Co_4(HL)_3(OAc)_5\}_2)^+$. Finally, two of these fragments are

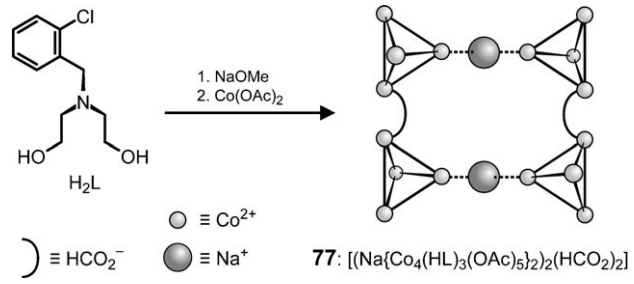

Scheme 31. Synthesis and schematic presentation of **77**.

fused by two formate anions across one base cobalt(II) ion of each of the four tetrahedra to give $[(Na\{Co_4(HL)_3(OAc)_5\}_2)_2(HCO_2)_2]$ (**77**; Figure 46).

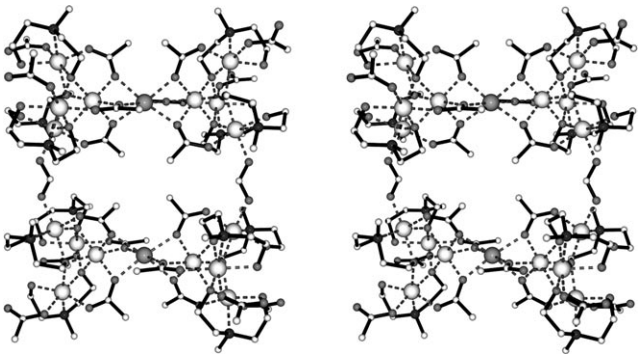

Figure 46. Stereo presentation of the structure of **77** in the crystal. View highlighting the linkage of the four $\{Co_4\}$ fragments by sodium and formate ions. The aromatic substituents are omitted for clarity.

11. Metal-Centered, Six-Membered Wheels of Manganese, Indium, and Iron

11.1. Metal-Centered, Homonuclear, Mixed-Valent Manganese Wheels

In Sections 9.2 and 10.1, a series of unoccupied, neutral, homovalent, hexanuclear ferric wheels **62** and hexanuclear copper wheels **71** and **72** were introduced. In contrast, starting from *N*-*n*-butyldiethanolamine H_2L^1, lithium hydride, and dilithium tetrachloromanganate(II), the neutral, metal-centered, homonuclear, mixed-valent, six-membered manganese wheel $[Mn^{II}\subset\{Mn^{II}_2Mn^{III}_4Cl_6(L^1)_6\}]$ (**78**) was generated in a one-pot reaction (Scheme 32).[52] However, upon reaction of N-substituted diethanolamines H_2L^2 with cesium carbonate and bis(tetraethylammonium)tetrachloromanganate(II), the metal-centered, mixed-valent manganese wheels $Et_4N[Mn^{II}\subset\{Mn^{II}_3Mn^{III}_3Cl_6(L^2)_6\}]$ (**79**) with an anionic core were generated (Scheme 32).[53]

In the solid state, the $\{Mn\subset Mn_6\}$ core[45d,m,54] of **78**·2 $CHCl_3$ possesses idealized S_6 symmetry. Detailed symmetry, bond-length, and charge considerations of **78** require the periphery to contain two Mn^{II} and four Mn^{III} centers, alternating one Mn^{II} and two Mn^{III} ions along the ring, and a Mn^{II} ion in the center (Figure 47). The anionic core of **79** is in principle

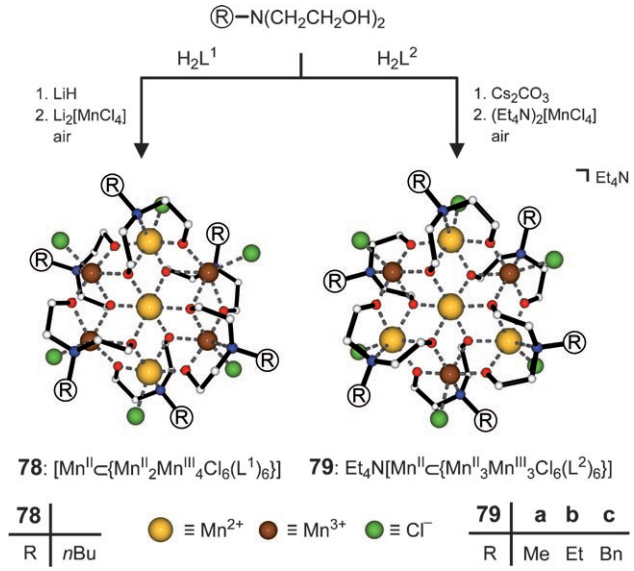

Scheme 32. Synthesis and schematic presentation of **78** and **79**.

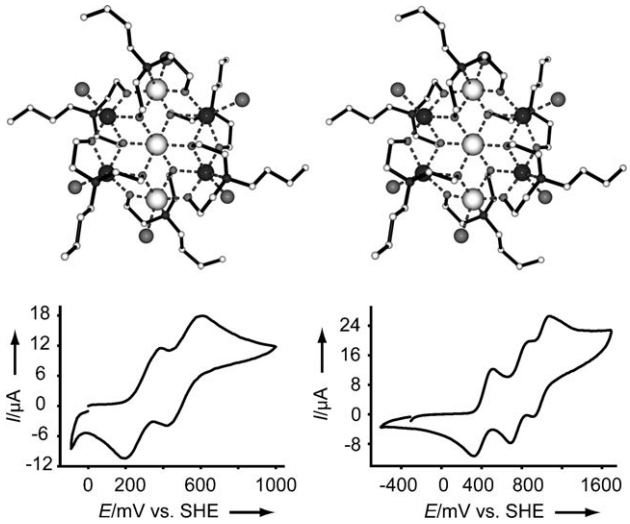

Figure 47. Top: Stereo presentation of the neutral mixed-valent $\{Mn\subset Mn_6\}$ wheel **78** in the crystal. Mn^{II} light gray (large), Mn^{III} dark gray (large), Cl gray (large). Bottom: CV of **78** (left) and **79a** (right).

isostructural with **78** but consists of a ring of alternating Mn^{II} and Mn^{III} ions centered by an additional Mn^{II} ion. The CV of **78** exhibits two quasi-reversible redox waves, which are assigned to the successive one-electron oxidations of the two Mn^{II} ions located at the periphery of the ring (Figure 47). As usual, oxidation of the central Mn^{II} ion is not observed within the applied potential.[9a,52–56] The CV of **79** displayed three quasi-reversible oxidation processes, which are attributed to the consecutive one-electron oxidations of the three peripheral Mn^{II} ions to Mn^{III}. Again, oxidation of the central Mn^{II} ion is not observed (Figure 47). The analysis of the SQUID magnetic susceptibility data for **78**·2 $CHCl_3$ showed that the intramolecular magnetic coupling of the manganese(II/III) ions is dominated by ferromagnetic exchange interactions. This results in a $S = 27/2$ ground-state multiplet.

Anisotropy SQUID measurements, high-frequency EPR spectroscopy, and 2DEG Hall magnetization measurements revealed that **78**·2 $CHCl_3$ shows SMM behavior (blocking temperature ca. 0.6 K) with closely spaced steps in the hysteresis owing to quantum tunneling of the magnetization.[57]

11.2. Metal-Centered, Heteronuclear Mixed-Valent Wheels

By combining our research on mixed-valent manganese wheels with our experience in heterotrinuclear thiazole thiazolylamide and star-shaped tetranuclear complexes (Sections 4.4 and 9.3), we were able to synthesize heterometallic wheels **80**–**82**. For this purpose, *N*-benzyldiethanolamine H_2L was deprotonated with cesium carbonate. In the case of the heteronuclear, neutral indium/manganese wheel $[Mn^{II}\subset\{Mn^{II}_2In^{III}_4Cl_6(L)_6\}]$ (**80**), a solution of a 3:4 mixture of $(Ph_4P)_2[MnCl_4]$ and $InCl_3$ was added to $(L)^{2-}$, while the anionic wheel $Ph_4P[Mn^{II}\subset\{Mn^{II}_3In^{III}_3Cl_6(L)_6\}]$ (**81**) was obtained with a solution of a 4:3 mixture of $(Ph_4P)_2[MnCl_4]$ and $InCl_3$ (Scheme 33).[56]

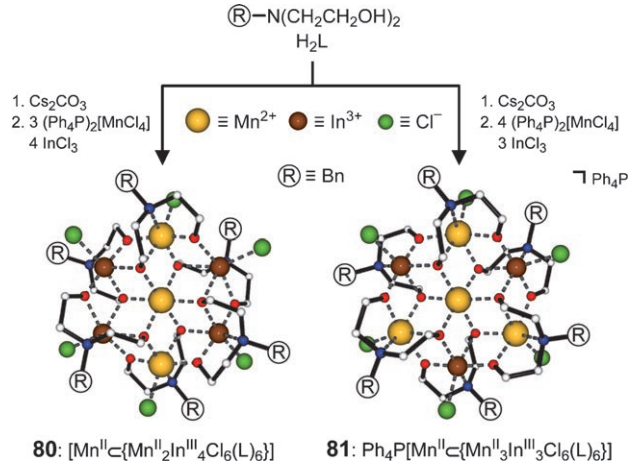

Scheme 33. Synthesis and schematic presentation of **80** and **81**.

The CV of $[Mn^{II}\subset\{Mn^{II}_2In^{III}_4Cl_6(L)_6\}]$ (**80**) exhibits two quasi-reversible one-electron Mn^{II}/Mn^{III} redox waves. This finding is consistent with the oxidation of two Mn^{II} ions located at the rim (Figure 48). On the other hand, $Ph_4P[Mn^{II}\subset\{Mn^{II}_3In^{III}_3Cl_6(L)_6\}]$ (**81**) displays three quasi-reversible waves, which are attributed to the consecutive oxidations

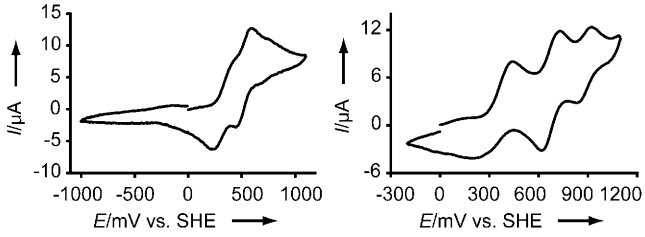

Figure 48. CV of **80** (left) and **81** (right).

of three Mn^{II} ions located at the periphery of the ring (Figure 48). As usual, the central Mn^{II} ions in **80** and **81** did not undergo oxidation in the given potential range.

The heteronuclear wheel $Ph_4P[Fe^{III}\subset\{Fe^{III}_2Mn^{III}_4Cl_6(L)_6\}]$ (**82**) was prepared in analogy to **80** and **81**, starting from *N*-benzyldiethanolamine H_2L, cesium carbonate, four equivalents of $(Ph_4P)_2[MnCl_4]$, and three equivalents of $FeCl_3$ (Scheme 34).[56] In principle, **82** is isostructural with the

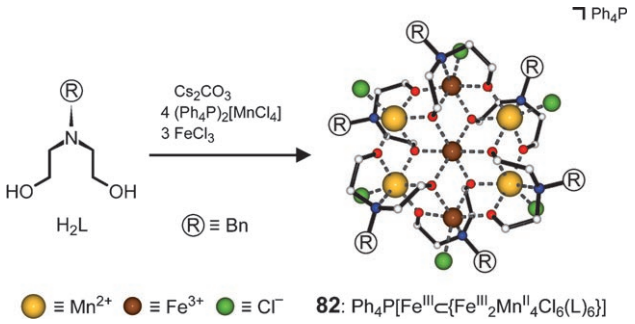

Scheme 34. Synthesis and schematic presentation of **82**.

wheels **78**–**81** (Sections 11.1, 11.2). The CV of **82** exhibits four quasi-reversible oxidation waves (Figure 49), suggesting that in **82** all four of the redox-active Mn^{II} ions are located in the ring and one Fe^{III} ion is placed in the center. The Mössbauer spectrum of **82** exhibits two quadrupole doublets with an area ratio of 1:2 for the three Fe^{III} ions (Figure 49).

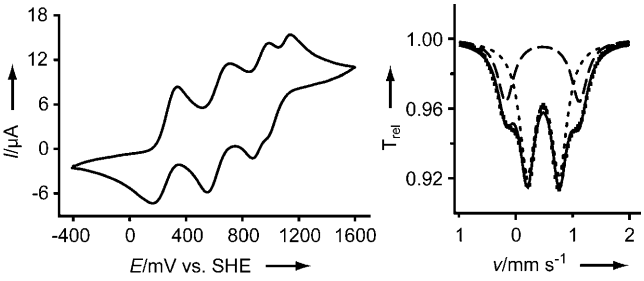

Figure 49. CV (left) and Mössbauer spectrum (right, $T = 100$ K) of **82**.

12. Mixed-Valent Octanuclear Iron-Defective Hexacubanes and a (CaCl)-Capped Body-Centered Six-Sided Iron(III) Polyhedron

12.1. Synthesis and Redox Properties of a Compact and a Linear Octanuclear Iron(II/III) Defective Hexacubane

All the metallic wheels discussed so far (Sections 9–11) were prepared with *N*-α-methylene-substituted diethanolamines. However, when α-branched *N*-*t*Bu-diethanolamine H_2L, instead of an *N*-α-methylene-substituted diethanolamine, was treated with mixtures of iron(II) and iron(III) chlorides ($Fe^{II}/Fe^{III} = 1{:}1$ for **83**; $Fe^{II}/Fe^{III} = 1{:}3$ for **84**), the mixed-valent octanuclear defective hexacubanes $[Fe^{II}_4Fe^{III}_4Cl_4(L)_6O_2]$ (**83**) and $[Fe^{II}_2Fe^{III}_6Cl_6(L)_6O_2]$ (**84**) were generated (Scheme 35).[58]

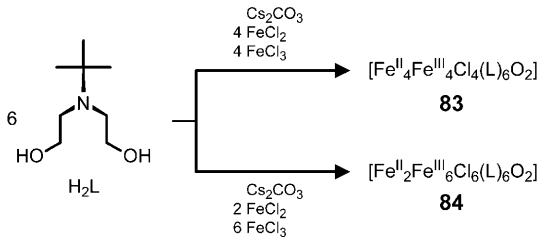

Scheme 35. Synthesis of the hexacubanes **83** and **84**.

Complex **83** is a compact defective hexacubane (Figure 50). The six tridentate ligands $(L)^{2-}$ of **83** exhibit two different bonding modes: four are tritopic, and two are

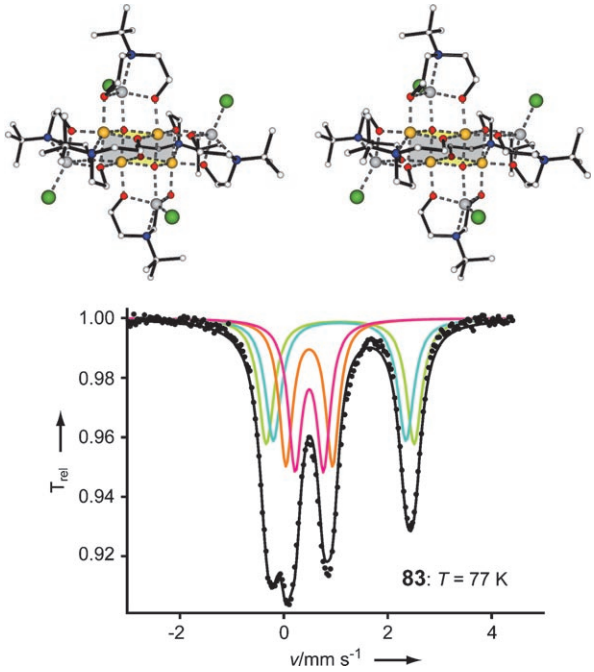

Figure 50. Top: stereo presentation of compact defective hexacubane **83**. Fe^{II} silver, Fe^{III} gold, Cl green. Bottom: Mössbauer spectrum of **83** (experiment black dots; simulation black line; peripheral Fe^{II} turquoise, green; central Fe^{III} magenta, orange).

tetratopic. The complex contains four distinct pairs of iron centers: two pairs of five-coordinate iron(II) and two pairs of six-coordinate iron(III) ions. Consequently, in **83**, six $\{Fe_3O_4\}$ defective cubane fragments are arranged in a cross-shaped manner. The CV of **83** exhibits four quasi-reversible waves, which are assigned to the consecutive one-electron oxidations of the four Fe^{II} ions. The Mössbauer spectrum of **83** at 77 K in the absence of an applied magnetic field consists of four quadrupole doublets with the relative intensity of 1:1:1:1, indicating four pairs of different iron ions (Figure 50).

Complex **84** is a linear defective hexacubane (Figure 51) and, in analogy to **83**, the six tridentate $(L)^{2-}$ ligands in **84** participate in two different bonding modes: four are tritopic, and two are tetratopic. Of four discrete pairs of metal centers, one pair of iron(II) ions is five-coordinate, and three pairs of iron(III) ions are six-coordinate. The core of **84** is composed

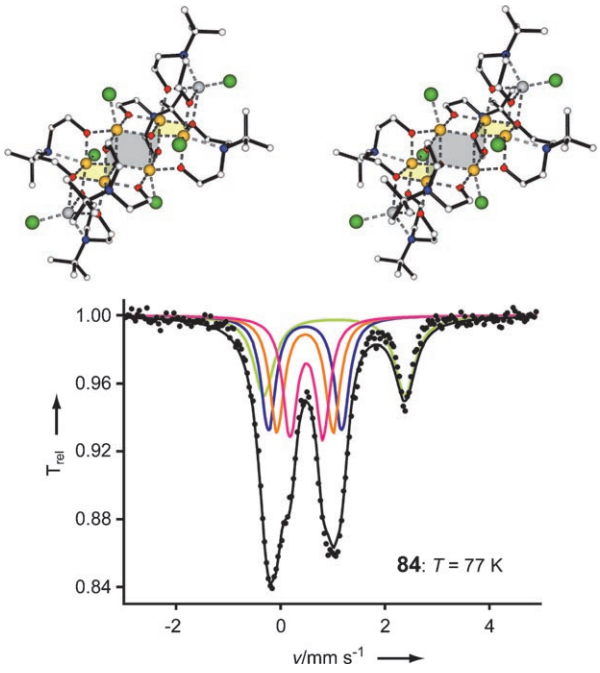

Figure 51. Top: stereo presentation of the linear defective hexacubane **84**. Fe^{II} silver, Fe^{III} gold, Cl green. Bottom: Mössbauer spectrum of **84** (experiment black dots; simulation black line; peripheral Fe^{II} green; central Fe^{III} magenta, orange, blue).

of a chain of six $\{Fe_3O_4\}$ defective cubane units in a zigzag arrangement. The CV of **84** shows two quasi-reversible waves, which correspond to reversible oxidation steps of two iron(II)/iron(III) redox couples. The Mössbauer spectrum of **84** at 77 K in the absence of an applied magnetic field consists of four quadrupole doublets with relative intensities of 1:1:1:1, indicating four different pairs of iron ions (Figure 51).

12.2. Synthesis and Characterization of an All-Iron(III) (CaCl)-Capped Body-Centered Six-Sided Polyhedron

When *N*-*t*Bu-diethanolamine H_2L (Scheme 36) was treated with calcium hydride, instead of cesium carbonate (Section 12.1), and subsequently with iron(III) chloride, the

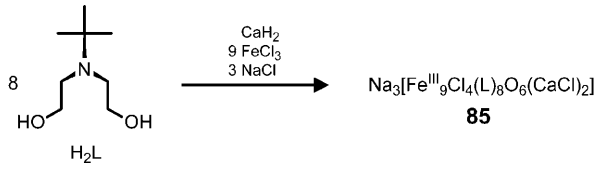

Scheme 36. Synthesis of (CaCl)-capped body-centered six-side polyhedron **85**.

heterometallic chelate complex $Na_3[Fe^{III}{}_9Cl_4(L)_8O_6(CaCl)_2]$ (**85**) was formed.[45i,58,59]

The complex **85** contains four octahedrally and four pseudotetragonal pyramidally coordinated homochiral iron centers and has nearly D_2 molecular symmetry (Figure 52).

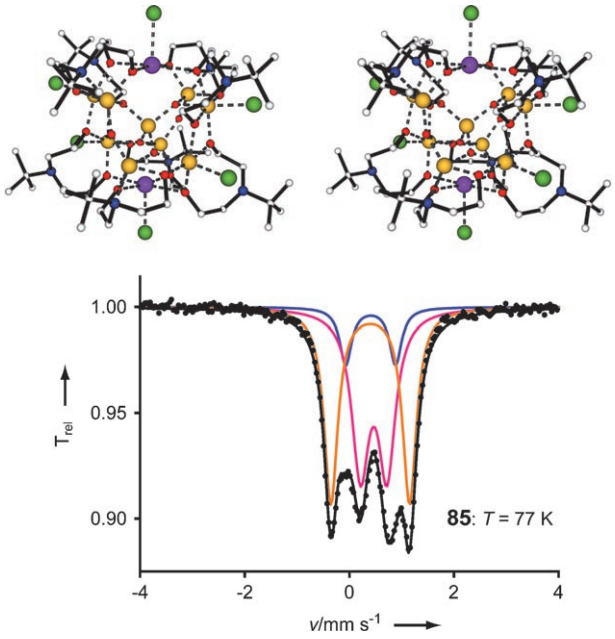

Figure 52. Top: stereo presentation of (CaCl)-capped body-centered six-sided all-Fe^{III} trianionic polyhedron (**85**)$^{3-}$. Fe gold, Ca purple, Cl green. Bottom: Mössbauer spectrum of **85** (experiment black dots, simulation black line; four-coordinate Fe^{III} blue; five-coordinate Fe^{III} orange; six-coordinate Fe^{III} magenta).

Four of the eight potentially tridentate $(L)^{2-}$ ligands function as such, whereas the remaining four act as bidentate ligands. All eight ligands are tritopic, each linking two iron centers and one calcium(II) ion. The central iron(III) ion is tetrahedrally coordinated by four μ_3-O^{2-} ions. The square-pyramidal coordination sphere of each of the two Ca^{2+} ions consists of four ligand ethoxide μ_2-O^- donors and one Cl^- ion. Note that the iron ions in **85** reveal three different types of coordination environments, including a tetrahedral coordination sphere for the iron ion in the center, which is uncommon for iron(III). The entire framework is fixed by the two (CaCl) caps. The Mössbauer spectrum of **85** at 77 K in the absence of an applied magnetic field consists of three quadrupole doublets with the relative intensity of 4:4:1, which indicate the existence of two sets of four and one different high-spin iron(III) ion (Figure 52).

13. Summary

The purpose of this Review is to demonstrate that the recognition of similarities in the synthesis of different supramolecular assemblies allows prediction of potential results in related cases. For example, we demonstrated that the assembly of metallotopomers of the classical purely organic coronates and of the bi- and tricyclic cryptates is possible starting from appropriate metal ions and tailor-made chelating ligands. This approach differs from multistep natural-product synthesis. It also turned out to be extremely productive to put stress on a successfully running reaction by changing the experimental parameters (stoichiometry, metal ion, coordination number, oxidation state, ligand geometry, denticity) and allowing nature to work for us. It is clear that this approach sometimes leads to serendipitous results which must be elucidated to gain insights that are useful for advanced studies. Consequently, this Review emphasizes the achievements in supramolecular coordination chemistry initiated by serendipity and their materialization based on rational design. This creative dialog represents the central theme of this Review, offering various new prospects. The breadth of this concept became progressively more apparent and has spontaneously uncovered a variety of new structures. In this regard, the discovery of the ferric wheels and their modification may serve as a paradigm for the productivity of this approach. Furthermore, the appealing structures are not merely products in their own rights, but present dynamic behavior and redox and magnetic properties, and they may serve as templates (assembly platforms) for the generation of large organic molecules. Finally, the highly interdisciplinary character of this research and the concentrated use and interplay of variable-temperature NMR spectroscopy, X-ray analysis, cyclic voltammetry, and Mössbauer spectroscopy guarantee an excellent broad training for young chemists and presents a nice example of "curiosity-driven research" as claimed by G. M. Whitesides on the occasion of his August-Wilhelm-von-Hofmann lecture.[60]

14. Outlook

It is evident that the majority of different structures given above provides excellent sources for further development, as illustrated exemplarily by the ferric wheels and the ferric star. A general feature of the metallocoronands $[Fe_6Cl_6(L)_6]$ (**62**; Section 9.2) is the fact that the *N*-alkyl substituents are alternately arranged above and below the plane of the six iron ions. Interestingly, this molecular geometry offers the possibility to construct container molecules such as $[K\subset\{Fe_6Cl_6(L^1)_2\}]^+$ starting from tripodal 1,3,5-tris(alkyldiethanolamine)benzenes H_6L^1 with six-coordinate iron(III) ions.

On the other hand, to achieve the high degree of selectivity that we are used to from natural processes, synthetic chemists must improve conventional multistep reactions. For that reason, tailor-made templates, which recognize matching reaction partners and bring them sufficiently close together to promote intermolecular reactions, are needed. In the past, numerous recognition motifs mimicking nature were offered, in which metal ions often play an important role.

Concerning our own research on ferric wheels $[M\subset\{Fe_n(L)_n\}]Cl$ (**60**,**61**), alkali ions act as templates (Section 9.1; Scheme 24).[39] In the case of metallosandwich $[Fe_6Cl_6(L^2)_6]$ (**86**; Scheme 37), the iron ions themselves function as templates (assembly platforms) to preorganize the olefinic diethoxyamine sidearms, suitable for threefold acyclic diene metathesis (ADMET) reactions in the presence of ruthenium alkylidene Grubbs catalysts.[61] Further transformations of **86** should finally produce the new class of extended calixarene analogues **87**.[62] Recently, viability for a similar system of this proposal was demonstrated by Stoddart, Grubbs et al.[63]

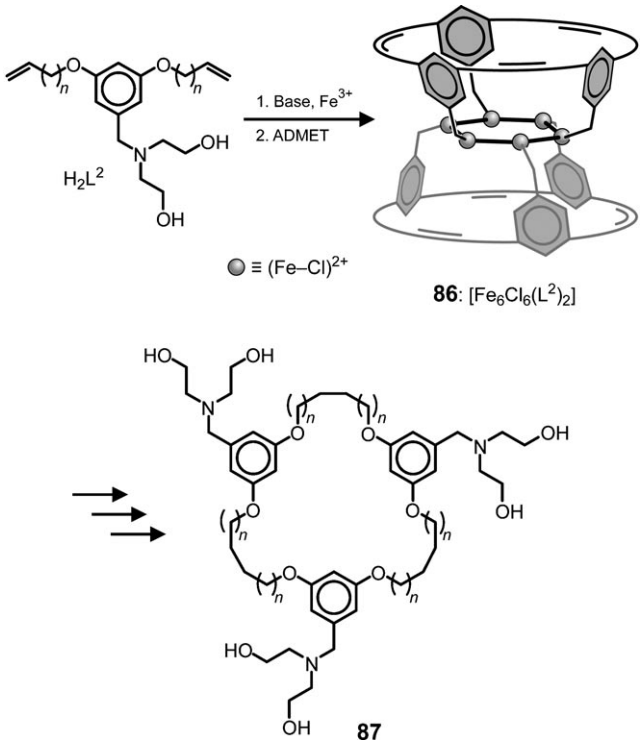

Scheme 37. Synthesis of **86** by template control and ADMET and its transformation to macrocycles **87**.

I would like to thank all the talented co-workers, crystallographers, and spectroscopists for their ideas, enthusiasm, and hard work over the past 20 years. Their names appear in the cited references. We would like further to thank Prof. K. N. Raymond, Berkeley University, for his collaboration in various supramolecular projects. Our work on supramolecular coordination chemistry would not have been possible without the generous financial support of the Deutsche Forschungsgemeinschaft, the Bayerisches Langzeitprogramm Neue Werkstoffe, the Fonds der Chemischen Industrie, and the Alexander von Humboldt Stiftung, which is gratefully acknowledged. Furthermore, I am very grateful to Prof. Dr. K. Meyer, Universität Erlangen-Nürnberg, for the broadminded allocation of premises after my retirement. I also would like to thank Prof. Dr. F. Vögtle, Universität Bonn, for stimulating discussions. Frontispiece: Conception: Rolf W. Saalfrank. Layout: Gerhard Brendel, Harald Maid. Background drawing based on snia cruz; http://flickr.com/photos/5415164@N00/. Copyright notice: Pablo Picasso, "Le taureau", 1. situation, 04.12.1954 Succession Picasso/VG Bild-Kunst, Bonn 2008; Pablo Picasso, "Le taureau", 11. situation, 17.01.1946 Succession Picasso/VG Bild-Kunst, Bonn 2008.

Received: May 11, 2007
Published online: October 20, 2008

[1] a) J.-M. Lehn, *Chem. Soc. Rev.* **2007**, *36*, 151 – 160; b) J.-M. Lehn, *Prog. Polym. Sci.* **2005**, *30*, 814 – 831; c) J.-M. Lehn, *Science* **2002**, *295*, 2400 – 2403; d) V. G. Machado, P. N. W. Baxter, J.-M. Lehn, *J. Braz. Chem. Soc.* **2001**, *12*, 431 – 462; e) J.-M. Lehn, *Chem. Eur. J.* **1999**, *5*, 2455 – 2463; f) J.-M. Lehn, *Supramolecular Chemistry: Concepts and Perspectives*, VCH, Weinheim, **1995**; g) J.-M. Lehn, *Acc. Chem. Res.* **1978**, *11*, 49 – 57.

[2] a) S. R. Seidel, P. J. Stang, *Acc. Chem. Res.* **2002**, *35*, 972 – 983; b) M. Tominaga, M. Fujita, *Bull. Chem. Soc. Jpn.* **2007**, *80*, 1473 – 1482; c) M. D. Pluth, K. N. Raymond, *Chem. Soc. Rev.* **2007**, *36*, 161 – 171; d) G. F. Swiegers, T. J. Malefetse, *Coord. Chem. Rev.* **2002**, *225*, 91 – 121; e) N. Gimeno, R. Vilar, *Coord. Chem. Rev.* **2006**, *250*, 3161 – 3189; f) G. Seeber, B. E. F. Tiedemann, K. N. Raymond, *Top. Curr. Chem.* **2006**, *265*, 147 – 183; g) J. M. Thomas, *Chem. Soc. Rev.* **2007**, *36*, 856 – 868; h) M. Albrecht, R. Fröhlich, *Bull. Chem. Soc. Jpn.* **2007**, *80*, 797 – 808; i) J. L. Boyer, M. L. Kuhlman, T. B. Rauchfuss, *Acc. Chem. Res.* **2007**, *40*, 233 – 242; j) R. W. Saalfrank, B. Demleitner in *Perspectives in Supramolecular Chemistry*, *Vol. 5* (Ed.: J.-P. Sauvage), Wiley, Chichester, **1999**, pp. 1 – 51; k) R. W. Saalfrank, E. Uller, B. Demleitner, I. Bernt, *Struct. Bonding (Berlin)* **2000**, *96*, 149 – 175; l) C. J. Jones, *Chem. Soc. Rev.* **1998**, *27*, 289 – 299; m) F. Hof, S. L. Craig, C. Nuckolls, J. Rebek, Jr., *Angew. Chem.* **2002**, *114*, 1556 – 1578; *Angew. Chem. Int. Ed.* **2002**, *41*, 1488 – 1508; n) B. J. Holliday, C. A. Mirkin, *Angew. Chem.* **2001**, *113*, 2076 – 2097; *Angew. Chem. Int. Ed.* **2001**, *40*, 2022 – 2043; o) E. Barea, J. A. R. Navarro, J. M. Salas, M. Quirós, M. Willermann, B. Lippert, *Chem. Eur. J.* **2003**, *9*, 4414 – 4421; p) R. E. P. Winpenny, in *Perspectives in Supramolecular Chemistry*, *Vol. 5* (Ed.: J.-P. Sauvage), Wiley, Chichester, **1999**, pp. 193 – 223; q) A. D. Cutland, R. G. Malkani, J. W. Kampf, V. L. Pecoraro, *Angew. Chem.* **2000**, *112*, 2801 – 2803; *Angew. Chem. Int. Ed.* **2000**, *39*, 2689 – 2692; r) H. Oshio, N. Hoshino, T. Ito, M. Nakano, F. Renz, P. Gütlich, *Angew. Chem.* **2003**, *115*, 233 – 235; *Angew. Chem. Int. Ed.* **2003**, *42*, 223 – 225; s) M. Albrecht, *Chem. Rev.* **2001**, *101*, 3457 – 3497; t) S. P. Watton, P. Fuhrmann, L. E. Pence, A. Caneschi, A. Cornia, G. L. Abbati, S. J. Lippard, *Angew. Chem.* **1997**, *109*, 2917 – 2919; *Angew. Chem. Int. Ed. Engl.* **1997**, *36*, 2774 – 2776; u) G. Mezei, C. M. Zaleski, V. L. Pecoraro, *Chem. Rev.* **2007**, *107*, 4933 – 5003; v) J. A. R. Navarro, E. Barea, M. A. Galindo, J. M. Salas, M. A. Romero, M. Quirós, N. Masciocchi, S. Galli, A. Sironi, B. Lippert, *J. Solid State Chem.* **2005**, *178*, 2436 – 2451.

[3] R. W. Saalfrank, A. Stark, K. Peters, H. G. von Schnering, *Angew. Chem.* **1988**, *100*, 878 – 880; *Angew. Chem. Int. Ed. Engl.* **1988**, *27*, 851 – 853.

[4] Roots: Part I.[42a] Serendipity has to hit a prepared mind. In order to pass the habilitation, all candidates are supposed to prepare three lectures on topics not related to their own research. As one of my pet subjects, I chose supramolecular chemistry. However, three weeks before the deadline, Jean-Marie Lehn was invited to give a plenary lecture at my university (1976). Instinctively, I felt it not to be smart to also talk about supramolecular chemistry. However, I was so fascinated by this rapidly developing new field of science that during the following years I kept an eye on it. One decade later, with completely different aspects in mind, I studied the double deprotonation of malonic ester with methyl grignard to generate its dianion, formally a tetradonor-substituted allene.[42a] However, this idea did not work. But, instead, in 1987 the first tetrahedral magnesium chelate complex (Section 5) was isolated. With the understanding of supramolecular chemistry in the back of my mind, it was straightforward to realize the fundamental relationship between this tetrahedral magnesium complex and the whole family of the classical, organic supramolecular species. From then on, numerous metallotopomers were rationally designed. The review is not organized chronologically and, for didactic reasons alone, starts with the plain metallocoronates.

[5] a) S. Leininger, B. Olenyuk, P. J. Stang, *Chem. Rev.* **2000**, *100*, 853 – 908; b) D. L. Caulder, K. N. Raymond, *Acc. Chem. Res.* **1999**, *32*, 975 – 982; c) L. R. MacGillivray, J. L. Atwood, *Angew. Chem.* **1999**, *111*, 1080 – 1096; *Angew. Chem. Int. Ed.* **1999**, *38*,

1018 – 1033; d) G. F. Swiegers, T. J. Malefetse, *Chem. Eur. J.* **2001**, *7*, 3636 – 3643; e) R.-D. Schnebeck, E. Freisinger, F. Glahé, B. Lippert, *J. Am. Chem. Soc.* **2000**, *122*, 1381 – 1390; f) M. Fujita, *Chem. Soc. Rev.* **1998**, *27*, 417 – 425.

[6] a) R. W. Saalfrank, N. Löw, S. Kareth, V. Seitz, F. Hampel, D. Stalke, M. Teichert, *Angew. Chem.* **1998**, *110*, 182 – 184; *Angew. Chem. Int. Ed.* **1998**, *37*, 172 – 175; b) R. W. Saalfrank, N. Löw, B. Demleitner, D. Stalke, M. Teichert, *Chem. Eur. J.* **1998**, *4*, 1305 – 1311; c) R. W. Saalfrank, N. Löw, F. Hampel, H.-D. Stachel, *Angew. Chem.* **1996**, *108*, 2353 – 2354; *Angew. Chem. Int. Ed. Engl.* **1996**, *35*, 2209 – 2210.

[7] a) V. L. Pecoraro, A. J. Stemmler, B. R. Gibney, J. J. Bodwin, H. Wang, J. W. Kampf, A. Barwinski, *Prog. Inorg. Chem.* **1996**, *45*, 83 – 177; b) A. J. Stemmler, J. W. Kampf, V. L. Pecoraro, *Angew. Chem.* **1996**, *108*, 3011 – 3013; *Angew. Chem. Int. Ed. Engl.* **1996**, *35*, 2841 – 2843; c) A. J. Stemmler, A. Barwinski, M. J. Baldwin, V. Young, V. L. Pecoraro, *J. Am. Chem. Soc.* **1996**, *118*, 11962 – 11963; d) B. R. Gibney, D. P. Kessissoglou, J. W. Kampf, V. L. Pecoraro, *Inorg. Chem.* **1994**, *33*, 4840 – 4849; e) M. S. Lah, B. R. Gibney, D. L. Tierney, J. E. Penner-Hahn, V. L. Pecoraro, *J. Am. Chem. Soc.* **1993**, *115*, 5857 – 5858; f) A. J. Blake, R. O. Gould, C. M. Grant, P. E. Y. Milne, D. Reed, R. E. P. Winpenny, *Angew. Chem.* **1994**, *106*, 208 – 210; *Angew. Chem. Int. Ed. Engl.* **1994**, *33*, 195 – 197; g) A. J. Blake, R. O. Gould, P. E. Y. Milne, R. E. P. Winpenny, *J. Chem. Soc. Chem. Commun.* **1991**, 1453 – 1454; h) G. M. Gray, C. H. Duffey, *Organometallics* **1995**, *14*, 245 – 250; i) L. F. Jones, C. A. Kilner, M. P. de Miranda, J. Wolowska, M. A. Halcrow, *Angew. Chem.* **2007**, *119*, 4151 – 4154; *Angew. Chem. Int. Ed.* **2007**, *46*, 4073 – 4076.

[8] R. W. Saalfrank, R. Burak, S. Reihs, N. Löw, F. Hampel, H.-D. Stachel, J. Lentmaier, K. Peters, E. M. Peters, H. G. von Schnering, *Angew. Chem.* **1995**, *107*, 1085 – 1087; *Angew. Chem. Int. Ed. Engl.* **1995**, *34*, 993 – 995.

[9] Cf.: a) M. Ruben, J. Rojo, F. J. Romero-Salguero, L. H. Uppadine, J.-M. Lehn, *Angew. Chem.* **2004**, *116*, 3728 – 3747; *Angew. Chem. Int. Ed.* **2004**, *43*, 3644 – 3662; b) G. S. Hanan, D. Volkmer, U. S. Schubert, J.-M. Lehn, G. Baum, D. Fenske, *Angew. Chem.* **1997**, *109*, 1929 – 1931; *Angew. Chem. Int. Ed. Engl.* **1997**, *36*, 1842 – 1844; c) J. Rojo, F. J. Romero-Salguero, J.-M. Lehn, G. Baum, D. Fenske, *Eur. J. Inorg. Chem.* **1999**, 1421 – 1428; d) A. M. Garcia, F. J. Romero-Salguero, D. M. Bassani, J.-M. Lehn, G. Baum, D. Fenske, *Chem. Eur. J.* **1999**, *5*, 1803 – 1808; e) M. Barboiu, G. Vaughan, R. Graff, J.-M. Lehn, *J. Am. Chem. Soc.* **2003**, *125*, 10257 – 10265; f) S. T. Onions, A. M. Frankin, P. N. Horton, M. B. Hursthouse, C. J. Matthews, *Chem. Commun.* **2003**, 2864 – 2865; g) M. Ruben, J.-M. Lehn, G. Vaughan, *Chem. Commun.* **2003**, 1338 – 1339; h) A.-M. Stadler, N. Kyritsakas, R. Graff, J.-M. Lehn, *Chem. Eur. J.* **2006**, *12*, 4503 – 4522.

[10] R. W. Saalfrank, A. Scheurer, R. Puchta, F. Hampel, H. Maid, F. W. Heinemann, *Angew. Chem.* **2007**, *119*, 269 – 272; *Angew. Chem. Int. Ed.* **2007**, *46*, 265 – 268.

[11] a) C. Piguet, G. Bernardinelli, G. Hopfgartner, *Chem. Rev.* **1997**, *97*, 2005 – 2062; b) J.-M. Lehn, A. Rigault, J. Siegel, J. Harrowfield, B. Chevrier, D. Moras, *Proc. Natl. Acad. Sci. USA* **1987**, *84*, 2565 – 2569; c) R. Krämer, J.-M. Lehn, A. De Cian; J. Fischer, *Angew. Chem.* **1993**, *105*, 764 – 767; J. Fischer, *Angew. Chem.* **1993**, *105*, 764 – 767; *Angew. Chem. Int. Ed. Engl.* **1993**, *32*, 703 – 706; d) E. J. Enemark, T. D. P. Stack, *Angew. Chem.* **1995**, *107*, 1082 – 1084; *Angew. Chem. Int. Ed. Engl.* **1995**, *34*, 996 – 998; e) E. J. Enemark, T. D. P. Stack, *Inorg. Chem.* **1996**, *35*, 2719 – 2720; f) B. Kersting, M. Meyer, R. E. Powers, K. N. Raymond, *J. Am. Chem. Soc.* **1996**, *118*, 7221 – 7222; g) D. Caulder, K. N. Raymond, *Angew. Chem.* **1997**, *109*, 1508 – 1510; *Angew. Chem. Int. Ed. Engl.* **1997**, *36*, 1440 – 1442; h) M. Meyer, B. Kersting, R. E. Powers, K. N. Raymond, *Inorg. Chem.* **1997**, *36*, 5179 – 5191; i) M. Albrecht, S. Kotila, *Angew. Chem.* **1995**, *107*, 2285 – 2287; *Angew. Chem. Int. Ed. Engl.* **1995**, *34*, 2134 – 2137; j) M. Albrecht, S. Kotila, *Angew. Chem.* **1996**, *108*, 1299 – 1300; *Angew. Chem. Int. Ed. Engl.* **1996**, *35*, 1208 – 1210; k) M. Albrecht, M. Schneider, R. Fröhlich, *New J. Chem.* **1998**, *22*, 753 – 754; l) M. Albrecht, M. Schneider, *Eur. J. Inorg. Chem.* **2002**, 1301 – 1306; m) M. J. Hannon, L. J. Childs, *Supramol. Chem.* **2003**, *16*, 7 – 22; n) M. Albrecht, *Chem. Soc. Rev.* **1998**, *27*, 281 – 287; o) R. M. Yeh, M. Ziegler, D. W. Johnson, A. J. Terpin, K. N. Raymond, *Inorg. Chem.* **2001**, *40*, 2216 – 2217; p) J. Xu, T. N. Parac, K. N. Raymond, *Angew. Chem.* **1999**, *111*, 3055 – 3058; *Angew. Chem. Int. Ed.* **1999**, *38*, 2878 – 2882; q) M. Albrecht, *Chem. Eur. J.* **2000**, *6*, 3485 – 3489.

[12] a) E. C. Constable, *Tetrahedron* **1992**, *48*, 10013 – 10059; b) E. C. Constable, *Angew. Chem.* **1991**, *103*, 1482 – 1483; *Angew. Chem. Int. Ed. Engl.* **1991**, *30*, 1450 – 1451; c) E. C. Constable, T. Kulke, M. Neuburger, M. Zehnder, *Chem. Commun.* **1997**, 489 – 490; d) R. C. Scarrow, D. L. White, K. N. Raymond, *J. Am. Chem. Soc.* **1985**, *107*, 6540 – 6546; e) C. J. Carrano, K. N. Raymond, *J. Am. Chem. Soc.* **1978**, *100*, 5371 – 5374; f) L. J. Charbonnière, A. F. Williams, U. Frey, A. E. Merbach, P. Kamalaprija, O. Schaad, *J. Am. Chem. Soc.* **1997**, *119*, 2488 – 2496; g) C. Piguet, G. Bernardinelli, A. F. Williams, B. Bocquet, *Angew. Chem.* **1995**, *107*, 618 – 621; *Angew. Chem. Int. Ed. Engl.* **1995**, *34*, 582 – 584; h) A. Williams, *Chem. Eur. J.* **1997**, *3*, 15 – 19.

[13] a) R. W. Saalfrank, A. Dresel, V. Seitz, S. Trummer, F. Hampel, M. Teichert, D. Stalke, C. Stadler, J. Daub, V. Schünemann, A. X. Trautwein, *Chem. Eur. J.* **1997**, *3*, 2058 – 2062; b) R. W. Saalfrank, V. Seitz, D. L. Caulder, K. N. Raymond, M. Teichert, D. Stalke, *Eur. J. Inorg. Chem.* **1998**, 1313 – 1317; for further examples, see: c) R. W. Saalfrank, V. Seitz, F. W. Heinemann, C. Göbel, R. Herbst-Irmer, *J. Chem. Soc. Dalton Trans.* **2001**, 599 – 603; d) D. L. Caulder, K. N. Raymond, *J. Chem. Soc. Dalton Trans.* **1999**, 1185 – 1200; e) R. Puchta, B. Roling, A. Scheurer, V. Weiskopf, F. Hampel, N. J. R. van Eikema Hommes, H.-U. Hummel, *Solid State Ionics* **2008**, *179*, 489 – 494.

[14] R. W. Saalfrank, N. Löw, S. Trummer, G. M. Sheldrick, M. Teichert, D. Stalke, *Eur. J. Inorg. Chem.* **1998**, 559 – 563.

[15] a) J. B. Howard, D. C. Rees, *Chem. Rev.* **1996**, *96*, 2965 – 2982; b) B. K. Burgess, D. J. Lowe, *Chem. Rev.* **1996**, *96*, 2983 – 3011.

[16] a) R. W. Saalfrank, R. Harbig, J. Nachtrab, W. Bauer, K.-P. Zeller, D. Stalke, M. Teichert, *Chem. Eur. J.* **1996**, *2*, 1363 – 1367; b) M. Kawano, M. Fujita, *Coord. Chem. Rev.* **2007**, *251*, 2592 – 2605.

[17] a) J. Sanders, *21th Solvay Conference on Chemistry*, 28.–30. November, **2007**, Brussels, Belgium; b) P. A. Brady, J. K. M. Sanders, *Chem. Soc. Rev.* **1997**, *26*, 327 – 336.

[18] R. W. Saalfrank, H. Maid, N. Mooren, F. Hampel, *Angew. Chem.* **2002**, *114*, 323 – 326; *Angew. Chem. Int. Ed.* **2002**, *41*, 304 – 307.

[19] R. W. Saalfrank, N. Mooren, A. Scheurer, H. Maid, F. W. Heinemann, F. Hampel, W. Bauer, *Eur. J. Inorg. Chem.* **2007**, 4815 – 4822.

[20] R. W. Saalfrank, C. Schmidt, H. Maid, F. Hampel, W. Bauer, A. Scheurer, *Angew. Chem.* **2006**, *118*, 322 – 325; *Angew. Chem. Int. Ed.* **2006**, *45*, 315 – 318.

[21] R. W. Saalfrank, C. Spitzlei, A. Scheurer, H. Maid, F. Heinemann, F. Hampel, *Chem. Eur. J.* **2008**, *14*, 1472 – 1481.

[22] a) R. W. Saalfrank, S. Trummer, H. Krautscheid, V. Schünemann, A. X. Trautwein, S. Hien, C. Stadler, J. Daub, *Angew. Chem.* **1996**, *108*, 2350 – 2352; *Angew. Chem. Int. Ed. Engl.* **1996**, *35*, 2206 – 2208; b) C. Stadler, J. Daub, J. Köhler, R. W. Saalfrank, V. Coropceanu, V. Schünemann, C. Ober, A. X. Trautwein, S. F. Parker, M. Poyraz, T. Inomata, R. D. Cannon, *J. Chem. Soc. Dalton Trans.* **2001**, 3373 – 3383; c) V. Coropceanu, V. Schünemann, C. Ober, M. Gerdan, A. X. Trautwein, J. Köhler, R. W. Saalfrank, *Inorg. Chim. Acta* **2000**, *300–302*, 875 – 881; d) Cf.: B. Hasenknopf, J.-M. Lehn, B. O. Kneisel, G. Baum, D.

Fenske, *Angew. Chem.* **1996**, *108*, 1987 – 1990; *Angew. Chem. Int. Ed. Engl.* **1996**, *35*, 1838 – 1840.

[23] a) S. J. Lippard, J. M. Berg, *Bioanorganische Chemie*, Spektrum Akademischer Verlag, Heidelberg **1995**, chap. 5, p. 136; b) S. M. Gorun, G. C. Papaefthymiou, R. B. Frankel, S. J. Lippard, *J. Am. Chem. Soc.* **1987**, *109*, 4244 – 4255; c) S. J. Lippard, *Angew. Chem.* **1988**, *100*, 353 – 371; *Angew. Chem. Int. Ed. Engl.* **1988**, *27*, 344 – 361; d) K. Wieghardt, K. Pohl, I. Jibril, G. Huttner, *Angew. Chem.* **1984**, *96*, 66 – 67; *Angew. Chem. Int. Ed. Engl.* **1984**, *23*, 77 – 78.

[24] J. A. Halfen, J. J. Bodwin, V. L. Pecoraro, *Inorg. Chem.* **1998**, *37*, 5416 – 5417.

[25] a) R. W. Saalfrank, S. Trummer, U. Reimann, M. M. Chowdhry, F. Hampel, O. Waldmann, *Angew. Chem.* **2000**, *112*, 3634 – 3636; *Angew. Chem. Int. Ed.* **2000**, *39*, 3492 – 3494; Erratum: R. W. Saalfrank, S. Trummer, U. Reimann, M. M. Chowdhry, F. Hampel, O. Waldmann, *Angew. Chem.* **2000**, *112*, 3885; *Angew. Chem. Int. Ed.* **2000**, *39*, 3736; b) R. W. Saalfrank, U. Reimann, F. Hampel, C. Goebel, R. Herbst-Irmer, *Z. Naturforsch. B* **2003**, *58*, 22 – 26; c) R. Koch, O. Waldmann, P. Müller, U. Reimann, R. W. Saalfrank, *Phys. Rev. B* **2003**, *67*, 094407.

[26] a) R. W. Saalfrank, U. Reimann, M. Göritz, F. Hampel, A. Scheurer, F. W. Heinemann, M. Büschel, J. Daub, V. Schünemann, A. X. Trautwein, *Chem. Eur. J.* **2002**, *8*, 3614 – 3619; b) R. W. Saalfrank, A. Scheurer, K. Pokorny, H. Maid, U. Reimann, F. Hampel, F. W. Heinemann, V. Schünemann, A. X. Trautwein, *Eur. J. Inorg. Chem.* **2005**, 1383 – 1387; c) R. W. Saalfrank, A. Scheurer, U. Reimann, F. Hampel, C. Trieflinger, M. Büschel, J. Daub, A. X. Trautwein, V. Schünemann, V. Coropceanu, *Chem. Eur. J.* **2005**, *11*, 5843 – 5848.

[27] a) R. W. Saalfrank, A. Stark, M. Bremer, H.-U. Hummel, *Angew. Chem.* **1990**, *102*, 292 – 295; *Angew. Chem. Int. Ed. Engl.* **1990**, *29*, 311 – 314; b) R. W. Saalfrank, B. Demleitner, H. Glaser, H. Maid, S. Reihs, W. Bauer, M. Maluenga, F. Hampel, M. Teichert, H. Krautscheid, *Eur. J. Inorg. Chem.* **2003**, 822 – 829; c) A. Stark, Ph.D. Thesis, Universität Erlangen-Nürnberg, **1990**.

[28] a) R. W. Saalfrank, B. Demleitner, H. Glaser, H. Maid, D. Bathelt, F. Hampel, W. Bauer, M. Teichert, *Chem. Eur. J.* **2002**, *8*, 2679 – 2683; b) H. Glaser, Ph.D. Thesis, Universität Erlangen-Nürnberg, **2002**.

[29] a) T. Beissel, R. E. Powers, T. N. Parac, K. N. Raymond, *J. Am. Chem. Soc.* **1999**, *121*, 4200 – 4206; b) G. Seeber, B. E. F. Tiedemann, K. N. Raymond, *Top. Curr. Chem.* **2006**, *265*, 147 – 183; c) P. Mal, D. Schultz, K. Beyeh, K. Rissanen, J. R. Nitschke, *Angew. Chem.* **2008**, DOI: 10.1002/ange.200803066; *Angew. Chem. Int. Ed.* **2008** DOI: 10.1002/anie.200803066.

[30] R. W. Saalfrank, R. Burak, A. Breit, D. Stalke, R. Herbst-Irmer, J. Daub, M. Porsch, E. Bill, M. Müther, A. X. Trautwein, *Angew. Chem.* **1994**, *106*, 1697 – 1699; *Angew. Chem. Int. Ed. Engl.* **1994**, *33*, 1621 – 1623.

[31] A. Breit, Ph.D. Thesis, Universität Erlangen-Nürnberg, **2001**.

[32] a) R. W. Saalfrank, B. Hörner, D. Stalke, J. Salbeck, *Angew. Chem.* **1993**, *105*, 1223 – 1225; *Angew. Chem. Int. Ed. Engl.* **1993**, *32*, 1179 – 1182; b) T. Beissel, R. E. Powers, K. N. Raymond, *Angew. Chem.* **1996**, *108*, 1166 – 1168; *Angew. Chem. Int. Ed. Engl.* **1996**, *35*, 1084 – 1086; c) D. L. Caulder, R. E. Powers, T. N. Parac, K. N. Raymond, *Angew. Chem.* **1998**, *110*, 1940 – 1943; *Angew. Chem. Int. Ed.* **1998**, *37*, 1840 – 1843; d) B. Hörner, Ph.D. Thesis, Universität Erlangen-Nürnberg, **1993**.

[33] a) R. W. Saalfrank, H. Glaser, B. Demleitner, F. Hampel, M. M. Chowdhry, V. Schünemann, A. X. Trautwein, G. B. M. Vaughan, R. Yeh, A. V. Davis, K. N. Raymond, *Chem. Eur. J.* **2002**, *8*, 493 – 497; b) D. W. Johnson, J. Xu, R. W. Saalfrank, K. N. Raymond, *Angew. Chem.* **1999**, *111*, 3058 – 3061; *Angew. Chem. Int. Ed.* **1999**, *38*, 2882 – 2885; c) C. Brückner, R. E. Powers, K. N. Raymond, *Angew. Chem.* **1998**, *110*, 1937 – 1940; *Angew. Chem. Int. Ed.* **1998**, *37*, 1837 – 1839; d) D. L. Caulder, C. Brückner, R. E. Powers, S. König, T. N. Parac, J. A. Leary, K. N. Raymond, *J. Am. Chem. Soc.* **2001**, *123*, 8923 – 8938; e) T. Yamaguchi, M. Fujita, *Angew. Chem.* **2008**, *120*, 2097 – 2099; *Angew. Chem. Int. Ed.* **2008**, *47*, 2067 – 2069.

[34] a) M. Albrecht, I. Janser, R. Fröhlich, *Chem. Commun.* **2005**, 157 – 165; b) M. Albrecht, I. Janser, J. Runsink, G. Raabe, P. Weis, R. Fröhlich, *Angew. Chem.* **2004**, *116*, 6832 – 6836; *Angew. Chem. Int. Ed.* **2004**, *43*, 6662 – 6666; c) M. Albrecht, I. Janser, S. Meyer, P. Weis, R. Fröhlich, *Chem. Commun.* **2003**, 2854 – 2855; d) I. M. Müller, R. Robson, F. Separovic, *Angew. Chem.* **2001**, *113*, 4519 – 4520; *Angew. Chem. Int. Ed.* **2001**, *40*, 4385 – 4386; e) I. M. Müller, D. Möller, *Angew. Chem.* **2005**, *117*, 3029 – 3033; *Angew. Chem. Int. Ed.* **2005**, *44*, 2969 – 2973; f) I. M. Müller, S. Spillmann, H. Franck, R. Pietschnig, *Chem. Eur. J.* **2004**, *10*, 2207 – 2213; g) S. Hiraoka, K. Harano, M. Shiro, Y. Ozawa, N. Yasuda, K. Toriumi, M. Shionoya, *Angew. Chem.* **2006**, *118*, 6638 – 6641; *Angew. Chem. Int. Ed.* **2006**, *45*, 6488 – 6491; h) T. Glaser, M. Heidemeier, T. Weyhermüller, R.-D. Hoffmann, H. Rupp, P. Müller, *Angew. Chem.* **2006**, *118*, 6179 – 6183; *Angew. Chem. Int. Ed.* **2006**, *45*, 6033 – 6037; i) I. M. Oppel (née Müller), K. Föcker, *Angew. Chem.* **2008**, *120*, 408 – 411; *Angew. Chem. Int. Ed.* **2008**, *47*, 402 – 405.

[35] H. Glaser, R. Puchta, N. J. R. van Eikema Hommes, D. Leusser, A. Murso, D. Stalke, W. Bauer, R. W. Saalfrank, *Helv. Chim. Acta* **2002**, *85*, 3828 – 3841.

[36] R. W. Saalfrank, H. Maid, A. Scheurer, F. W. Heinemann, R. Puchta, W. Bauer, D. Stern, D. Stalke, *Angew. Chem.* **2008**, *120*, DOI: 10.1002/ange.200804225; *Angew. Chem. Int. Ed.* **2008**, *47*, DOI: 10.1002/anie.200804225, accepted.

[37] R. W. Saalfrank, O. Struck, M. G. Davidson, R. Snaith, *Chem. Ber.* **1994**, *127*, 2489 – 2492.

[38] S. Mann, G. Huttner, L. Zsolnai, K. Heinze, *Angew. Chem.* **1996**, *108*, 2983 – 2984; *Angew. Chem. Int. Ed. Engl.* **1996**, *35*, 2808 – 2809.

[39] R. W. Saalfrank, I. Bernt, E. Uller, F. Hampel, *Angew. Chem.* **1997**, *109*, 2596 – 2599; *Angew. Chem. Int. Ed. Engl.* **1997**, *36*, 2482 – 2485.

[40] a) O. Waldmann, R. Koch, S. Schromm, P. Müller, I. Bernt, R. W. Saalfrank, *Phys. Rev. Lett.* **2002**, *89*, 246401; b) O. Waldmann, R. Koch, S. Schromm, J. Schülein, P. Müller, I. Bernt, R. W. Saalfrank, F. Hampel, E. Balthes, *Inorg. Chem.* **2001**, *40*, 2986 – 2995.

[41] a) R. W. Saalfrank, C. Deutscher, S. Sperner, T. Nakajima, A. M. Ako, E. Uller, F. Hampel, F. W. Heinemann, *Inorg. Chem.* **2004**, *43*, 4372 – 4382; b) R. W. Saalfrank, I. Bernt, M. M. Chowdhry, F. Hampel, G. B. M. Vaughan, *Chem. Eur. J.* **2001**, *7*, 2765 – 2769; c) A. M. Ako, H. Maid, S. Sperner, S. H. H. Zaidi, R. W. Saalfrank, M. S. Alam, P. Müller, F. W. Heinemann, *Supramol. Chem.* **2005**, *17*, 315 – 321.

[42] a) R. W. Saalfrank, H. Maid, *Chem. Commun.* **2005**, 5953 – 5967; b) R. W. Saalfrank, H. Maid, F. Hampel, K. Peters, *Eur. J. Inorg. Chem.* **1999**, 1859 – 1867.

[43] P. N. W. Baxter, R. G. Khoury, J.-M. Lehn, G. Baum, D. Fenske, *Chem. Eur. J.* **2000**, *6*, 4140 – 4148.

[44] a) R. W. Saalfrank, A. Scheurer, I. Bernt, F. W. Heinemann, A. V. Postnikov, V. Schünemann, A. X. Trautwein, M. S. Alam, H. Rupp, P. Müller, *Dalton Trans.* **2006**, 2865 – 2874; b) A. F. Takács, M. Neumann, A. V. Postnikov, K. Kuepper, A. Scheurer, S. Sperner, R. W. Saalfrank, K. C. Prince, *J. Chem. Phys.* **2006**, *124*, 044503; c) M. Ruben, J.-M. Lehn, P. Müller, *Chem. Soc. Rev.* **2006**, *35*, 1056 – 1067.

[45] Cf.: a) R. Sessoli, D. Gatteschi, A. Caneschi, M. A. Novak, *Nature* **1993**, *365*, 141 – 143; b) K. L. Taft, G. C. Papaefthymiou, S. J. Lippard, *Science* **1993**, *259*, 1302 – 1305; c) D. Gatteschi, A. Caneschi, L. Pardi, R. Sessoli, *Science* **1994**, *265*, 1054 – 1058; d) B. Pilawa, M. T. Kelemen, S. Wanka, A. Geisselmann, A. L. Barra, *Europhys. Lett.* **1998**, *43*, 7 – 12; e) B. Barbara, L. Thomas,

F. Lionti, I. Chiorescu, A. Sulpice, *J. Magn. Magn. Mater.* **1999**, *200*, 167 – 181; f) E. Coronado, J.-R. Galán-Mascarós, C.-J. Gómez-García, J. Ensling, P. Gütlich, *Chem. Eur. J.* **2000**, *6*, 552 – 563; g) D. Gatteschi, R. Sessoli, *Angew. Chem.* **2003**, *115*, 278 – 309; *Angew. Chem. Int. Ed.* **2003**, *42*, 268 – 297; h) C. J. Milios, C. P. Raptopoulou, A. Terzis, F. Lloret, R. Vicente, S. P. Perlepes, A. Escuer, *Angew. Chem.* **2004**, *116*, 212 – 214; *Angew. Chem. Int. Ed.* **2004**, *43*, 210 – 212; i) A. K. Boudalis, B. Donnadieu, V. Nastopoulos, J. M. Clemente-Juan, A. Mari, Y. Sanakis, J.-P. Tuchagues, S. P. Perlepes, *Angew. Chem.* **2004**, *116*, 2316 – 2320; *Angew. Chem. Int. Ed.* **2004**, *43*, 2266 – 2270; j) L. M. Wittick, K. S. Murray, B. Moubaraki, S. R. Batten, L. Spiccia, K. J. Berry, *Dalton Trans.* **2004**, 1003 – 1011; k) M. Murugesu, W. Wernsdorfer, K. A. Abboud, G. Christou, *Angew. Chem.* **2005**, *117*, 914 – 918; *Angew. Chem. Int. Ed.* **2005**, *44*, 892 – 896; l) D. Foguet-Albiol, T. A. O'Brien, W. Wernsdorfer, B. Moulton, M. J. Zaworotko, K. A. Abboud, G. Christou, *Angew. Chem.* **2005**, *117*, 919 – 923; *Angew. Chem. Int. Ed.* **2005**, *44*, 897 – 901; m) S. Koizumi, M. Nihei, M. Nakano, H. Oshio, *Inorg. Chem.* **2005**, *44*, 1208 – 1210; n) A. L. Barra, A. Caneschi, A. Cornia, F. Fabrizi de Biani, D. Gatteschi, C. Sangregorio, R. Sessoli, *J. Am. Chem. Soc.* **1999**, *121*, 5302 – 5310; o) D. Gatteschi, R. Sessoli, A. Cornia, *Chem. Commun.* **2000**, 725 – 732; p) A. Bouwen, A. Caneschi, D. Gatteschi, E. Goovaerts, D. Schoemaker, L. Sorace, M. Stefan, *J. Phys. Chem. B* **2001**, *105*, 2658 – 2663; q) J. Kortus, M. R. Pederson, T. Baruah, N. Bernstein, C. S. Hellberg, *Polyhedron* **2003**, *22*, 1871 – 1876; r) A. Cornia, A. C. Fabretti, P. Garrisi, C. Mortalò, D. Bonacchi, D. Gatteschi, R. Sessoli, L. Sorace, W. Wernsdorfer, A.-L. Barra, *Angew. Chem.* **2004**, *116*, 1156 – 1159; *Angew. Chem. Int. Ed.* **2004**, *43*, 1136 – 1139; s) S. Carretta, P. Santini, G. Amoretti, T. Guidi, R. Caciuffo, A. Candini, A. Cornia, D. Gatteschi, M. Plazanet, J. A. Stride, *Phys. Rev. B* **2004**, *70*, 214403; t) J. Ribas-Arino, T. Baruah, M. R. Pederson, *J. Chem. Phys.* **2005**, *123*, 044303; u) N. T. Madhu, J.-K. Tang, I. J. Hewitt, R. Clérac, W. Wernsdorfer, J. van Slageren, C. E. Anson, A. K. Powell, *Polyhedron* **2005**, *24*, 2864 – 2869; v) A. M. Ako, O. Waldmann, V. Mereacre, F. Klöwer, I. J. Hewitt, C. E. Anson, H. U. Güdel, A. K. Powell, *Inorg. Chem.* **2007**, *46*, 756 – 766; w) A. M. Ako, I. J. Hewitt, V. Mereacre, R. Clérac, W. Wernsdorfer, C. E. Anson, A. K. Powell, *Angew. Chem.* **2006**, *118*, 5048 – 5051; *Angew. Chem. Int. Ed.* **2006**, *45*, 4926 – 4929.

[46] Cf.: a) C. J. Hawker, K. L. Wooley, J. M. J. Fréchet, *J. Chem. Soc. Chem. Commun.* **1994**, 925 – 926; b) C. Hawker, J. M. J. Fréchet, *J. Chem. Soc. Chem. Commun.* **1990**, 1010 – 1013.

[47] R. W. Saalfrank, C. Deutscher, H. Maid, A. M. Ako, S. Sperner, T. Nakajima, W. Bauer, F. Hampel, B. A. Heß, N. J. R. van Eikema Hommes, R. Puchta, F. W. Heinemann, *Chem. Eur. J.* **2004**, *10*, 1899 – 1905.

[48] Animations to visualize the dynamics of $(\Delta,\Delta,\Delta,\Delta)$-$[(NH_4)_4\cap\{Mg_4(L)_6\}]\rightleftarrows(\Lambda,\Lambda,\Lambda,\Lambda)$-$[(NH_4)_4\cap\{Mg_4(L)_6\}]$ and S_6-$[In_6Cl_6(L^1)_6]\rightleftarrows S_6'$-$[In_6Cl_6(L^1)_6]$: http://www.chemie.uni-erlangen.de/oc/saalfrank/gallery.html.

[49] a) R. W. Saalfrank, I. Bernt, F. Hampel, *Angew. Chem.* **2001**, *113*, 1745 – 1748; *Angew. Chem. Int. Ed.* **2001**, *40*, 1700 – 1703; b) I. Bernt, Ph.D. Thesis, Universität Erlangen-Nürnberg, **2001**; c) Z. Grote, R. Scopelliti, K. Severin, *J. Am. Chem. Soc.* **2004**, *126*, 16959 – 16972.

[50] R. W. Saalfrank, I. Bernt, F. Hampel, A. Scheurer, T. Nakajima, S. H. Z. Huma, F. W. Heinemann, M. Schmidtmann, A. Müller, *Polyhedron* **2003**, *22*, 2985 – 2989.

[51] R. W. Saalfrank, I. Bernt, F. Hampel, *Chem. Eur. J.* **2001**, *7*, 2770 – 2774.

[52] R. W. Saalfrank, A. Scheurer, R. Prakash, F. W. Heinemann, T. Nakajima, F. Hampel, R. Leppin, B. Pilawa, H. Rupp, P. Müller, *Inorg. Chem.* **2007**, *46*, 1586 – 1592.

[53] R. W. Saalfrank, T. Nakajima, N. Mooren, A. Scheurer, H. Maid, F. Hampel, C. Trieflinger, J. Daub, *Eur. J. Inorg. Chem.* **2005**, 1149 – 1153.

[54] a) G. L. Abbati, A. Cornia, A. C. Fabretti, A. Caneschi, D. Gatteschi, *Inorg. Chem.* **1998**, *37*, 3759 – 3766; b) M. A. Bolcar, S. M. J. Aubin, K. Folting, D. N. Hendrickson, G. Christou, *Chem. Commun.* **1997**, 1485 – 1486; c) N. C. Harden, M. A. Bolcar, W. Wernsdorfer, K. A. Abboud, W. E. Streib, G. Christou, *Inorg. Chem.* **2003**, *42*, 7067 – 7076; d) S. Koizumi, M. Nihei, T. Shiga, M. Nakano, H. Nojiri, R. Bircher, O. Waldmann, S. T. Ochsenbein, H. U. Güdel, F. Fernandez-Alonso, H. Oshio, *Chem. Eur. J.* **2007**, *13*, 8445 – 8453; e) T. Liu, B.-W. Wang, Y.-H. Chen, Z.-M. Wang, S. Gao, *Z. Anorg. Allg. Chem.* **2008**, *634*, 778 – 783.

[55] Cf.: L. Zhao, C. J. Matthews, L. K. Thompson, S. L. Heath, *Chem. Commun.* **2000**, 265 – 266.

[56] R. W. Saalfrank, R. Prakash, H. Maid, F. Hampel, F. W. Heinemann, A. X. Trautwein, L. H. Böttger, *Chem. Eur. J.* **2006**, *12*, 2428 – 2433.

[57] L. Thomas, F. Lionti, R. Ballou, D. Gatteschi, R. Sessoli, B. Barbara, *Nature* **1996**, *383*, 145 – 147.

[58] R. Prakash, R. W. Saalfrank, H. Maid, A. Scheurer, F. W. Heinemann, A. X. Trautwein, L. H. Böttger, *Angew. Chem.* **2006**, *118*, 6017 – 6022; *Angew. Chem. Int. Ed.* **2006**, *45*, 5885 – 5889.

[59] Cf.: W. Schmitt, C. E. Anson, W. Wernsdorfer, A. K. Powell, *Chem. Commun.* **2005**, 2098 – 2100.

[60] *Wissenschaftsforum Chemie*, 16 – 19 September, **2007**, Ulm, Germany.

[61] As is generally known, the German tax system is much too complicated, and therefore it will never be possible to do one's taxes in writing on a beer coaster, as was proposed by Friedrich Merz. However, this is possible for a chemistry problem, a science which is traditionally regarded as being far from simple. Please, see for yourself: the catalytic cycle of the metathesis reaction (Noble Prize in chemistry, 2005) indeed fits on a beer coaster. R. W. Saalfrank, *Nachr. Chem.* **2006**, *54*, 401.

[62] a) E. Uller, Ph.D. Thesis, Universität Erlangen-Nürnberg, **2001**; b) T. Gottschalk, diploma thesis, Universität Erlangen-Nürnberg, **2005**.

[63] H. Hou, K. C.-F. Leung, D. Lanari, A. Nelson, J. F. Stoddart, R. H. Grubbs, *J. Am. Chem. Soc.* **2006**, *128*, 15358 – 15359.

